INCORPORATING WIND POWER CURTAILMENT IN RELIABILITY AND WIND ENERGY BENEFIT ASSESSMENT

A Thesis Submitted to the College of

Graduate Studies and Research

In Partial Fulfillment of the Requirements

For the Degree of Master of Science

In the Department of Electrical Engineering

University of Saskatchewan

Saskatoon, Canada

By

Malhar Padhee

PERMISSION TO USE

In presenting this thesis in partial fulfilment of the requirements for a Postgraduate degree from the University of Saskatchewan, I agree that the Libraries of this University may make it freely available for inspection. I further agree that permission for copying of this thesis in any manner, in whole or in part, for scholarly purposes may be granted by the professor or professors who supervised my thesis work or, in their absence, by the Head of the Department or the Dean of the College in which my thesis work was done. It is understood that any copying or publication or use of this thesis or parts thereof for financial gain shall not be allowed without my written permission. It is also understood that due recognition shall be given to me and to the University of Saskatchewan in any scholarly use which may be made of any material in my thesis.

Requests for permission to copy or to make other use of material in this thesis in whole or part should be addressed to:

Head of the Department of Electrical Engineering

57 Campus Drive

University of Saskatchewan

Saskatoon, Saskatchewan, S7N 5A9

Canada

ABSTRACT

Fossil fuel is presently a major source for electricity production, but it contributes significantly to Green House Gas emissions. Wind is a promising alternative, and can potentially become a major power resource in future power systems. Wind power installations are growing significantly for producing clean energy in electric power systems. As the wind penetration continues to increase to relatively high levels, it can significantly affect the overall performance and reliability of the power system. Hence, it becomes very important to accurately model the behaviour of wind, its interaction with conventional sources and also with other wind resources connected to the power system in order to conduct a realistic assessment of system reliability and benefits from wind energy utilization.

When the wind penetration levels are low, all the wind energy generated is utilized to serve the load. However, at higher wind penetration levels, wind energy is spilled due to limitations in the operating reserve or ramping capability of the scheduled generating units. The system reliability and the wind energy benefits are reduced as the wind energy spillage increases due to wind curtailment. Hence, accurate wind models should be researched and developed to include wind energy curtailment in the reliability modelling, considering factors such as the system load level, priority loading order of the generating unit and response rates of the generating units. Researchers have not incorporated these factors in wind power modelling and in the adequacy evaluation of wind integrated power systems. A new analytical technique is developed in the subsequent chapters to carry out a comprehensive wind absorption capability evaluation of the power system, and also to incorporate this characteristic in reliability modelling of the system.

Wind curtailments can take place not only due to generation constraints, but also due to transmission line constraints depending on the capacity and location of the wind energy resource

in the power system, and the power transfer capacity of the transmission lines connected to the wind farm bus. Therefore, reliability modelling of the power system considering wind curtailments due to both generation and transmission constraints should be carried out to assess the impact of wind farms on bulk system reliability and the wind energy benefits. Wind curtailment is incorporated in the composite power system reliability evaluation by modelling the wind resource both as generation and as negative load. The techniques can be utilized to conduct system adequacy and wind energy benefit assessment both at the capacity planning stages and composite generation/transmission planning stages, incorporating wind power curtailment due to generating unit response limitations.

As the wind penetration in a power system increases, the wind farms connected to the system are distributed at different geographical locations. Both analytical and Monte Carlo Simulation based techniques have previously been used by the research group at the University of Saskatchewan to include the cross correlation between the wind characteristics of different wind farms in the wind modelling for reliability evaluation of power systems. However, the combined effect of wind diversity and wind curtailments due to both transmission and generation constraints on the system reliability and wind energy benefit assessment has not been considered. The techniques developed for system adequacy and wind energy benefit assessment considering wind curtailment due to generation and transmission constraints are further modified and presented in this thesis to include wind diversity in the analysis. The developed techniques for adequacy evaluation of wind integrated power systems considering wind power curtailment and diversity should be extremely useful for system planning engineers and policy makers as wind power penetration in power systems continues to increase throughout the world.

ACKNOWLEDGMENTS

First and foremost, I am extremely thankful to my supervisor, Dr. Rajesh Karki for the invaluable guidance and constant encouragement I received through the course of my research work as well as during the preparation of this thesis. His prodigious knowledge, experience in the field and support was critical for the completion of my M.Sc. research work. I would also like to thank the College of Graduate Studies and Research, the Department of Electrical and Computer Engineering, SaskPower and Natural Sciences and Engineering Research Council of Canada (NSERC) for providing the financial support throughout my graduate program.

I would like to sincerely thank my committee members for the valuable suggestions and inputs which greatly improved the quality of my thesis. I am really thankful to my former project supervisor and research advisor in India, Prof. (Dr.) P. K. Dash, and my former colleague, Dr. Suman Thapa for guiding me on several occasions. With their immense knowledge in the field, they provided me with valuable research related suggestions. I am very grateful to my graduate study teachers, Dr. Ramakrishna Gokaraju and Dr. Sherif O. Faried for strengthening my knowledge on power system protection and power system analysis. I would also like to thank all my colleagues in the Power Systems Research Group for their support.

Last but definitely not the least, I would like to express my deepest gratitude to my parents, Dr. Ambarish Padhee and Sujata Padhee and my sister, Varsha for their constant love, encouragement and support during my time as a graduate student.

TABLE OF CONTENTS

PERMISSION TO USE i

ABSTRACT ii

ACKNOWLEDGEMENTS iv

TABLE OF CONTENTS v

LIST OF TABLES vii

LIST OF FIGURES ix

LIST OF ABBREVIATIONS xi

1 INTRODUCTION 1
1.1 Power system reliability evaluation 1
1.2 Inclusion of wind in power system adequacy evaluation 4
1.3 Problem statement and research objective 8
1.4 Outline of the thesis 13

2 BASIC CONCEPTS FOR RELIABILITY AND WIND ENERGY UTILIZATION EVALUATION IN POWER SYSTEMS 15
2.1 Introduction 15
2.2 Generating system adequacy evaluation 15
2.2.1 Conventional generation modelling 18
2.2.2 Wind power modelling 21
2.2.3 Load modelling and incorporation of wind power as negative load 23
2.2.4 Risk indices 26
2.3 Bulk system adequacy evaluation 30
2.3.1 Sequential MCS 31
2.3.2 Non-sequential MCS 33
2.3.2.1 State sampling approach 33
2.3.2.2 State transition sampling approach 34
2.3.3 Risk indices 35
2.3.4 The MECORE software 37
2.4 Conclusions 38

3 WIND POWER ABSORPTION CAPABILITY ASSESSMENT IN A POWER SYSTEM 40
3.1 Introduction 40
3.2 Proposed technique to assess the wind power absorption capability of a power system 40
3.2.1 Wind power absorption capability assessment for a system operating state 41

3.2.2 Wind power absorption capability at different operating conditions 42
3.3 Application of the proposed method 45
3.4 Conclusions 51

4 INCORPORATION OF WIND CURTAILMENT IN GENERATION SYSTEM RELIABILITY AND WIND ENERGY BENEFIT ASSESSMENT 52
4.1 Introduction 52
4.2 Power system modelling to include wind power curtailment 53
4.2.1 Conventional generation modelling 53
4.2.2 Load modelling and wind modelling to include wind energy curtailment 53
4.3 Proposed indices to quantify the wind energy benefits 55
4.4 Application of the proposed method 57
4.4.1 Generation and load model 58
4.4.2 System evaluation 59
4.5 Impact of wind growth on the reliability and wind energy utilization 64
4.6 Impact of wind diversity on power system reliability and wind energy benefit assessment 68
4.7 Conclusions 73

5 INCORPORATION OF WIND CURTAILMENT IN BULK SYSTEM RELIABILITY AND WIND ENERGY BENEFIT ASSESSMENT 75
5.1 Introduction 75
5.2 Proposed HL II reliability and wind energy benefit assessment technique considering wind curtailment 76
5.2.1 Conventional generation modelling 76
5.2.2 Transmission line modelling 76
5.2.3 Load and wind modelling 76
5.2.4 Load modelling for MECORE application to include wind curtailment in the HL II adequacy evaluation 79
5.2.5 Load model approximation 81
5.2.6 Validation of the proposed technique 84
5.3 Generation and transmission contribution to wind curtailments and the impact on bulk system reliability 86
5.3.1 The modified IEEE-RTS 86
5.3.2 Evaluation of the HL II reliability indices 88
5.4 Impact of wind growth on the reliability and wind energy utilization 89
5.5 Consideration of wind diversity in bulk power system reliability and wind energy benefit assessment 96
5.5.1 Development of HL II evaluation technique considering wind speed correlation and wind power curtailment 97
5.5.2 Sensitivity studies considering increase in wind penetration 99
5.6 Conclusions 102

6 SUMMARY AND CONCLUSIONS 104

LIST OF REFERENCES 108

LIST OF TABLES

Table page no.

Table 2.1: Conventional generating unit models 20

Table 2.2: Total conventional generation model 20

Table 2.3: Hourly wind power, hourly load and modified load of the example power system.... 24

Table 2.4: Modified hourly loads arranged in descending order 25

Table 2.5: Differences between system models for HL I and HL II adequacy assessment..... 31

Table 3.1: System generation data 45

Table 3.2: Generating unit ramp rate data 47

Table 3.3: Generation schedule for the system load of 2047 MW 47

Table 3.4: WPAC for different response times..... 48

Table 3.5: WPAC at different operating conditions 48

Table 3.6: Calculation of the expected WPAC during the low load period 50

Table 3.7: Expected WPAC for different response times..... 50

Table 4.1: Impact of wind curtailment on system adequacy 60

Table 4.2: Impact of wind curtailment on wind energy utilization..... 61

Table 4.3: Generating unit load dispatch to serve 1667 MW of load 62

Table 4.4: Thermal and gas power absorption capability for different operating conditions..... 63

Table 4.5: Impact of wind curtailment on GHG emissions 63

Table 4.6: Impact of wind power growth and wind curtailments on wind capacity credit..... 65

Table 4.7: Reduction in GHG emissions and impact of wind curtailment 68

Table 4.8: Impact of wind diversity on system reliability indices 71

Table 4.9: Impact of wind diversity on wind capacity credit 72

Table 4.10: Impact of wind diversity on wind energy indices 72

Table 4.11: Reduction in GHG emissions and impact of wind diversity 73

Table 5.1: The HL I annual system indices considering a system peak load of 2850 MW..... 82

Table 5.2: The HL I annual system indices considering a system peak load of 3500 MW..... 82

Table 5.3: The HL II annual system indices without any wind resource 82

Table 5.4: The HL II annual system indices in presence of 198 MW Swift Current wind farm.. 82

Table 5.5: Validation of the proposed technique using the HL-I analytical technique 85

Table 5.6: Generating units added to the IEEE-RTS 88

Table 5.7: System LOLE considering wind curtailment due to generation and transmission constraints 89

Table 5.8: Impact of wind power growth and wind curtailments on load carrying capability 91

Table 5.9: Impact of wind power curtailment on GHG emissions 96

Table 5.10: Impact of wind diversity on system reliability and wind energy utilization 99

Table 5.11: Impact of wind growth on wind capacity credit 100

Table 5.12: Impact of wind diversity on system reliability and wind energy utilization 101

Table 5.13: Impact of wind growth on wind capacity credit 102

LIST OF FIGURES

Figure page no.

Figure 1.1: Subdivisions of system reliability 1

Figure 1.2: Structure of hierarchical levels in a power system 2

Figure 1.3: Global cumulative installed wind capacity (Source: Global Wind Energy Council (GWEC), www.gwec.net) 6

Figure 2.1: Basic system model for generating system adequacy assessment 16

Figure 2.2: Wind-integrated system model for generating system adequacy assessment. (a) Wind capacity modelled as generation; (b) Wind capacity modelled as negative load 17

Figure 2.3: Conventional generating unit Markov models (a) 2-state model; (b) 3-state model.....

..... 19

Figure 2.4: Wind turbine generator power curve 23

Figure 2.5: Per unit LDC for the test power system 25

Figure 2.6: Calculation of risk indices using the generation and load model 27

Figure 2.7: System PLCC and LOLE with and without wind energy 29

Figure 2.8: Wind-integrated power system model for bulk system adequacy assessment 30

Figure 3.1: Flowchart of the proposed technique to determine WPAC for different system operating conditions 43

Figure 4.1: Hourly load variation and wind power output for 198 MW Wind farm 1 for 8760 hours 54

Figure 4.2: Hourly load variation and wind power output for a 48 hour period 58

Figure 4.3: Effect of wind curtailment on the modified load model for the winter season 59

Figure 4.4: Impact of wind growth on system LOLE 64

Figure 4.5: Impact of wind growth on the IPLCC 66

Figure 4.6: Impact of wind power growth on the wind energy utilization 67

Figure 4.7: Impact of wind growth on the fuel savings 68

Figure 4.8: Winter load models modified by 728 MW wind capacity with and without considering wind diversity 70

Figure 5.1: Annual 30-step load model of the IEEE-RTS 83

Figure 5.2: Modified annual 30-step load model incorporating wind curtailment from a 198 MW wind farm 84

Figure 5.3: Single line diagram of the IEEE-RTS 87

Figure 5.4: Impact of wind growth on system LOLE 91

Figure 5.5: Impact of wind growth on the CC 93

Figure 5.6: Impact of wind growth on the wind energy utilization considering wind curtailment due to generation constraints 94

Figure 5.7: Impact of wind growth on the wind energy utilization considering wind curtailment due to generation and transmission constraints 94

Figure 5.8: Impact of wind growth on the fuel savings 95

LIST OF ABBREVIATIONS

ARMA	Autoregressive Moving Average
CC	Capacity Credit
CCGT	Combined Cycle Gas Turbine
COPT	Capacity Outage Probability Table
ENS	Energy Not Supplied
FOR	Forced Outage Rate
GHG	Green House Gas
HL I	Hierarchical Level I
HL II	Hierarchical Level II
HL III	Hierarchical Level III
IEEE	Institute of Electrical and Electronics Engineers
IEEE-RTS	IEEE- Reliability Test System
IPLCC	Increase in Peak Load Carrying Capability
LDC	Load Duration Curve
LOEE	Loss of Energy Expectation
LOLE	Loss of Load Expectation
MCR	Maximum Continuous Rating
MCS	Monte Carlo Simulation
MW	Megawatt
NERC	North American Electric Reliability Corporation
PLCC	Peak Load Carrying Capability
RI	Reliability Index
SCGT	Simple Cycle Gas Turbine
SM	System Minutes
U	Unavailability
UPM	Units Per Million
WC	Wind Curtailment
WEA	Wind Energy Available
WECS	Wind Energy Conversion System
WES	Wind Energy Supplied
WESP	Wind Energy Spilled
WIPS	Wind Integrated Power System
WPA	Wind Power Absorbed
WPAC	Wind Power Absorption Capability
WTG	Wind Turbine Generator

1 INTRODUCTION

1.1 Power system reliability evaluation

Electric power systems should be designed and operated in a manner such that reliable and economic electrical energy supply is continuously provided to the customers. A loss of service to the customer can result in significant socio-economic impacts to both the electric energy suppliers and consumers. Power system reliability is the ability of the system to meet the electricity needs of the end use customers, considering unanticipated failures of equipment and changes in the customer demand. Power system reliability generally consists of two aspects: system security and system adequacy [1], which is shown in Figure 1.1.

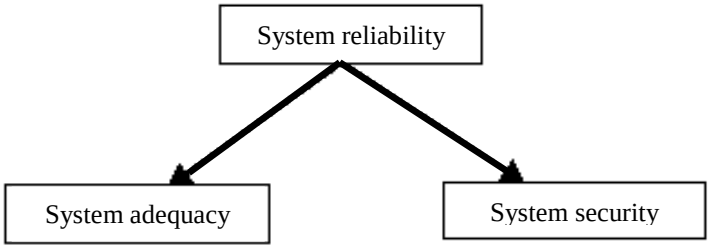

Figure 1.1: Subdivisions of system reliability

System adequacy is concerned with whether or not sufficient infrastructure, such as generating capacity, transmission and distribution capacity, is present in the power system in order to fulfil the customer electricity requirements. Such studies are normally performed during the planning phases, in order to ensure that the system is capable of maintaining the expected reliability. System security studies are concerned with dynamic disturbances that the power

system may encounter and withstand during its operation [1]. The system is considered to be secure if it has the ability to respond to the disturbances and operate in an acceptable manner.

A power system comprises of three hierarchical levels (HL) denoted as HL I, HL II and HL III [1] shown in Figure 1.2. HL I reliability assessment considers the ability of the total system generation to satisfy the total system load demand. HL II reliability evaluation of a power system is involved with the assessment of the ability of both the generation and the transmission system to generate and transport electrical energy to the system load points. Such an evaluation is also known as bulk power system reliability evaluation or composite system reliability evaluation. HL III considers all of the generation, transmission and distribution systems. The research described in this thesis is conducted at both the HL I and HL II levels and is focused on system adequacy analysis.

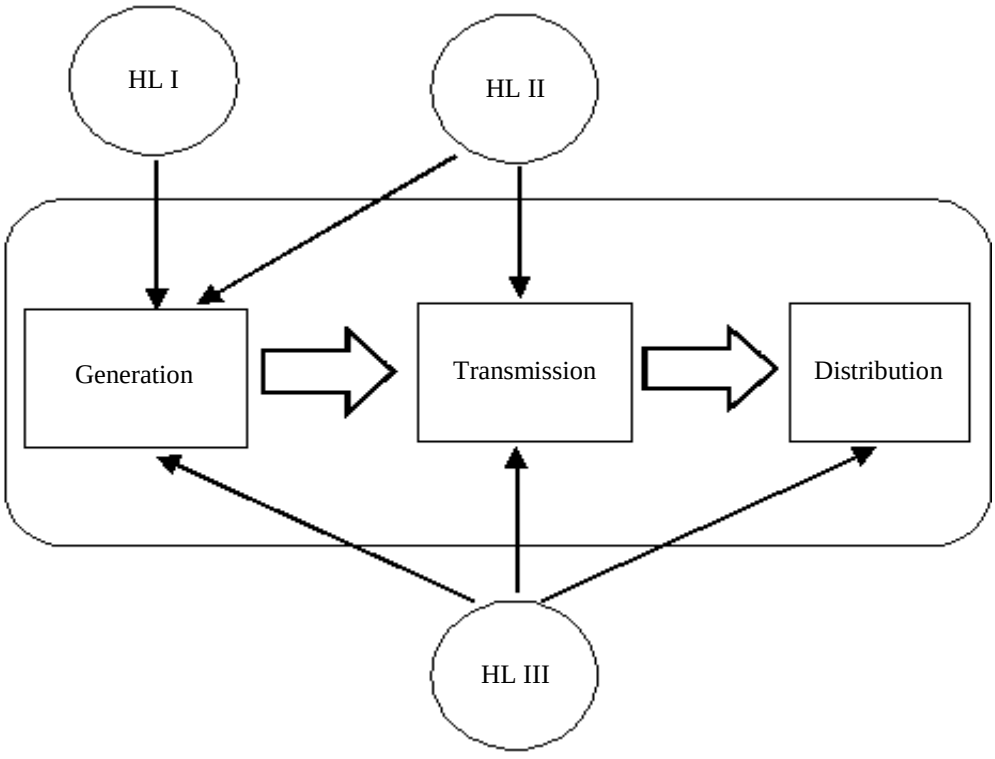

Figure 1.2: Structure of hierarchical levels in a power system

Historically, power system reliability analyses have been carried out utilizing deterministic methods. These techniques use simple rule of thumb methods and are easy to apply. A major drawback of the deterministic approach is that it cannot respond adequately to the random behaviour of the power system and customer demands. Probabilistic reliability evaluation methods can recognize random system characteristics, and are more suitable in modern power system applications. Many power system planners apply probabilistic methods in reliability evaluation at the HL I level [2]. With increasing uncertainties in modern power systems, the applications of probabilistic methods are receiving increased attention in system operation and at the HL II level. The work reported in this thesis makes use of probabilistic methods in adequacy evaluation of power systems.

Analytical and simulation techniques are the two fundamental methodologies for probabilistic power systems reliability evaluation [1]. The analytical technique involves the formulation and utilization of mathematical models of system components using direct numerical solutions, to obtain the desired reliability indices. These techniques have been utilized in different forms by researchers in the adequacy assessment of power systems [3-5]. A Monte Carlo simulation (MCS) technique uses random numbers produced by computers to simulate the system operating states. Subsequently, risk indices are computed from the simulation of these system states conducted over a period of interest, and repetition of the simulation runs until a convergence criterion is met.

Two fundamental techniques are generally utilized in Monte Carlo applications to power system reliability evaluation. These are the sequential and non-sequential MCS techniques. The operating states of all the system components are sampled in the non-sequential technique and a non-chronological system state is obtained. The sequential approach simulates the operating and

failure mode cycles of all the components and a system operating cycle is obtained by combining all the component cycles. Dependent and sequential events can be considered by using the sequential simulation technique. This technique can be used to obtain the distributions of reliability indices in addition to the more common expected indices. Reference [6] uses the sequential Monte Carlo simulation technique in the adequacy evaluation of a power system. References [7] and [8] use the non-sequential Monte Carlo simulation approach for the system adequacy assessment at the HL I and HL II levels respectively.

Analytical techniques require significantly less computation time than that required by the MCS technique. A MCS application in a practical scenario usually requires customized computer programs developed for the particular application in the relevant field. Analytical techniques are therefore more readily applied in practical systems, and have been used for HL I studies in this work. However, Monte Carlo Simulation can incorporate more complexity in the power system since it simulates the operation of the system. A software tool called MECORE [9] was available and has been utilized to carry out HL II studies in this research. The MECORE software is a Monte Carlo based bulk power system reliability evaluation tool capable of performing reliability assessment of an electric power system.

1.2 Inclusion of wind in power system adequacy evaluation

The utilization of conventional energy resources like coal and fossil fuel-based resources cause several environmental problems such as the greenhouse effect, carbon dioxide emissions and acid rain due to sulphur dioxide emissions. The greenhouse gas (GHG) emissions can cause adverse environmental impacts and result in irreversible changes to the climate. Wind has become a promising alternative and is being recognized as an important power source to offset

the GHG emissions from conventional energy resources. The gradual reduction in fossil fuel reserves and rapid increase in the energy demands has resulted in considerable amount of investment in wind power technology.

Presently, about 4% of the total power generation capacity in Canada is from wind, which is approximately 9219 MW [10]. By the end of 2015, the wind penetration level in Canada is expected to increase to about 6%, with an extra 7000 MW of wind capacity expected to contribute to the total generation capacity [10]. The rapid increase in global cumulative installed wind capacity from the year 1996 to 2013 is shown in Figure 1.3. There has been a substantial increase in the installed wind capacity from 6,100 MW in 1996 to 318,105 MW in 2013. The present installed wind power in the province of Saskatchewan, Canada is 198 MW [11]. The wind farms located in Saskatchewan are: 150 MW Centennial wind farm located in the Rural Municipality of Coulee near Swift Current [11], 11 MW Cypress and 11.2 MW Sunbridge wind farms located near Gull Lake [11] and the 26.4 MW Red Lily wind farm located near Moosomin. The installed capacity is projected to grow to about 428 MW by 2017 with a 177 MW facility in Chaplin along with several smaller projects with independent power producers (IPPs) [11]. The installed wind capacity in Saskatchewan is projected to grow by another 300 MW within the next decade.

A Wind Turbine Generator (WTG) converts wind energy into electrical energy. Electric power generation from a wind farm can be highly variable and uncertain depending on the wind regime at the geographic site. The power output profile of a wind farm is therefore very different from that of a conventional power plant. It is therefore necessary to develop methods which can take into account the uncertainties and variability associated with a wind resource. The uncertainty and variation in wind power output poses significant difficulties to system engineers.

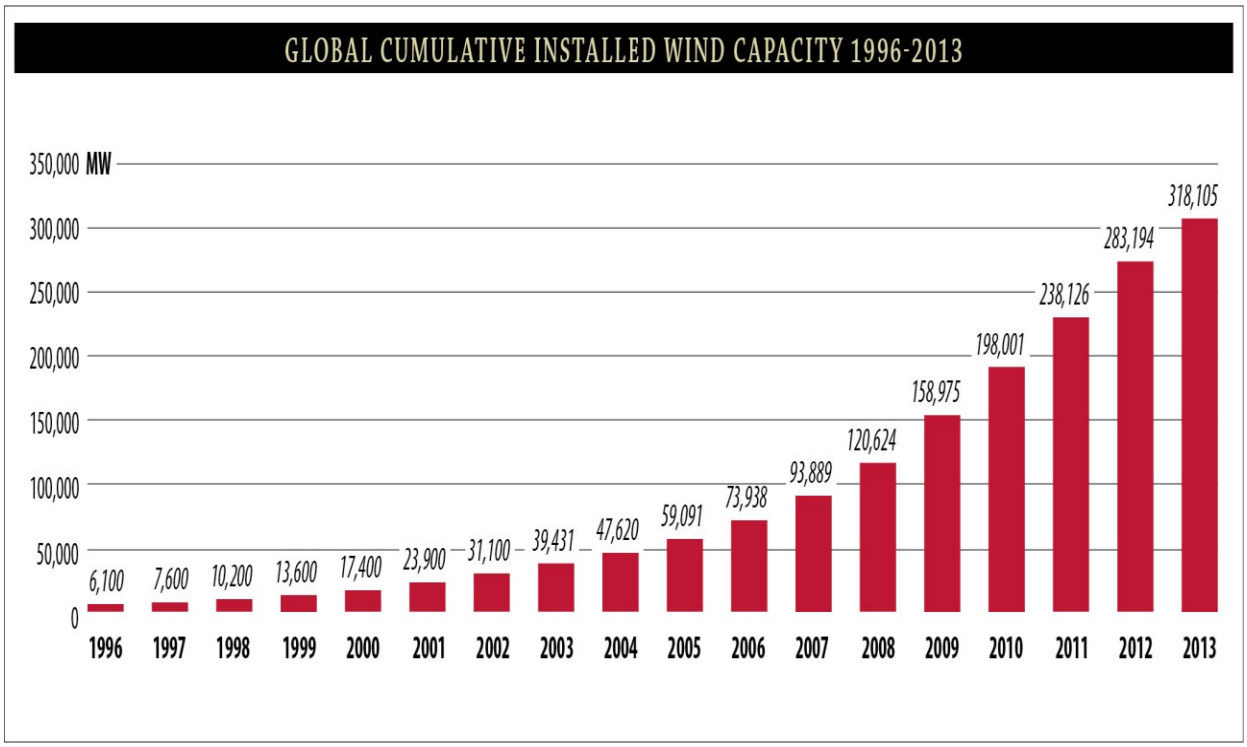

Figure 1.3: Global cumulative installed wind capacity (Source: Global Wind Energy Council (GWEC), www.gwec.net)

These difficulties refer to the planning and operation of the power system while maintaining an acceptable reliability. Power systems had little wind capacity in the past, and therefore, the impact of wind power on system performance was insignificant. As the wind power generation increases to high levels, the consideration of the effect of wind capacity on system reliability indices becomes particularly important. At high wind penetration levels, very accurate wind power models are required for wind integrated power system reliability assessment.

Researchers have used analytical and MCS techniques to conduct the adequacy assessment of wind integrated power systems both at the HL I and HL II levels. References [12-14] present simple and accurate analytical techniques to conduct the generating capacity adequacy assessment of wind integrated power systems (WIPS), and references [15-18] present MCS

techniques for the HL I adequacy assessment of WIPS. References [18-22] present MCS techniques for composite generation and transmission system adequacy assessment of WIPS.

References [17, 21, 23-27] have incorporated the cross correlation between the wind characteristics of different wind farms connected to the power system in the wind modelling during the reliability evaluation of a WIPS. References [23-25] utilize analytical techniques and references [17, 26] use the MCS for the HL I adequacy assessment of power systems with multiple wind farms considering wind speed correlation. References [21] and [27] utilize the state sampling MCS approach for conducting HL II reliability studies on a modified version of the IEEE Reliability Test System considering different wind speed correlation levels and generation and transmission deficient power systems.

Several methods have been used to model the wind speed and wind power in the power system reliability evaluation. Reference [28] has used both the observed hourly wind speeds and the mean observed hourly wind speeds in the reliability evaluation of WIPS. References [29] and [30] use the autoregressive moving average (ARMA) model to predict the wind speeds in the reliability evaluation procedure. Reference [29] also uses the moving average (MA) model to predict the wind speeds in the reliability evaluation procedure. Reference [5] utilizes a wind model which considers both the probability and the frequency and duration characteristics of wind speed. In this model, a Markov chain with a finite number of states is used to represent the wind speed. The available observed wind speeds are used to obtain the parameters of the wind model. In order to include wind power in the calculation process using an analytical technique or a Monte Carlo state sampling approach, the apportioning method is used in [31] to build multi-state wind energy conversion system (WECS) models. Either the observed wind speeds or the

simulated wind speeds [29, 30] are used to build the multi-state models of the wind power output.

With the growth of the installed wind capacity in power systems, system operators encounter significant difficulties in determining suitable unit commitment, reserve requirements and in making dispatch decisions to meet the predicted load with minimal operating risk and cost. A limited number of techniques have been proposed for evaluating the operating risks related to wind power estimation, and quantify operating reliability associated with unit commitment and operating reserves while incorporating the wind variation uncertainties. Reference [32] presents a new approach to assess the contribution of wind power to the peak load carrying capability of the power generating system in the operating domain. The concepts of unit commitment risk analysis are extended to include the wind power variations by building short-term probability distributions of the wind power output.

1.3 Problem statement and research objective

Wind power penetration continues to increase in electric power systems throughout the world [10] causing increased concerns related to system planning and operation in a reliable manner. As wind penetration increases to relatively large scales, it becomes important in system planning to assess the capacity value and reliability impacts of wind resources, as well as the renewable energy utilization and the environmental benefits from them. Wind farms are generally at the top of the generating unit dispatch order, and all the wind energy generated were utilized to serve the load in the past scenarios where wind penetration was relatively low. In high wind penetration scenario, however, wind energy is occasionally spilled or curtailed [33] due to the limitations in operating reserve or ramping capability of the scheduled generating units [33].

Increase in wind penetration, however results in additional wind power curtailments and an increase in the wind energy spilled.

References [33-36] analyze the various factors affecting wind power curtailment in large scale power systems and also present techniques to quantify the wind power curtailment. In reference [33], the wind curtailment estimation effects of natural inter-yearly wind profile variability, system demand-profile, and minimum system inertial constraints are examined in detail. Reference [33] also presents several case studies which show that the size of the wind farms connected to the power system greatly impacts the wind power curtailment. Reference [34] presents a model-based approach to estimate the wind curtailment in Ireland utilizing high-resolution wind speed and demand data over a four year period, particularly focusing on the temporal characteristics of curtailment and factors that affect it. The model is also able to forecast the wind curtailment levels in the future years. References [35] and [36] propose accurate analytical techniques to quantify the wind curtailments occurring due to transmission congestion in the modified version of IEEE-RTS and an actual large scale power system. The proposed approaches however cannot be used for reliability assessment of power systems.

With the increase in wind energy spillage due to wind curtailment, the system reliability and the wind energy benefits are reduced. Therefore, accurate wind models should be developed to incorporate wind energy curtailment in reliability modelling. In order to develop such wind models, important factors such as the system load level, priority loading order of the generating unit and the response rate or ramping capabilities of the generating units should be considered. References [33] and [35-38] have considered some of these important factors to quantify the wind energy curtailment in power systems. However, the incorporation of these factors in the wind model and in the adequacy assessment of wind integrated power systems has not been

considered. Therefore, a simple analytical technique should be developed which can carry out a comprehensive wind absorption capability evaluation of the power system.

There is a need to develop a method that can be used to assess the wind power absorption capability of a power system, and incorporate this characteristic in reliability modeling of the system. Such models suited to adequacy evaluation both at the HL I and HL II levels will be very useful to system planners since existing methods do not incorporate wind power curtailment due to generating unit response limitations. As analytical methods are relatively easy to apply, a simple analytical technique that can accurately model the wind power curtailment in generation system reliability evaluation would be very useful to system capacity planners. Important factors such as maintenance of generating units and seasonal correlation between system load and wind power [39] can be considered by conducting a period analysis [1, 39]. The developed techniques should be able to accurately quantify the wind energy benefits in addition to the reliability assessment as these are important considerations in capacity planning.

It has been discussed in [33, 36, 40] that wind curtailments can take place not only due to generation constraints, but also due to transmission line constraints depending on the location of the wind energy resource in the power system, capacity of the wind resource, and also the power transfer capacity of the transmission lines connected to the wind farm bus. Reference [40] presents real case studies which show that wind curtailments also occur due to the presence of high wind power ramp rates for a certain time period, high wind generation during off-peak hours, and the line constraints which limit the transmission of the excess wind power generation to the other balancing areas. Therefore, accurate reliability modeling of the power system considering wind curtailments due to both generation and transmission constraints will be important in assessing the impact of wind farms on bulk system reliability, and on the economic

and environmental benefits from wind energy. Wind curtailment can be incorporated in the composite power system reliability evaluation by following the negative load approach for wind modelling [18, 41]. Further modifications should also be made in the developed HL II technique to include wind diversity in the system adequacy assessment.

With the growth in wind penetration, the wind farms in a power system are distributed at different geographical locations, which could result in better system reliability as compared to a scenario where the entire wind capacity is at one wind site. References [17, 23-26] have included the cross correlation between the wind characteristics of different wind farms in the wind modeling during the reliability evaluation of the power generation system. References [23-25] use analytical techniques and references [17, 26] use the MCS for the HL I adequacy assessment of power systems with multiple correlated wind farms. References [21, 22, 27] present techniques to conduct adequacy assessment in composite power systems with multiple wind farms considering wind speed correlation. A state sampling MCS based approach is used in [21, 27] to conduct reliability studies on a wind-integrated power system considering different values of wind speed correlation. Reference [27] concluded that the reliability improvements are better for lower values of wind speed correlation between two wind farms. Reference [22] presents a reliability assessment technique for a composite power system including wind power generation, and also compares the HL II reliability indices by changing the location of the wind resources and the wind penetration in the power system.

From the results in [17, 21-27], it is seen that wind diversity leads to noticeable improvement in the system reliability. However, the combined effect of wind diversity and wind curtailments due to both transmission and generation constraints on the system reliability has not been considered by previous researchers. Some researchers have considered the utilization of

compressed air energy storage (CAES) [42] and a generic energy storage model [43] for mitigating the effects of wind energy curtailment. The diversification of wind resources should also be considered as an alternative method to mitigate the impact of wind curtailments on the system reliability.

The total installed wind capacity in the Saskatchewan province is predicted to increase to 428 MW by 2017. The diversification of the wind resources at multiple geographic locations, and the resulting reliability benefits to the Saskatchewan power system has been reported in a previous system reliability study [44]. However, the wind energy curtailment and its impact on the system reliability and wind energy benefits have not been considered. The research work in this thesis was part of a collaborative research project jointly funded by the Saskatchewan Power Corporation (SaskPower) and the Natural Sciences and Engineering Research Council of Canada (NSERC). The research work aims to address the problems discussed in this section. The major objectives are listed below:

- To develop an analytical technique to assess the wind power absorption capability of a power system considering factors such as system loading conditions and operating characteristic of the conventional generating units
- To develop new techniques to incorporate wind curtailment and wind diversity in the reliability and wind energy benefit assessment at the HL I level
- To develop new techniques to incorporate wind curtailment and wind diversity in the reliability and wind energy benefit assessment of the bulk power system
- To compare the performance of the proposed techniques with previously developed methods

1.4 Outline of the thesis

This thesis consists of six chapters:

Chapter 1 describes the basic concepts concerning the reliability assessment of wind-integrated power systems. The research problem and objectives of the research work are also described in the chapter.

Chapter 2 presents the preliminary reliability concepts for HL I and HL II adequacy evaluation of a wind-integrated power system. A simple test power system is used to describe the concepts used in the studies in the subsequent chapters.

Chapter 3 introduces a new probabilistic technique to accurately assess the wind power absorption capability of a power system. A realistic power system was used in the studies, which consisted of different types of generating units. The proposed method for wind power absorption capability assessment is subsequently described, considering different possible operating conditions of the system. Factors such as the response rate and dispatch order of generating units can affect actual wind energy utilization in a power system, and hence the reliability of the power system. These important factors have been incorporated in the technique presented Chapter 3, and in the reliability and wind energy utilization assessment methods described in Chapters 4 and 5.

Chapter 4 proposes a new analytical technique for generating system adequacy evaluation and wind energy benefit assessment that incorporates the wind power absorption capability of a power system at different loading conditions. A new approach to wind power modelling has been proposed in this chapter to account for the wind power curtailment and also the correlation between different wind farms connected to the power system. The proposed methodology is capable of assessing the wind energy-based indices in addition to the system reliability indices.

Sensitivity studies are also conducted in the chapter considering increases in the wind penetration and the effect on the wind energy curtailments.

Chapter 5 presents a new technique for reliability and wind energy utilization assessment at the HL II level. Wind energy curtailment is also considered in the composite generation and transmission system evaluation technique by following the negative load approach to wind modelling. The proposed evaluation technique considers wind curtailments due to both transmission and generation constraints. Further modification is made in the HL II evaluation technique to include wind speed correlation between diverse wind sites and also wind sites with different types of wind regimes in the analysis. Further sensitivity studies are also conducted by varying the wind penetration level in the bulk power system.

Chapter 6 outlines the research conducted in this thesis and presents the conclusions.

2 BASIC CONCEPTS FOR RELIABILITY AND WIND ENERGY UTILIZATION EVALUATION IN POWER SYSTEMS

2.1 Introduction

The adequacy evaluation of power systems incorporating wind energy involves building the probabilistic models of the various power system components. The developed models are subsequently utilized to evaluate the power system reliability indices. The basic modeling concepts which have been used in subsequent chapters are described in this chapter. This chapter presents the development of conventional generation, wind power and also the load models suitable for both HL I and HL II reliability evaluation. The chapter also discusses a negative load approach to wind modeling and its incorporation in the system load model. The detailed procedure of evaluation of the risk indices, peak load carrying capability and wind capacity credit are subsequently described. Lastly, the various Monte Carlo Simulation approaches for power system reliability evaluation and a MCS based composite generation and transmission system reliability evaluation tool are described.

2.2 Generating system adequacy evaluation

The generating system adequacy assessment is concerned with the evaluation of the ability of all the generating resources to meet the total system load. The transmission network is not included in such an assessment. Figure 2.1 shows the basic system model.

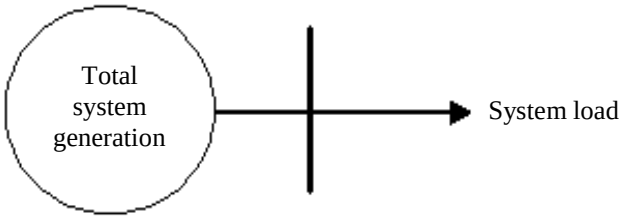

Figure 2.1: Basic system model for generating system adequacy assessment

A generation model is created for each generating unit in the system by representing the unit by a two-state or a multi-state Markov model [1] depending on its type and operating characteristic. A recursive algorithm [1] included in a computer program is used to combine the individual generating unit models to obtain the overall system generation model, which is in the form of a capacity outage probability table (COPT) [1]. This table consists of the various capacity outage states in increasing order and the corresponding cumulative probabilities.

The adequacy evaluation model for a wind-integrated power system is shown in Figure 2.2. In Figure 2.2 (a), the total generating system consists of two subsystems: wind turbine generators (WTG) and conventional generators. Wind power is modelled as a negative load as part of the system load model in Figure 2.2 (b). The hourly wind power output is subtracted from the corresponding hourly load value to obtain the modified system load for every hour, to subsequently build a modified system load model.

The system load can be represented by an hourly load model. The hourly load data for a year are first collected and sorted in descending order. Subsequently, an annual load duration curve is built by showing the loads in per unit of the peak load, and plotting them against time. The various risk indices are obtained by convolving the system generation model with the load model [1].

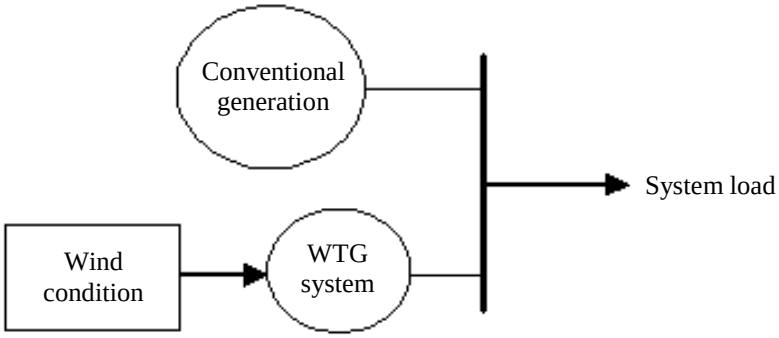

(a)

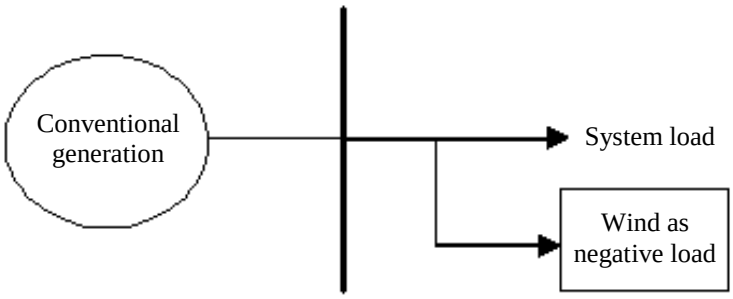

(b)

Figure 2.2: Wind-integrated system model for generating system adequacy assessment. (a) Wind capacity modelled as generation; (b) Wind capacity modelled as negative load.

Many situations can occur in which the generation and the load models vary within the period of analysis. Period analysis [1] can be conducted by dividing the year into several periods in order to incorporate scheduled maintenance of generating units, generating unit deratings during some seasons, seasonal variation of wind speed and system load, and also the correlation between the wind speed and system load in the reliability analysis. In a period analysis, the analysis period (say 8760 hours) is divided into sub-periods; conventional generation, wind generation and load models are built for each period. Subsequently, the reliability indices are calculated for each sub-period, and finally the reliability indices for the entire period are obtained

by adding the corresponding indices for each sub-period, as shown in (2.1). Important information about the contribution of each sub-period to the annual indices can also be obtained from a period analysis.

$$RI = \sum_{p=1}^{n} RI_p \tag{2.1}$$

Where, n: number of sub-periods within the total period

RI_p: reliability index for sub-period p

RI: reliability index for the entire period

2.2.1 Conventional generation modelling

The hydro units and thermal units are the main conventional generation units, which are generally represented by a 2-state Markov model as shown in Figure 2.3 (a). Such units are either fully available (Up) or completely out of service (Down). In Figure 2.3 (a), λ and μ are the unit failure rate and the unit repair rate, respectively. These units are modelled in terms of probability of a generating unit being in a forced outage state, which is known as the forced outage rate (FOR) or unavailability (U) of the generating unit.

$$FOR = \frac{\sum \text{forced outage time}}{\text{Total operating time}} \tag{2.2}$$

Some types of generating units may be forced to operate at reduced capacity for significant amount of time [1]. Such units can be modelled by a multistate Markov model. Figure 2.3 (b) shows a generating unit represented by a 3-state Markov model. The transition rates between the different states are also shown in the figure.

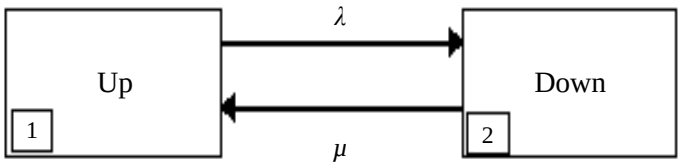

(a)

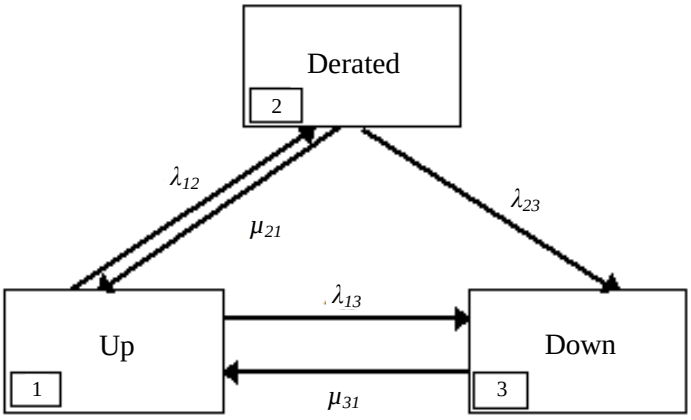

(b)

Figure 2.3: Conventional generating unit Markov models (a) 2-state model; (b) 3-state model.

This section illustrates the method to create a generation model using an example power system that has four conventional generating units as shown in Table 2.1. The units #1, #2 and #3 have rated capacities of 110 MW, 42 MW and 34 MW, and FOR of 8.6%, 1.5% and 1% respectively. These units are modelled as 2-state generating units. The unit #4 is a hydro unit modelled as 3-state generating unit. The total system conventional generating capacity is 241 MW.

A recursive algorithm [1] is used to combine the generating unit models shown in Table 2.1 to build the total generation model for the power system. The algorithm combines the generating unit models one at a time to create overall system model, which is shown in Table 2.2.

Table 2.1: Conventional generating unit models

Unit #	Type	Rated capacity (MW)	FOR	Derated capacity (MW)	Derated state probability
1	Thermal	110	0.086	-	-
2	Hydro	42	0.015	-	-
3	Hydro	34	0.010	-	-
4	Hydro	55	0.030	35	0.270

The cumulative probability of a specific capacity outage state of *Y*, after a unit with a rated capacity of *C* and forced outage rate *FOR* is added is found as,

$$P(Y) = (1 - FOR)P'(Y) + (FOR)P'(Y - C) \tag{2.3}$$

In (2.3), *P'(Y)* and *P(Y)* represent the cumulative probabilities of the capacity outage state of *Y* before and after the addition of the unit. Equation (2.3) is initialized by setting *P'(Y)* = 1.0 for *Y* ≤ 0 and *P'(Y)* = 0 otherwise.

To include multistate generating unit models, (2.3) can be modified as,

$$P(Y) = \sum_{i=1}^{n} p_i P'(Y - C_i) \tag{2.4}$$

Where, *n* is the number of capacity states, C_i is capacity outage of the *i*th state for the added unit and p_i is the probability of the *i*th capacity state. Equation (2.4) reduces to (2.3) if *n* = 2.

The first column in Table 2.2 shows the capacity outage states of the total generation system and the second column shows the corresponding probabilities of occurrence.

Table 2.2: Total conventional generation model

Capacity out (MW)	Probability
0.00	0.62390097
20.00	0.24064752
34.00	0.00630203

Table 2.2 (Continued): Total conventional generation model

Capacity out (MW)	Probability
42.00	0.00950103
54.00	0.00243078
55.00	0.02673861
62.00	0.00366468
76.00	0.00009597
89.00	0.00027009
96.00	0.00003702
97.00	0.00040719
110.00	0.05870403
130.00	0.02264298
131.00	0.00000411
144.00	0.00059297
152.00	0.00089397
164.00	0.00022872
165.00	0.00251589
172.00	0.00034482
186.00	0.00000903
199.00	0.00002541
206.00	0.00000348
207.00	0.00003831
241.00	0.00000039

2.2.2 Wind power modelling

Historical wind speed data for a large number of years must be obtained for the wind sites in order to develop accurate wind models for reliability evaluation of wind integrated power systems. For the studies in the subsequent chapters, the wind farms connected to the power system were assumed to be located at various locations in Saskatchewan, Canada with different wind regimes. For the wind farm locations, several years of hourly wind speed data was obtained from Environment Canada [45]. In general, past wind speed data is accessible at an anemometer height of 10 m [46] for weather stations. However, the hub height of a wind turbine is typically between 60 m and 80 m. Therefore, the wind speed values are scaled to the hub height of the

wind turbine. Reference [47] uses a logarithmic velocity profile assuming the atmosphere to be adiabatic, which is shown in (2.5).

$$\overline{u_x}(h_h) = \frac{u_*}{K} \ln \frac{h_h}{z_0} \tag{2.5}$$

Where, $u_* = \dfrac{K}{\ln \dfrac{h_h}{z_0}} \overline{u_x}(h_r)$

h_h = hub height in m

h_r = reference height which is 10 m

z_0 = surface roughness length

K = von Karman constant ~ 0.4

The surface roughness length is approximately 0.03 m for the airport sites [48].

The output power of a WTG is dependent on wind speed of the site at the time, forced outage rate (FOR) and the characteristics of the wind turbine. The output power of a WTG can be calculated for a given wind speed using (2.6) [21].

$$P(v) = \begin{cases} 0, & 0 \le v < V_{ci} \\ (A + Bv + Cv^2)\mathrm{P_r}, & V_{ci} \le v < V_r \\ P_r, & V_r \le v < V_{co} \\ 0, & v \ge V_{co} \end{cases} \tag{2.6}$$

Where, P_r is the rated capacity of the WTG, and the constants A, B and C depend on the values of V_{ci}, V_r and V_{co} [21]. The cut-in speed, V_{ci} is the minimum speed at which the wind turbine blades overcome friction and start rotating. The rated speed, V_r is the minimum wind speed at which the wind turbine generates its rated power. The cut-out speed, V_{co} is the speed at which the wind turbine blades are brought to rest to prevent damage due to high wind speeds. Equation

(2.6) is shown graphically in Figure 2.4, and is known as the wind power curve. The V_{ci}, V_r and V_{co} of 15 km/h, 50 km/h, and 90 km/h respectively were used in the subsequent studies.

The impact of the forced outage rate of WTGs in a wind farm can also be included while developing the wind power model. However, studies conducted in [49] have shown that the FOR of a WTG have little impact and can be neglected during the adequacy assessment of a wind integrated power system. Hence, to simplify the wind model the FOR of the WTG has been excluded in subsequent studies. Adequacy evaluation of power systems is generally conducted using hourly time resolution. Hourly average wind speed data obtained from Environment Canada [45] is therefore used in the evaluation. It is assumed that all the WTGs in a wind farm experience the same wind speed for a particular hour of the year.

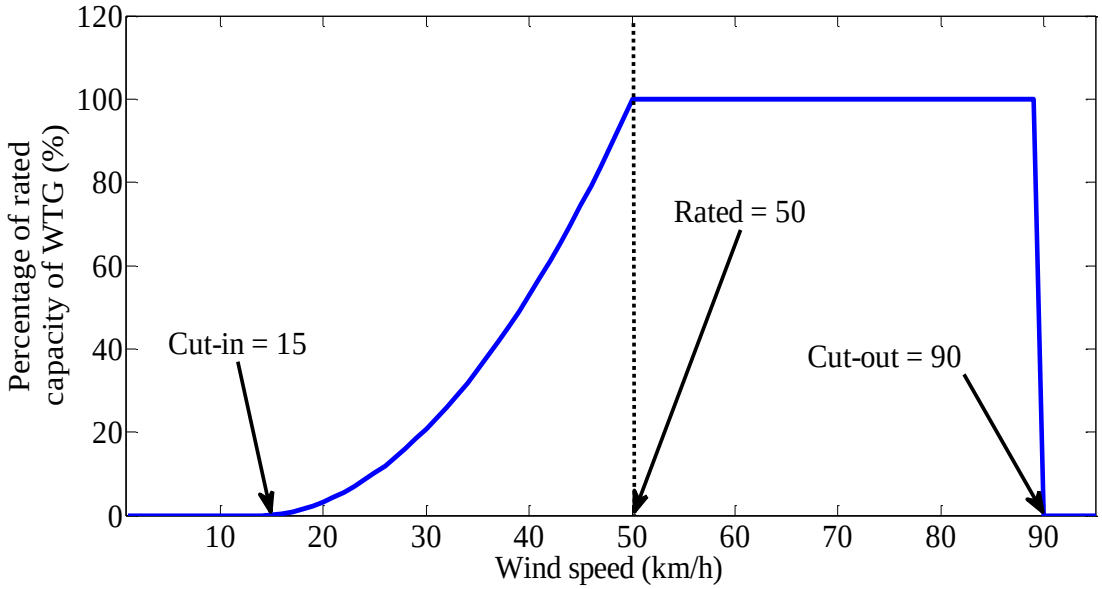

Figure 2.4: Wind turbine generator power curve

2.2.3 Load modelling and incorporation of wind power as negative load

The system load characteristic is represented as a Load Duration Curve (LDC) in this thesis. The LDC is built by collecting the hourly average loads over a period of time and sorting them in descending order of magnitude. Wind power, if present in the power system, was included in the reliability evaluation by considering it as a negative load. The hourly wind power output was subtracted from the corresponding hourly load value to obtain the modified system load for that particular hour. A cumulative load model is formed, by ordering the modified hourly system load for a particular time period in a descending order. The load model subsequently obtained shows the load levels and also the time duration of occurrence of the load levels in a specific time period. The negative load approach of modelling the wind resource is also used for wind energy utilization assessment in the subsequent chapters. Table 2.3 shows the hourly peak load, the hourly wind power output and the modified hourly load for a ten hour period using the hypothetical power system described previously. The system peak load is assumed to be 131 MW and a wind farm with a rated capacity of 18 MW is connected to the power system.

Table 2.3: Hourly wind power, hourly load and modified load of the example power system

Hour	Load (MW)	Wind power output (MW)	Modified load (MW)
0	87	5	82
1	116	15	101
2	47	8	39
3	70	10	60
4	36	12	24
5	96	13	83
6	74	2	72
7	58	7	51
8	109	4	105
9	122	9	113
10	73	3	70
11	102	6	96

Table 2.4 shows the modified hourly peak loads arranged in descending order, after incorporating the hourly wind power outputs as negative loads. The time period is 12 hours. The total number of hours in the 12 hour period that each load level is exceeded is then evaluated, and the normalized values are shown in column 4. Figure 2.5 shows the LDC, which is created from the load levels arranged in descending order. The load levels in the LDC are normalized with respect to the maximum modified load value, and are shown in column 3.

Table 2.4: Modified hourly loads arranged in descending order

Hour	Modified load (MW)	Modified load (p.u.)	Duration (p.u.)
9	113	1.0000	0.0000
8	105	0.9292	0.0909
1	101	0.8938	0.1818
11	96	0.8495	0.2727
5	83	0.7345	0.3636
0	82	0.7256	0.4545
6	72	0.6371	0.5455
10	70	0.6194	0.6364
3	60	0.5309	0.7273
7	51	0.4513	0.8182
2	39	0.3451	0.9091
4	24	0.2123	1.0000

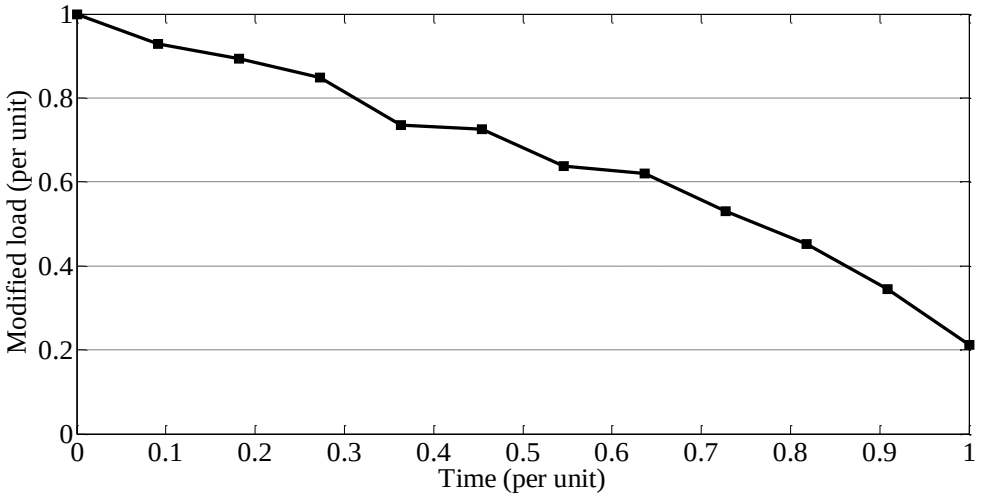

Figure 2.5: Per unit LDC for the test power system

2.2.4 Risk indices

In order to estimate the system risk indices, the total conventional generation model in Table 2.2 was combined with the load model in Table 2.4. A loss of load situation can take place if the available generating capacity is not able to meet the load demand. A commonly used reliability index is the Loss of Load Expectation (LOLE) [1] which shows the expected amount of time during which a loss of load takes place in the power system. The LOLE is shown in hours/period, when the load model is the LDC. Here, 'period' refers to the total time period covered by the LDC. For the system used in this chapter, this is 12 hours. The combination of the generation model with the load model in order to estimate the LOLE is shown in Figure 2.6. The reserve capacity, installed capacity and the different capacity levels of the generation model and load model are shown in the figure. Figure 2.6 shows that load curtailment takes place whenever there is a capacity outage greater than the reserve. For instance, the load cannot be supplied for time period t_k due to a capacity outage of CO_k. The system LOLE is evaluated using (2.7).

$$LOLE = \sum_{i=1}^{n} p_i \times t_i \tag{2.7}$$

Where,

n: number of capacity outage states in the generation model

p_i: probability of the capacity outage CO_i

t_i: duration of outage for which loss of load occurs during outage CO_i

A widely used metric in generation adequacy assessment is the loss of load expectation of one day in ten years or 0.1 days/year [2]. This reliability criterion has also been used in several NERC reliability studies. References [2, 50] also show a range of indices used by Canadian electric power utilities for HL I adequacy assessment. Most of the Canadian utilities use days/year LOLE criteria which are 0.1 days/pear and 0.2 days/year. Hydro Quebec uses an

hours/year LOLE criterion which is 2.4 hours/year. The LOLE for the example system with 241 MW of conventional capacity, an 18 MW wind farm and a system peak load of 131 MW is computed by using the generation model in Table 2.2, the load model in Table 2.4 and Eq. (2.7). The system LOLE value is found to be 0.2857 hrs/period.

Another widely used risk index for a power system is the Loss of Energy Expectation (LOEE). LOEE is the total expected amount of energy curtailed due to the system outages considering the evaluation period. The total energy demand is represented by the area under the LDC. The energy not supplied due to outage CO_i is represented by the area E_i in Figure 2.6. The LOEE is computed using (2.8).

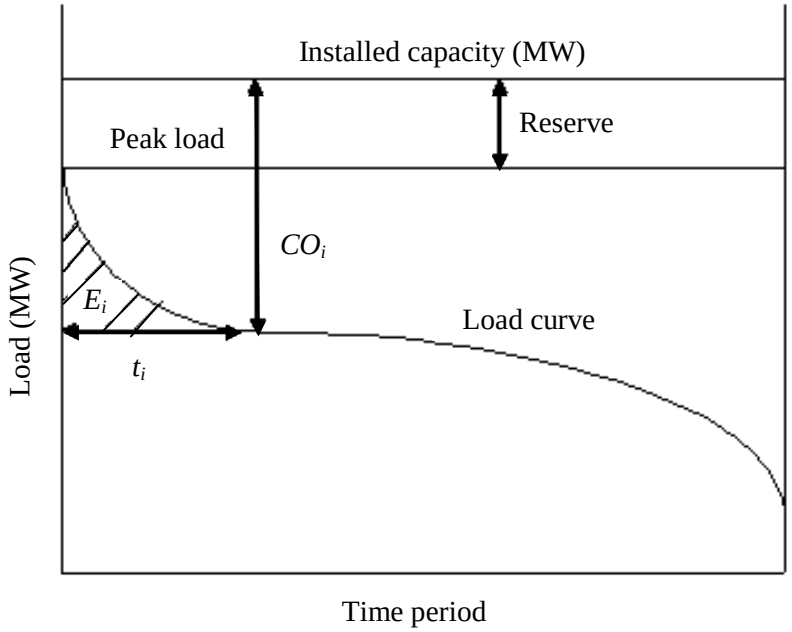

Figure 2.6: Calculation of risk indices using the generation and load model

$$LOEE = \sum_{i=1}^{n} p_i \times E_i \tag{2.8}$$

It is difficult to compare the reliability of systems of different sizes using the LOEE index as the LOEE of the large system will be greater than that of the small system. Therefore, LOEE can be normalized by the total energy demand of the system or the system peak to obtain reliability indices which can be utilized to compare various power systems. The units per million (UPM) index is obtained when the LOEE index is normalized by the annual energy demand. The resulting small number is multiplied by one million as shown in (2.9).

$$UPM = \frac{\text{LOEE}}{\text{Annual energy demand}} \times 10^6 \tag{2.9}$$

The Saskatchewan Power Corporation utilizes a reliability criterion of 200 UPM [2] and has also increased it further to 350 UPM for HL I adequacy assessment.

Another reliability index which can be derived from LOEE is system minutes (SM), and is used by Ontario Hydro [2]. This is obtained by normalizing the LOEE by the system annual peak load as shown in (2.10).

$$SM = \frac{\text{LOEE}}{\text{Annual peak load}} \times 60 \tag{2.10}$$

The load model shown in Table 2.4 can also be used to evaluate the LOLE values at different peak load values for the example power system. In Figure 2.7, the LOLE values for different values of peak load are shown. The generation facilities are normally planned such that a specific risk criterion is always met for the system peak load. The assessment of the peak load which a planned or existing generation can carry while maintaining the risk criterion, is an important part of the planning process. The peak load carrying capability (PLCC) of a power system is the maximum peak load the power system can serve without violating the pre-defined risk criterion. The LOLE, UPM and SM based risk criteria used by different utility companies has been discussed in [2, 50].

In general, system planners are interested to know the capacity worth of wind farm addition to the power system. The Capacity Credit (CC) of a wind farm is an index which can be used to evaluate the capacity worth of a wind farm. CC is the increase in PLCC taking place in the power system when a wind resource is added to it. The LOLE and PLCC values of the test power system with and without the wind resource are shown in Figure 2.7. Considering a LOLE risk criterion of 1 hr/period, the PLCC values with and without the addition of a wind resource are represented as $PLCC_2$ and $PLCC_1$, respectively. As shown in Figure 2.7, the increase in PLCC (IPLCC) due to the addition of the wind resource to the example power system is ($PLCC_2$ – $PLCC_1$).

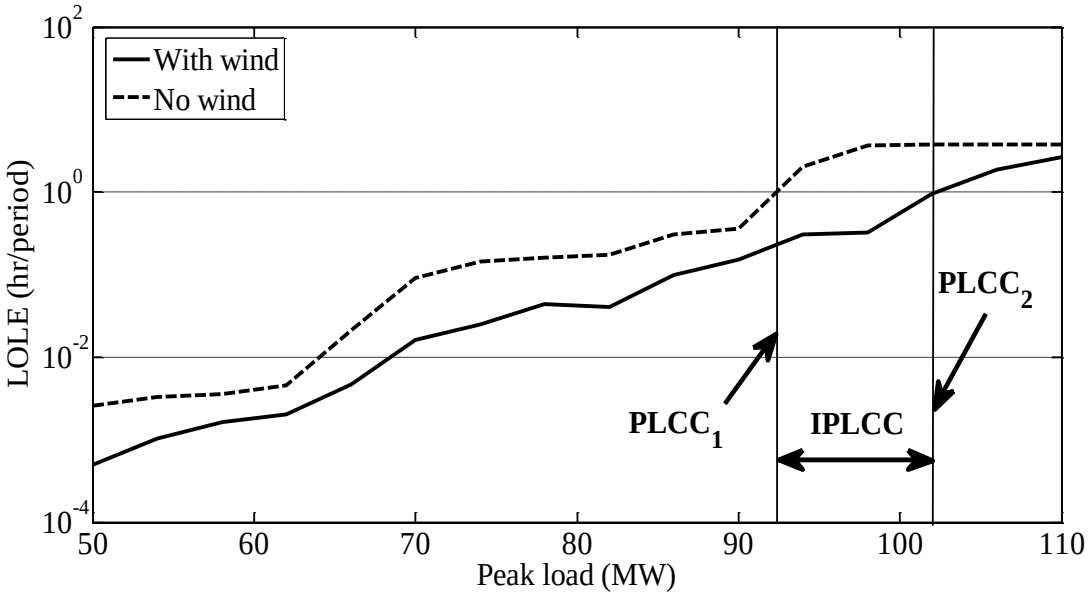

Figure 2.7: System PLCC and LOLE with and without wind energy

2.3 Bulk system adequacy evaluation

Bulk system reliability evaluation is involved with the assessment of the ability of both the generation and the transmission system to generate and transport electrical energy to the system load points. This evaluation is also known as composite system reliability assessment. Figure 2.8 shows a basic wind-integrated bulk power system model. This model differs from the HL I model in a number of ways, as shown in Table 2.5. The power system consists of generator buses, load buses, conventional generators and wind farms. The conventional generating units and the wind farms are located at different locations in the power system network. The conventional generation modelling, wind power modelling, and load modelling are carried out in a similar manner as described in Section 2.2.

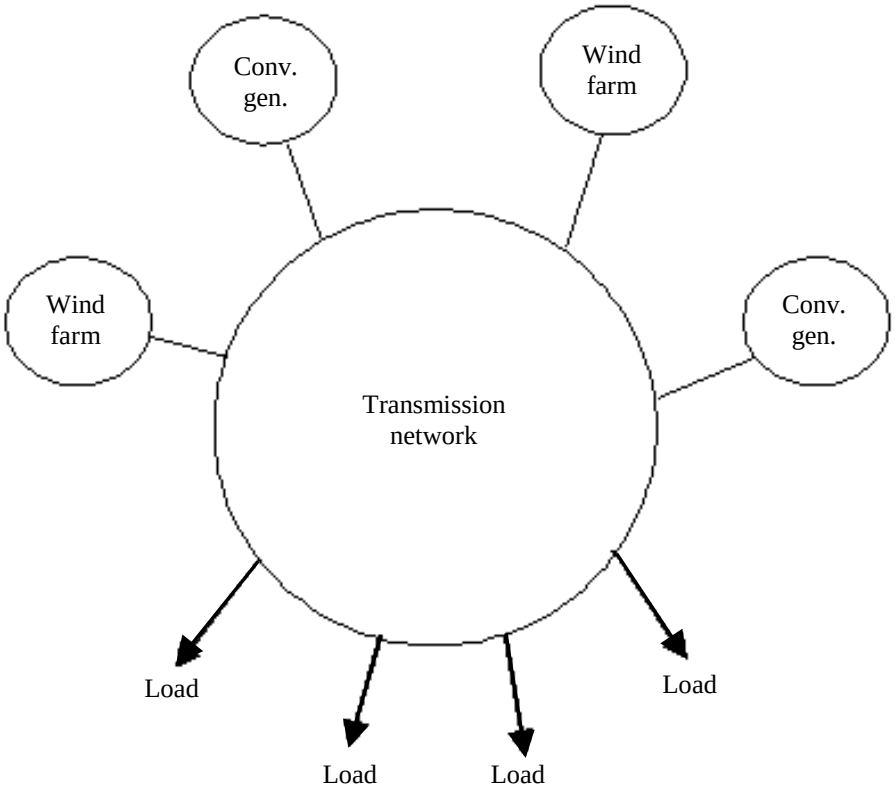

Figure 2.8: Wind-integrated power system model for bulk system adequacy assessment

Table 2.5: Differences between system models for HL I and HL II adequacy assessment

HL I model	HL II model
1. Does not include transmission line modeling.	1. Transmission line constraints are considered, and are a part of the system modeling.
2. All the system generation are lumped together to create an overall generation model.	2. There are multiple generation models, dispersed at different locations in the bulk power system.
3. A single LDC is used for the adequacy assessment, which is modified by including the entire wind resource as a negative load.	3. The system loads at different load buses use different modified LDCs depending on the presence or absence of a wind farm at the bus.

In HL II analysis, the impact of the transmission line constraints and the locational impacts of generating resources and the load points are considered. The reliability level at each load point in the power system is evaluated, and these reliability indices are finally aggregated to find the overall reliability level of the power system. It has been discussed in Sections 1.1 and 1.2 that both analytical and MCS techniques [18-22, 27] can be used for HL II adequacy assessment. A Monte Carlo based bulk power system reliability evaluation tool called MECORE [9, 51] was available for the HL II studies. Monte Carlo Simulation can include more complexity in the power system since it actually simulates the system operation and evaluates the reliability indices. This approach has been used for the subsequent HL II studies. The two basic MCS techniques used in power system reliability evaluation are: sequential and non-sequential Monte Carlo Simulation.

2.3.1 Sequential MCS

The sequential simulation technique simulates the operating and failure mode cycles of all the components and a system operating cycle is obtained by combining all the component cycles.

In this approach, the probability distributions of times to failure and repair are used to simulate operating and failure component state durations in time chronology. The technique includes chronological load models in specific time intervals. The procedure can be described by the following steps [52]:

1. The initial state of each component is defined.

2. The distribution functions of the component repair and failure rates and the inverse transform technique [53] are used to sample the duration of each component residing in its present state. For instance, if the times to failure is described by an exponential distribution function, $f(t) = \lambda e^{-\lambda t}$, then for the operating state duration (T) the sampling value is,

$$T_k = -\frac{1}{\lambda_k} \ln U_k \tag{2.11}$$

In (2.11), U_k is a uniformly distributed random number between [0, 1] referring to the kth component and λ_k is the failure rate of the kth component.

3. Step 2 is repeated for a specific time period, which is normally one year (8760 hours). A sequential set of operating and failure states is subsequently built for every component for a specific time period.

4. Subsequently the process simulated in steps 1 to 3 is analyzed for time interval of the simulation period to determine the overall system performance.

5. Finally, reliability indices are computed and updated after the simulation is complete for every year.

6. Steps 1 to 5 are repeated updating the indices until a specific convergence criterion is met.

This method can be used to obtain both the frequency and the duration indices. The main advantage of this method is that dependent events which are related in time chronology can be easily modelled. Another feature of this technique is that different state duration distributions can

be incorporated. However, since the generation and storage of information regarding the sequential state transition processes of all the system components is an essential requirement, the storage and computation time requirements of this technique are higher than that of the non sequential approach.

2.3.2 Non-sequential MCS

In the non-sequential MCS, the state of the system is obtained by sampling all component states without maintaining the chronology of the events. The non-sequential MCS consists of two approaches: state sampling approach and the state transition sampling approach.

2.3.2.1 State sampling approach

The fundamental sampling procedure is carried out by assuming that the behaviour of every component can be designated by a uniform distribution between [0, 1]. A two-state or multi-state model can be used to represent a component. For a two-state component, each component has the two states which are failure and success. In this case, component failures are independent events. A vector S can be used to represent the system state consisting of n components which include generators, lines and transformers. Here, $S = (S_1, \ldots, S_k, \ldots, S_n)$, S_k is the state of the kth component. The system is in the normal state when S is zero; or else the system is in a contingency state occurring due to the outage of components. The process can be described by the following steps:

1. A uniform random number, U_k is generated for the kth component.

2. The state of the kth component is found using (2.12):

$$S_k = \begin{cases} 0 \ \text{(Normal state)} & \text{if } U_k \geq FOR_k \\ 1 \ \text{(Outage state)} & \text{if } U_k < FOR_k \end{cases} \tag{2.12}$$

Where, FOR_k is the forced outage rate of the *k*th component.

3. Step 2 is applied to all the components to determine the operating state *S*.

4. Determine the operating state of the entire system from the operating states of all the system components.

5. If the system state is a normal state, then load curtailment does not occur. If the system state is a contingency state, then load curtailment may be needed. A DC load flow technique is used to compute the transmission line power flows.

6. A linear programming optimization model is utilized to reschedule generation, reduce line overloads and to avoid load curtailment if possible or to minimize the total load curtailment if unavoidable [51].

7. By repeating steps 1 to 6, for every load point the reliability indices are computed until a stopping criterion is reached.

The main advantage of the system state sampling technique is that multi-state components can be included in the analysis without a substantial increase in the computation time. Equation (2.13) shows the probabilities of the *k*th component considering one derated state. Similar to step 2, the state of the *k*th component is found using (2.13):

$$S_k = \begin{cases} 0 \ \text{(Normal state)} \ \text{if} \ U_k \geq PD_k + FOR_k \\ 1 \ \text{(Derated state)} \ \text{if} \ FOR_k \leq U_k < PD_k + FOR_k \\ 2 \ \text{(Outage state)} \ \text{if} \ U_k < FOR_k \end{cases} \quad (2.13)$$

Where, PD_k is the probability of the derated state for the *k*th component. If additional derated states are present, they can be simulated in a similar manner.

2.3.2.2 State transition sampling approach

This approach considers the state transitions of the system, instead of the component states. It is assumed that all state residence times are exponentially distributed and state transition of

any component leads to the state transition of the system. The procedure can be described by the following steps:

1. Start the simulation process from the system state where all the system components are available.

2. Use the minimization model of load curtailment to evaluate the adequacy of the system state if it is a contingency state in which at least one component is in the outage state. Or else, do not use the minimization model and proceed to the subsequent step.

3. Generate uniformly distributed random numbers to deduce the next system state by using the process of state transition sampling. This process directly creates a system state transition sequence, which can be used to compute both the load point and system frequency indices.

4. Steps 2 to 3 are repeated until an appropriate convergence criterion is fulfilled.

Exact frequency indices can be evaluated using the state transition sampling approach without sampling the distribution function and storing chronological information. However, this approach can only be utilized for exponentially distributed component state durations, which is a major limitation. As compared to the state sampling approach, this technique is also computationally less efficient.

2.3.3 Risk indices

The basic indices to evaluate the adequacy of a generating system are the LOLE, LOEE, PLCC and capacity credit as described in Section 2.2. The risk indices used for HL I adequacy assessment can be extended to composite system adequacy assessment. Monte Carlo simulation based techniques can be utilized to compute these indices. However, both system indices and load point indices are required to carry out a complete bulk system assessment. The bulk power

system reliability indices can be either annualized or annual values. Annualized risk indices can be computed using a single load level for the entire year and the system peak load is also used in the analysis. However, the actual chronological annual load values are used for the evaluation of the annual adequacy indices. The basic bulk system adequacy indices are described as follows.

(1) Probability of load curtailment (PLC)

$$PLC = \sum_{i \in SS} P_i \tag{2.14}$$

Where the probability of the system state i is given by P_i and SS represents the group of system states linked with load curtailments.

(2) Expected duration of load curtailment (EDLC)

$$EDLC = PLC \times 8760 \text{ hr/yr.} \tag{2.15}$$

(3) Expected energy not supplied (EENS)

$$EENS = \sum_{i \in SS} 8760 C_i P_i \tag{2.16}$$

In (2.16), the load curtailment associated with system state i is given by C_i.

MCS based techniques are capable of evaluating the reliability indices both for the entire power system and individual load points. For example, the overall EDLC of a power system, $EDLC_{system}$ is found as,

$$EDLC_{system} = \sum_{i=1}^{LP} EDLC_i \tag{2.17}$$

Where, LP is the number of load points in the power system and the EDLC for an individual load point is represented by $EDLC_i$. The LOLP, LOLE and LOEE utilized for generation reliability studies are similar to the PLC, EDLC and EENS indices, respectively evaluated for HL II

adequacy assessment. The PLCC and the capacity credit in a wind-integrated power system can be estimated using the EDLC index using the procedure described in Section 2.2.4.

2.3.4 The MECORE software

The MECORE software is a Monte Carlo based bulk power system reliability evaluation tool capable of performing reliability assessment of the electric power system. After preliminary development at the University of Saskatchewan, the software was developed further at BC Hydro [9, 51].

The software can be used to evaluate the generation reliability in a composite system, transmission reliability in a composite system and the composite generation and transmission reliability. Various reliability indices can be estimated both for the overall power system and for every load point separately. MECORE was built by using the state sampling MCS technique and enumeration techniques. The simulation of the components states in the system and calculation of annualized indices using a peak load value is carried out using the state sampling technique. Annual indices using the annual LDC are estimated by using a hybrid enumeration technique [51]. MECORE can be used to conduct reliability studies for power systems with up to 1000 buses and 2000 branches.

Multi-state random variables are used for modeling the generating units. The MECORE program can recognize up to ten derated states to incorporate multistate renewable energy models in the reliability analysis. Two-state models are used to represent the transmission lines. In order to change generation patterns, reduce line overloads and to reduce load curtailments, DC load flow and linear programming Optimal Power Flow models are used by the software.

A brief description of the capabilities of MECORE is as follows [9]:

I. Failure modes:

- Independent failures of generators, lines and transformers
- Transmission line common mode outages
- Derated states of generating units

II. Failure criteria:

- Capacity deficiency
- Line overload
- Load loss due to system separation
- Bus isolation-load loss

III. Load model:

- Annual and seasonal load models
- Multi-step models

IV. Probability indices:

- Load bus and system indices
- Annual and annualized indices

The basic HL II reliability indices discussed in Section 2.3.3 can be evaluated for individual load points and the overall power system using MECORE. This program can also be used in HL I studies, by assuming the transmission lines in the system to be 100% reliable.

2.4 Conclusions

In this chapter, the basic concepts for reliability evaluation of a wind integrated power system were introduced. The chapter describes the process of modelling the system load,

conventional generation and the wind generation. In order to explain the different concepts and the procedure of reliability and wind energy utilization assessment, a small power system with four conventional generating units and one wind farm was considered. The wind resource was modelled as a negative load and a modified system load model was created. By using a simple wind integrated power system model, the basic concepts and reliability evaluation techniques were clearly explained, and would be applied to larger and realistic power systems in the subsequent chapters. The essential concepts required to conduct Monte Carlo simulations and obtain the reliability indices of a bulk power system were also discussed in this chapter.

3 WIND POWER ABSORPTION CAPABILITY ASSESSMENT IN A POWER SYSTEM

3.1 Introduction

Wind power penetration has been rapidly increasing in electric power systems throughout the world as mentioned earlier. At high wind scenarios, spillage of wind energy can occasionally occur as discussed in Section 1.3. Wind energy spillage due to wind curtailment will have a significant impact on the benefits from wind power, including the contribution to system reliability. Hence, accurate wind models are required to include wind energy curtailment in the reliability modelling.

The importance of considering factors such as the system load level, priority loading order of the generating unit and the ramping capabilities of the generating units to develop such accurate wind models was discussed in Section 1.3. This chapter presents an analytical method to determine the wind power absorption capability of a wind-integrated power system. Wind curtailment scenarios in different operating conditions have been analyzed by considering typical unit types and operating characteristic of the conventional generating units in their priority loading order. Finally, a realistic power system is analyzed in order to assess the amount of wind power that can be absorbed during different load scenarios considering the standard operating practices and operating data related to the stability of the scheduled generating units.

3.2 Proposed technique to assess the wind power absorption capability of a power system

This section presents the analysis to assess the amount of wind power that can be absorbed by a power system during different loading scenarios considering different types of generating units. The data on the types of power plants, the parameters of the individual generating units, such as the FOR, the Maximum Continuous Rating (MCR), the minimum capacities and the

ramp rates are required for the analysis. The typical conventional generating plants in a power system are coal, hydro and natural gas plants. Many systems also have a number of generating units designated as “must use” units that will be operated at all times. A number of generating units are scheduled to supply the load at a given operating condition, such that the total scheduled capacity exceeds the load by a capacity margin also known as the spinning reserve. The operating margin is conventionally determined using the N-1 criterion [1].

A methodology is developed in this research work to assess the amount of wind power that can be absorbed by the system in a particular state. The method is then utilized to evaluate the wind absorption capability of the system in all possible system operating states and the result is aggregated using a probability expectation technique as described in the following sub-sections.

3.2.1 Wind power absorption capability assessment for a system operating state

The total operating capacity *Cop* must be equal to the load level *L* as shown in (3.1), and the spinning reserve is shared by a number of the scheduled units.

$$L = \sum_{i=1}^{N} Cop_i \tag{3.1}$$

Where, *N* is the number of scheduled generating units in the operating condition.

The maximum spinning reserve on any unit is limited by its minimum capacity. The spinning reserve R_i of the *i*th scheduled unit with MCR C_i and minimum capacity $Cmin_i$ is given by (3.2).

$$R_i = C_i - Cop_i \tag{3.2}$$

Where $Cop_i \geq Cmin_i$, and Cop_i is the operating capacity the *i*th unit.

The total power generated by the scheduled generating units must be equal to the load at all times as mentioned above. If wind power becomes available during the above operating

condition, the conventional units must ramp down within an acceptable response time in order to utilize the wind power. The maximum ramp down capacity $RMP_{max,i}$ of the ith unit in the response time T, in minutes is given by (3.3).

$$RMP_{\max,i} = \begin{cases} RR_i * T, & (Cop_i - RR_i * T) \geq C\min_i \\ Cop_i - C\min_i, & (Cop_i - RR_i * T) < C\min_i \end{cases} \quad (3.3)$$

Where, RR_i is the ramp rate of ith unit in MW per minute.

The total maximum ramp down capacity RMP_{max} for the selected system operating state is given by (3.4), and is equal to the maximum wind power that can be absorbed during the operating state.

$$RMP_{\max} = \sum_{i=1}^{N} RMP_{\max,i} \quad (3.4)$$

The system can therefore, absorb a maximum wind capacity of RMP_{max} during this generation schedule. The maximum wind power that can be absorbed by the generation schedule is expressed in percentage of the load served in (3.5), and is designated as the wind power absorption capability (WPAC) in this chapter.

$$WPAC = \frac{RMP_{\max}}{L} \times 100 \quad (3.5)$$

3.2.2 Wind power absorption capability at different operating conditions

Section 3.2.1 described a technique to evaluate the WPAC of a particular generation schedule. This section presents a procedure for conducting WPAC studies for different possible operating conditions for a power system. The system load varies throughout the year, and there will be a number of different generation schedules in a year to satisfy the system demand between the minimum and the maximum load levels. Figure 3.1 illustrates the process to determine all possible generation schedules or operating conditions for a power system.

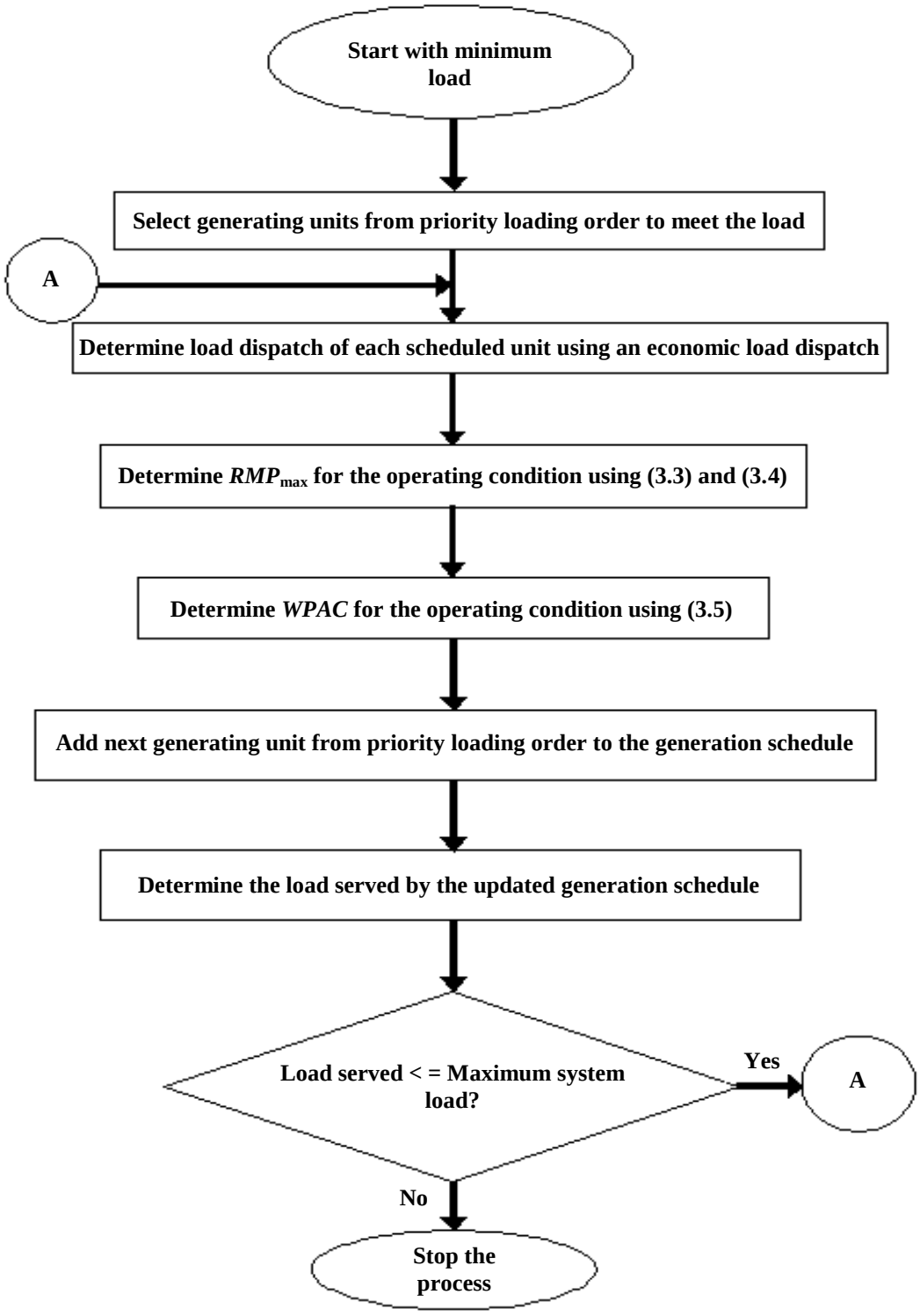

Figure 3.1: Flowchart of the proposed technique to determine WPAC for different system operating conditions

Starting with the minimum power system load, the generating units from the priority loading order are selected based on the unit commitment criteria to meet this load. The "*N*-1" criterion has been widely used to determine the operating reserve requirement in the generation schedule. Probabilistic criteria, such as the unit commitment risk have been published [54] and receive increasing attention in recent years. The load dispatch of each scheduled generating unit is then determined using an economic load dispatch. Probabilistic methods to determine risk based load dispatch [54] are also described in literature [55]. The maximum ramp down capacity of the conventional scheduled units can be determined using Equations (3.3) and (3.4) and the WPAC for the operating condition can then be evaluated using Equation (3.5). The generating units from the priority loading order are sequentially added, one at a time, to the generation schedule, and the load served by the resulting generation schedule is determined for each schedule. The aforementioned procedure is repeated as shown in Figure 3.1 to calculate the WPAC for each generation schedule. The procedure of adding units by priority loading order is continued until the load served for a generation schedule reaches the system peak load value.

The large number of WPAC values corresponding to the different operating conditions to meet the varying load levels adds significant complexity to the reliability modeling process and the evaluation method. The number can be reduced by grouping the load levels into *n* intervals. For example, if *n* is reduced to 2, only two intervals are considered: the low load and the high load interval. The $WPAC_{\text{int}}$ for each interval is calculated using (3.6).

$$WPAC_{\text{int}} = \sum_{i=1}^{m} WPAC_i * P_i \tag{3.6}$$

Where, $WPAC_i$ is the wind power absorption capability in the *i*th generation schedule within the interval, P_i is the probability of the load being at the level for the *i*th generation schedule, and *m* is the number of different operating conditions within the load interval.

3.3 Application of the proposed method

The proposed wind model that incorporates wind energy curtailment, and the method to evaluate the adequacy and energy indices in a wind-integrated power system is illustrated on a practical large-scale power system.

The total generation capacity of the power system is 4134 MW, and the system generation data is shown in Table 3.1. The generating plants include coal, hydro, biomass, combined cycle gas turbine (CCGT), simple cycle gas turbine (SCGT) and wind power. Data on the generating unit forced outage rate (FOR), priority loading order, maximum and the minimum capacities were obtained from actual industry data, and are also shown in the table. Table 3.2 shows the generating unit ramp rate data obtained from industry experience and references [37, 38]. The annual peak load and minimum load of the system are 3700 MW and 1787 MW respectively.

Table 3.1: System generation data

Unit type	Unit name	Priority order	FOR (%)	MCR (MW)	Minimum capacity (MW)
Coal	C1	Base load plant	6.12	291	160
	C2		11.12	291	166
	C3		8.56	110	110
	C4		9.08	139	80
	C5		6.14	139	80
	C6		3.54	284	181
	C7		6.89	276	180
Hydro	H1	11	0.58	62	0
	H2	12	6.91	62	0
	H3	13	0.29	62	0
	H4	Base load plant	0.55	34	25 MW from one unit
	H5		1.61	34	
	H6		0.64	34	
	H7		1.14	34	
	H8		1.04	34	
	H9		1.72	34	
	H10		1.47	42	
	H11		0.30	42	

Table 3.1 (Continued): System generation data

Unit type	Unit name	Priority order	FOR (%)	MCR (MW)	Minimum capacity (MW)
Hydro	H12	Base load plant	0.18	14	14
	H13		0.14	14	14
	H14		2.10	14	14
	H15		1.38	14	14
	H16		0.14	15	15
	H17		0.20	15	15
	H18		0.10	15	15
	H19	14	0.05	85	0
	H20	15	0.09	85	0
	H21	16	0.13	85	0
	H22	Base load plant	1.77	23	15
	H23		2.50	50	50
CCGT	CC1	1	4.50	260	162.9
	CC2	2	3.00	228	165.4
	CC3	Base load plant	6.00	246	80
	CC4	3	5.18	312	151
	CC5 (1)	4	2.63	38	17
	CC5 (2)	5	2.03	38	17
	CC5 (3)	7	3.26	38	17
	CC5 (4)	8	1.57	38	17
	CC5 (5)	9	1.23	38	17
	CC5 (6)	10	1.39	38	17
	CC5 (7) (Steam)	6	4.50	60	20
	CC6 (Steam)	26	4.68	95	57
SCGT	SC1	17	2.40	46	25
	SC2	18	2.40	46	25
	SC3	19	2.40	46	25
	SC4	20	2.40	46	25
	SC5	21	2.40	46	25
	SC6	22	2.20	43	25
	SC7	23	2.20	43	25
	SC8	24	33.31	44	20
	SC9	25	16.94	79	20

Table 3.2: Generating unit ramp rate data

Unit	Ramp rate (%/min)
Hydro	35
Gas	10
Coal	2
Steam	3

The methodology for computing the WPAC of a power system for different power system operating conditions is presented in Section 3.2. The process is started from the minimum power system load of 1787 MW. A total operating reserve of 374 MW is considered to account for the loss of the largest unit of 291 MW (C1) and a regulation margin requirement of 83 MW. Table 3.3 shows the generation schedule when the system load is 2047 MW. Certain generating units or capacity must be operated at all times, and are the "must use" units, which are represented as MU1-6. The maximum ramp down capacity $RMP_{\max,i}$ of each generating unit in the generation schedule for the different response times are evaluated using (3.3), and are shown in Table 3.3. The maximum wind power that can be absorbed by this generation schedule is evaluated using (3.4) and the corresponding WPAC is evaluated using (3.5). The WPAC values were calculated for 15, 10 and 5 minutes response times, and are shown in Table 3.4.

Table 3.3: Generation schedule for the system load of 2047 MW

Type	Unit Name	$RMP_{\max,i}$ (MW)		
		15 min	10 min	5 min
Must Use	MU1	0	0	0
	MU2	0	0	0
	MU3-6	2	2	2
Coal	C1	87.3	58.2	29.1
	C3	0	0	0
	C4	41.7	27.8	13.9
	C5	41.7	27.8	13.9
	C6	85.2	56.8	28.4
	C7	82.8	55.2	27.6

Table 3.3 (Continued): Generation schedule for the system load of 2047 MW

Type	Unit Name	$RMP_{max,i}$ (MW)		
		15 min	10 min	5 min
Hydro	H9	9	9	9
	H12-15	0	0	0
	H16-18	0	0	0
	H22	8	8	8
	H23	0	0	0
CCGT	CC3	166	166	123

Table 3.4: WPAC for different response times

Response time (min)	WPAC (%)
15	22
10	14
5	7

Table 3.5 shows the WPAC for different system operating conditions. The calculation of WPAC values illustrated in Tables 3.3 and 3.4 are shown in the third row of Table 3.5. The subsequent rows in Table 3.5 show the WPAC values for the operating states obtained by sequentially adding the generating units, one at a time, according to the priority loading order shown in Table 3.1 until the peak load was reached. The loads served by the resulting generation schedules are also shown in Table 3.5.

Table 3.5: WPAC at different operating conditions

No. of committed units	Total MCR (MW)	Load served (MW)	Load probability	WPAC for different response times (% of the load served)		
				15 min	10 min	5 min
26	2166	1787	0.00000000	20.12	13.08	5.26
27	2426	2047	0.00091047	22.23	14.76	7.28

Table 3.5 (Continued): WPAC at different operating conditions

No. of committed units	Total MCR (MW)	Load served (MW)	Load probability	WPAC for different response times (% of the load served)		
				15 min	10 min	5 min
28	2654	2275	0.04222324	23.05	15.33	8.92
29	2966	2592	0.22556996	24.08	16.34	9.20
30	3140	2766	0.21100237	24.64	18.24	10.07
31	3254	2880	0.15698570	25.86	19.71	11.65
32	3316	2942	0.07139714	27.42	21.40	13.51
33	3378	3004	0.05511551	28.92	23.02	15.29
34	3463	3089	0.04796480	30.87	25.14	17.62
35	3548	3174	0.05896590	32.72	27.14	19.83
...	...	...	...	...	...	...
55	4134	3700	0.00011001	45.49	40.78	33.03

The studies to assess the amount of wind power that can be absorbed by the system were carried out considering 15 minute, 10 minute and 5 minute response times. These response times have been considered in [37, 38] to follow wind variability with conventional unit ramping. The results are shown in Table 3.5. The load probabilities are also shown in the table.

There are 30 different generation schedules for the different load level intervals in the system shown in Table 3.5. The number of intervals is reduced to two in this example, which are, 1) high load and 2) low load. The system load above and below the average annual load of 2766 MW was considered as the high load and the low load respectively. All load steps above the

average load were grouped in the high load period and load steps below the average load were grouped in the low load period. It was assumed that wind power curtailment occurs both during the low load and high load periods. The WPAC for each operating condition within the low load period were combined using a probability method to obtain an expected value for the entire low load period. Table 3.6 shows the calculation considering the 15 minutes response time. The same technique was used to obtain the expected WPAC for the high load period. Table 3.7 presents the expected WPAC for both the low load and high load periods for the 10 and 5 minutes response times as well.

Table 3.6: Calculation of the expected WPAC during the low load period

(1) Load served (MW)	**(2) Load probability**	**(3) Load probability given low load**	**(4) WPAC (% of load served)**	**(5) Col. (3) x Col. (4)**
1787.3	0.00000000	0.00000000	20.12	0.000000
2047.3	0.00091047	0.00189798	22.23	0.042170
2275.3	0.04222324	0.08801898	23.05	2.014782
2592.3	0.22556996	0.47022539	24.08	11.261253
2766.3	0.21100237	0.43985765	24.64	10.83809
Expected WPAC (%)				**23.57**

Table 3.7: Expected WPAC for different response times

Response time (min)	**Low load period**	**High load period**
15	23%	31%
10	15%	23%
5	8%	14%

3.4 Conclusions

This chapter proposes a new technique to accurately assess the wind power absorption capability of a power system. A practical large-scale power system was considered in the analysis, consisting of different types of generating units. The response rates of the various generating units to change in loading were considered in the analysis. A detailed analysis of the wind power absorption capability of the system is carried out for all possible operating conditions for the system, with generating units being added, one at a time according to the priority loading order, to the base case generation schedule. The WPAC at the different response times were then evaluated for each operating condition. The loading conditions were grouped into the low load and high load periods, and expected WPAC values were assessed for each period. Factors such as the dispatch order of generating units and response rate of generating units to load change can affect the wind energy utilization in the power system, and hence the reliability of the power system. These important factors have been incorporated in the reliability and wind energy utilization assessment techniques described in the subsequent chapters.

4 INCORPORATION OF WIND CURTAILMENT IN GENERATION SYSTEM RELIABILITY AND WIND ENERGY BENEFIT ASSESSMENT

4.1 Introduction

In Chapter 3, a simple technique to conduct an accurate assessment of the wind power absorption capability of a power system was proposed. The importance of incorporating this characteristic in reliability modeling of the power system has been discussed in Section 1.3. Such models suited to adequacy assessment at the HL I level will be very useful to system planners as existing methods do not include wind power curtailment due to generating unit response limitations. As the wind penetration continues to increase, the wind farms in a power system are distributed at different geographical locations. This chapter presents an analytical method to combine the effects of wind diversity and wind curtailments due to generation constraints to evaluate the reliability, energy and environmental benefits of wind power.

A negative load approach for wind modelling has been proposed to incorporate wind power curtailment and wind power correlation in the reliability studies. An analytical method to determine the wind absorption capability of the power system at different loadings has been developed in Chapter 3. Important factors such as maintenance of generating units and seasonal correlation between system load and wind power [39] can be considered by conducting a period analysis [1, 39]. The proposed analytical technique is capable of estimating not only the system reliability indices, but also wind energy utilization and wind energy benefit indices.

4.2 Power system modelling to include wind power curtailment

4.2.1 Conventional generation modelling

Generating unit data such as the location, type, capacity rating, derated capacity and forced outage rate (FOR) [1] are the required inputs to the probabilistic models discussed in Section 2.2 for the conventional generating units. Large coal fired thermal units and combined cycle gas turbine (CCGT) units generally reside in one or more derated states in addition to the fully available and outage states. Such units can be represented by a multi-state model. The hydro units and the simple cycle gas turbine (SCGT) can be represented by two-state generation models. An overall generation model is developed combining all the conventional generating units as discussed in Section 2.2.1. The generation model was represented as a Capacity Outage Probability Table (COPT).

A period analysis was carried out by dividing the year into four seasonal periods: Winter (November-February), Spring (March-May), Summer (June-August), and Fall (September-October). A maintenance schedule is approximated to determine the number of units in the four seasonal periods. Seasonal deratings are also incorporated by considering the reduced capacities of the generating units in different seasons. Firm import and export capacities are also considered to determine the available capacities in different seasons. An overall generation model is developed for each season considering the number of generating units and available seasonal capacity.

4.2.2 Load and wind modelling to incorporate wind energy curtailment

This section describes the procedure of building the load models taking into account the

available wind generation that can be utilized to serve the load. The WPAC calculated using the method described in the Chapter 3 is utilized to modify the system load model by considering wind generation as negative load. Figure 4.1 shows a sample of the hourly chronological system load model for a period of one year (8760 hours). Figure 4.1 also shows the wind power output of an actual wind farm located near Swift Current, Saskatchewan, Canada for the same period. The wind power is expressed in per unit of the rated wind farm capacity. The hourly system load is then modified by subtracting the wind power absorbed by the system in the corresponding hours. The WPAC values are used to determine the wind power absorbed at the different hours of the year. The horizontal lines in Figure 4.1 divide the system load into *n* number of intervals. *Pi* is the probability that the load level *Li* lies in the interval *i*. The wind power absorbed (WPA) in hour *t* is calculated using (4.1).

$$WPA(t,i) = \begin{cases} WP(t), & WP(t) \le \text{WPACi} * L(t,i) \\ \text{WPACi} * L(t,i), & WP(t) > \text{WPACi} * L(t,i) \end{cases} \tag{4.1}$$

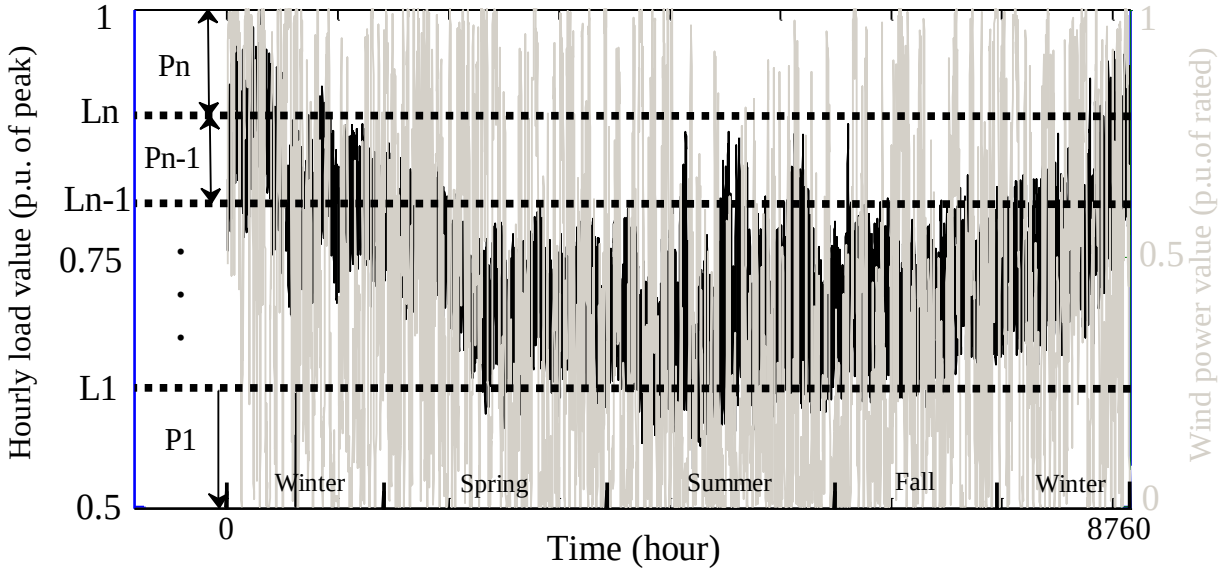

Figure 4.1: Hourly load variation and wind power output for 198 MW Wind farm 1 for 8760 hours

In (4.1), *WP*(t) is the wind farm power output at hour *t*, and *L(t,i)* is the load at hour *t* and lies in the interval *i*.

The chronological series of the modified load *ML*(t) can then be obtained for a period of one year by subtracting the wind power absorbed by the system from the total system load. The diurnal and seasonal variation in wind power can be quite different from one year to the next. Hence, wind power data for a large number of years are used in the study. The corresponding modified load models therefore obtained by repeating the above procedure using *s* number of different yearly samples of wind power data are averaged for each hour of the year as shown in Equation (4.2).

$$\{ML(t)\}_{t=1\text{ to }8760} = \{(1/\text{s})SUM_{j=1\text{ to s}}(L(t) - WPA(t)_j)\}_{t=1\text{ to }8760} \tag{4.2}$$

The modified hourly loads from (4.2) are sorted in a descending order to obtain the load duration curve. The load duration curve can be created using this approach for different periods in a year to perform a period analysis. The load model for each period is then convolved with the system generation model for the same period to obtain the period risk indices. The period risk indices are aggregated to obtain the annual risk indices.

4.3 Proposed indices to quantify the wind energy benefits

Important indices are proposed and introduced in this section to quantify the energy and environmental benefits from wind energy utilization. The total wind energy absorbed by the system in a year is termed as the expected wind energy supplied (WES), and is obtained using (4.3).

$$WES = \sum_{p=1}^{n} WES_p \tag{4.3}$$

Where, WES_p is the expected wind energy supplied in period p, and is calculated using (4.4); n is the number of periods in the year.

$$WES_p = ENS_{p,\text{no wind}} - ENS_p \tag{4.4}$$

Where, ENS_p is the total energy not supplied in period p, and $ENS_{p,\text{ no wind}}$ is the energy not supplied when wind is excluded.

The annual expected wind energy spilled (WESP) can be calculated using (4.5).

$$WESP = \sum_{p=1}^{n} (WEA_p - WES_p) \tag{4.5}$$

Where, WEA_p is the expected wind energy available in period p, and can be obtained using (4.6).

$$WEA_p = \left(\sum_{i=1}^{CS_p} (C_i \times P_i) \right) \times T_p \tag{4.6}$$

Where, CS_p is the number of the discrete capacity states in the wind generation model in the period p, T_p is the number of hours in that period, and C_i and P_i are the capacity and probability of the ith state, respectively.

The utilization of wind energy, results in a reduction of harmful greenhouse gas (GHG) emissions due to reductions in coal and natural gas combustion. The data for average GHG emissions from conventional fuel were obtained from the US Environmental Protection Agency (US-EPA) [56]. The energy offset from these units by wind energy was evaluated to assess the reduction in GHG emissions.

A probabilistic method developed to quantify the reduction in GHG emissions due to wind energy utilization is presented in this section. A discrete probability distribution of the system load is first created, where the number of discrete steps, M can be obtained using the Sturges' rule [57]. The generation schedule is determined as discussed in Section 3.2 for each load step,

and the percentage of the loads served by the scheduled fossil fuel units are calculated using (4.7).

$$PLS_{fk} = \frac{LS_{fk}}{L_k} \times 100 \tag{4.7}$$

Where, LS_{fk} represents the load served by type f fossil fuel unit, for the kth load step, L_k.

The expected percentage of load served $EPLS_f$ by the different types of fossil fuel units, such as coal and natural gas, is calculated using (4.8).

$$EPLS_f = \sum_{k=1}^{M} p_k * PLS_{fk} \tag{4.8}$$

Where, p_k is the probability of the kth load step and PLS_{fk} is the percentage of load served by f type of fossil fuel units in the kth generation schedule.

The reduction in CO_2, SO_x and NO_x emissions in lbs/year due to wind energy by offsetting the energy from conventional fuel can be calculated using (4.9-4.11).

$$CO_2 \text{ reduction} = \sum_{\text{all fuels}} \left(CO2_f * \frac{EPLS_f}{100} * WES \right) \tag{4.9}$$

$$SO_x \text{ reduction} = \sum_{\text{all fuels}} \left(SOx_f * \frac{EPLS_f}{100} * WES \right) \tag{4.10}$$

$$NO_x \text{ reduction} = \sum_{\text{all fuels}} \left(NOx_f * \frac{EPLS_f}{100} * WES \right) \tag{4.11}$$

Where, $CO2_f$, SOx_f and NOx_f are the amount of CO_2, SO_x and NO_x emissions in lbs/MWh of energy produced by burning fossil fuel. The data for average GHG emissions for coal and gas units were obtained from the US Environmental Protection Agency (US-EPA) [56].

4.4 Application of the proposed method

The proposed method to evaluate the adequacy and energy indices in a wind-integrated

power system including wind energy curtailment is illustrated on a practical power system. The details of the large-scale power system are described in Section 3.3.

4.4.1 Generation and load model

This section illustrates the development of the wind-integrated load models using the methodology described in Section 4.2. The WPAC values shown in Table 3.7 are utilized to modify the system load model by considering wind generation as negative load. Figure 4.2 shows a sample of the hourly chronological system load model for a 48-hour period. The figure also shows the per unit wind power output of a wind farm considered at a site near Swift Current for the same period. Historical hourly wind power data collected over six years for the site was used in the evaluation. The system load is divided into two periods, high load and low load period by considering $n = 2$ in Eq. (4.1). The horizontal dotted line in the Figure 4.2 separates the two periods. It should be noted that the annual load factor of the power system is 0.75. The wind power absorbed by the system in time chronology was calculated using (4.1). The average modified hourly load values were subsequently obtained from (4.2) using the six years of historical wind power data.

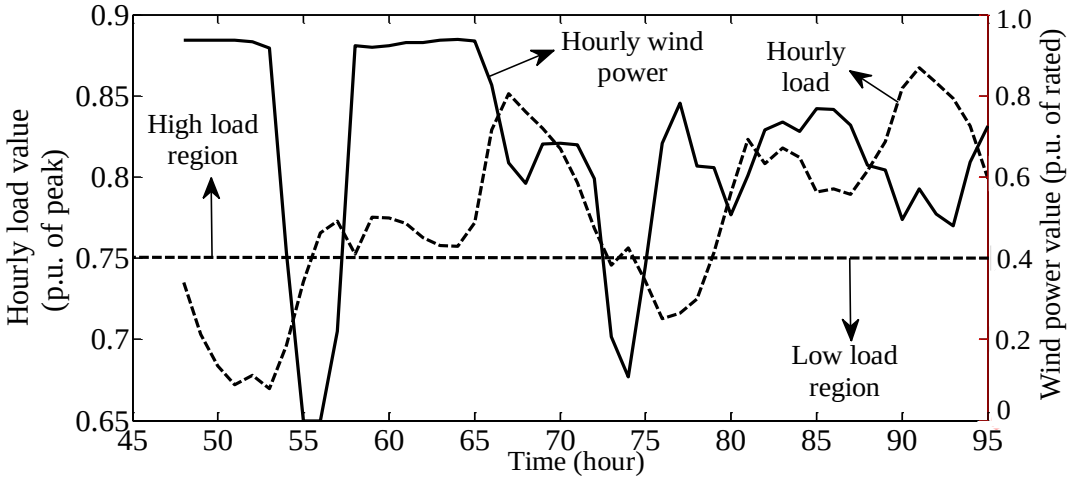

Figure 4.2: Hourly load variation and wind power output for a 48 hour period

A period analysis was conducted and the average modified hourly load values were divided into the four seasonal periods: Winter, Spring, Summer and Fall. A LDC was built for each season from the chronological modified load profiles. The LDC thus created for the winter season is shown in Figure 4.3 for illustration, and is compared with the LDC obtained without considering wind curtailment. The dotted curve shows the actual winter LDC before being modified by wind power. A significant difference between the load models with and without considering wind curtailment can be observed in the figure.

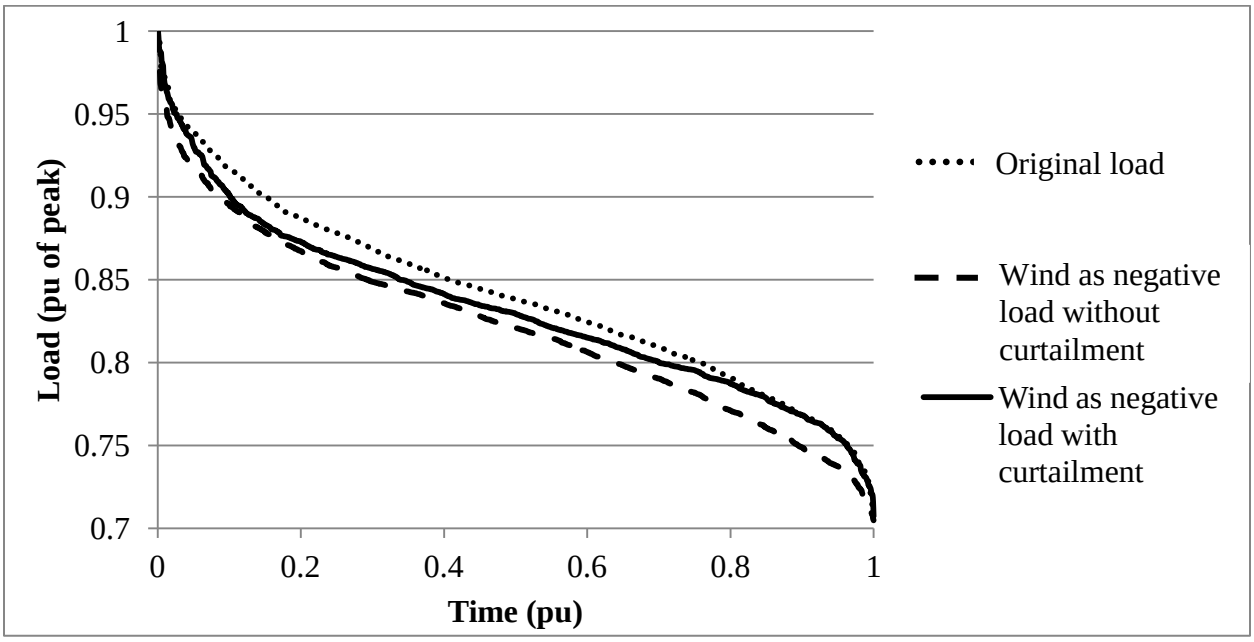

Figure 4.3: Effect of wind curtailment on the modified load model for the winter season

4.4.2 System evaluation

A system adequacy evaluation was carried out using the developed models. Data in Table 3.1 were used to create a generation model for the conventional generating units in the system. A period analysis was considered to include the effect of generating unit maintenance and seasonal

capacity deratings. It was assumed that the units H12-H18, C7, H1 and H4 are on maintenance during the spring season, units CC5 (1)-CC5 (6) and SC1-3 during the summer season, and units C1-2, H1 and H4 during the fall season. The capacity of the hydro, CCGT and SCGT generating units were derated by 6.47%, 8.37% and 6% in Spring, Summer and Fall seasons respectively. Load forecast uncertainty was considered in the evaluation assuming a standard deviation of 4% of the forecast expected load. A 728 MW wind farm located near Swift Current was considered to be connected to the power system. The conventional generation models developed for the four seasons were convolved with the corresponding seasonal modified LDCs to obtain the adequacy indices of the system.

Table 4.1 shows the loss of load expectation (LOLE) and the loss of energy expectation (LOEE) obtained with and without considering the wind curtailment in the evaluation. It can be seen that the system LOLE substantially increases when wind curtailments due to generation ramping limitations are recognized in the evaluation. The wind curtailment contributes to an additional 116.6 MWh of expected energy not supplied per year. Existing adequacy evaluation techniques that do not account for the wind curtailments result in highly optimistic results.

Table 4.1: Impact of wind curtailment on system adequacy

	No wind curtailment	**With wind curtailment**
LOLE (h/yr)	9.82	11.13
LOEE (MWh/yr)	881.0	997.6
PLCC (MW)	3235.7	3230.4
IPLCC (MW)	142.6	137.3
CC (%)	19.6	18.9

Table 4.1 also shows the peak load carrying capability (PLCC) of the system evaluated considering a LOLE criterion of 1 hour/year. It can be seen that the system can carry 5.3 MW

less load due to wind curtailment. The PLCC of the system without considering wind power is 3093.1 MW. The contribution of the 728 MW wind farm in carrying additional system load was also assessed. This is measured by the increase in PLCC (IPLCC) in Table 4.1. The capacity credit of a wind farm is the additional load it can carry at the original LOLE criterion, and is expressed as a percentage of the installed wind farm capacity. Table 4.1 shows the capacity credit of the 728 MW wind farm with and without considering wind curtailment. Wind curtailment results in a 3.7% decrease in the wind capacity credit.

The energy contribution of the wind farm was quantified in the practical power system by evaluating the proposed energy indices. The annual expected wind energy supplied to the system (WES) and the wind energy spilled were calculated using (4.3) and (4.5) respectively, and are shown in Table 4.2. There is a reduction in the wind energy utilized by the system due to wind power curtailment. It can be seen that all the wind energy is absorbed by the system and there is no wind energy spillage if there is no wind curtailment. The fact that wind is curtailed due to generation ramping limitations actually causes a wind energy spillage of 261.9 GWh per year. Table 4.2 shows that the WES by the 728 MW farm is reduced by 261.9 GWh per year due to wind power curtailment. Table 4.2 also shows the fuel energy saved with and without considering wind curtailment. It can be seen that the fuel savings is reduced by approximately 10 million dollars per year due to the wind power curtailment.

Table 4.2: Impact of wind curtailment on wind energy utilization

	No wind curtailment	**With wind curtailment**
WES (GWh/yr)	1838.488	1576.582
WESP (GWh/yr)	0.000	261.906
Fuel saving (M$/yr)	69.12	59.27

The offset in conventional fuel, mainly coal and natural gas, due to wind energy utilization results in the reduction in greenhouses gas emissions as discussed earlier. The probabilistic method described in Section 4.3 was used to quantify the reduction in GHG emissions due to wind energy utilization. Using the Sturges' rule [57], an 11-step discrete probability distribution of the system load was created. The generation schedule for each load step was then determined considering an operating reserve of 373.7 MW, which includes an Automatic Generation Control (AGC) margin of 82.7 MW assigned to hydro units H4-9. The generation scheduling was performed using the same loading priority assumptions as discussed in Section 3.3.

As an example, for the first load step of the load probability distribution, 1667 MW, it is found that coal and natural gas units serve 74.32% and 17.52% of the load, respectively. Table 4.3 shows the load dispatch from the scheduled generating units for this load level. It can be seen that coal and natural gas units provide a total of 1239 MW and 292 MW to the system load, which is 74.32% and 17.52% of the 1667 MW load.

Table 4.3: Generating unit load dispatch to serve 1667 MW of load

Unit	**Coal**							**Hydro**		**Nat. Gas**		**Total**
	C3	**C4**	**C5**	**C6**	**C1**	**C2**	**C7**	**H4-9**	**H22**	**CC3**	**CC1**	
MCR (MW)	110	139	139	284	291	291	276	204	23	246	260	2263
Loading (MW)	110	139	139	284	291	291	276	204	15	80	132	1667

The percentage of the loads served by the scheduled coal and natural gas units were computed for each load step using (4.7), and the results are shown in Table 4.4. The expected percentage of load served by the coal and natural gas units were calculated as 51.2% and 35.9% respectively using (4.8) and shown in Table 4.4. The reduction in CO_2, SO_x and NO_x emissions

due to offset in coal and natural gas energy were calculated using Eq. (4.9)-(4.11) for the wind penetration level of 728 MW, and are shown in Table 4.5.

Table 4.4: Thermal and gas power absorption capability for different operating conditions

Load (MW)	**Load probability**	**Load served by coal (%)**	**Load served by natural gas (%)**	**Col. (2) × Col. (3) (%)**	**Col. (2) × Col. (4) (%)**
1667	0.00000189	74.316	17.523	0.000121	0.000045
1861	0.00001256	70.328	18.260	0.000758	0.000355
2054	0.00091048	65.316	22.966	0.050364	0.030015
2248	0.00125639	63.104	24.186	0.066719	0.042951
2442	0.16255689	61.914	26.506	8.438978	5.934432
2635	0.22565698	60.298	27.035	11.350095	8.357342
2829	0.18100237	59.703	25.570	8.996361	6.438363
3022	0.22652849	57.926	25.969	10.856604	8.148049
3216	0.14854325	55.184	26.398	6.711778	5.406796
3401	0.07352638	53.411	28.971	3.191854	2.865455
3603	0.00125368	51.907	30.666	0.052538	0.050982
Expected percentage of load served (EPLS) =				**51.2**	**35.9**

Table 4.5: Impact of wind curtailment on GHG emissions

Reduction in emission of	**No wind curtailment**	**With wind curtailment**
CO_2 (T/yr)	1176220	1060036
SO_x (T/yr)	5034	4537
NO_x (T/yr)	2806	2528

4.5 Impact of wind growth on the reliability and wind energy utilization

The studies presented in this section illustrate the impact of wind power growth on wind energy curtailments, and the resulting reliability and energy indices. It is assumed that the wind penetration in the example power system grows from 4.8%, to 9.5%, and then to 16.2% in this study. The resulting installed wind capacities are 198 MW, 428 MW and 728 MW respectively. The wind penetration is the installed wind capacity expressed as a percentage of the total available generation capacity.

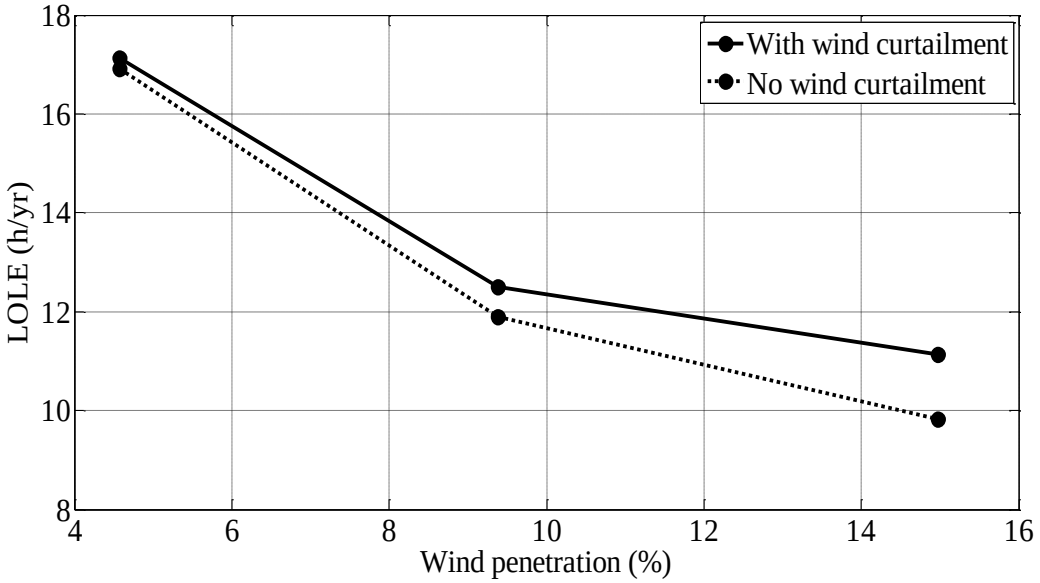

Figure 4.4: Impact of wind growth on system LOLE

The system LOLE for the three wind penetration levels with and without considering wind curtailments are shown in Figure 4.4. It can be seen that the LOLE decreases with the increase in wind penetration. It should be noted however, that the incremental reliability benefit decreases. A comparison of the indices obtained with and without considering wind curtailment shows that the system reliability decreases when wind power curtailment is considered as shown by the earlier studies. The reduction in reliability due to wind curtailment increases with wind power

growth in a system. It can be concluded that as wind penetrations in power systems increase with time, it becomes more important to consider wind energy curtailments because it causes significant reductions in the reliability contribution of wind power in a wind-integrated power system. Ignoring wind power curtailment will provide very optimistic results in such cases.

Table 4.6 shows the PLCC of the system and the wind capacity credit at the three wind penetration levels with and without considering wind power curtailments. The system PLCC increases with the increase in wind penetration. The wind power curtailment, however, causes a reduction in the increase in PLCC due to wind power. It can be observed from Figure 4.5 that the increase in PLCC (IPLCC) due to wind power is reduced by 0.5 MW, 3.0 MW and 5.3 MW as a result of wind power curtailment when the installed wind capacities are 198 MW, 428 MW and 728 MW respectively. It can be seen that there are larger reductions in PLCC benefits due to wind power curtailment at higher wind penetrations. Table 4.6 also shows that wind capacity credit decreases with wind power growth in the system. There is a further reduction in the capacity credit (CC) of wind when wind power curtailment is considered in the evaluation. The CC are reduced by 0.8%, 3.0% and 3.7% respectively due to wind power curtailment at the three wind penetration levels in the increasing order.

Table 4.6: Impact of wind power growth and wind curtailments on wind capacity credit

	PLCC (MW)			**CC (%)**		
Wind farm capacity (MW)	**198 MW**	**428 MW**	**728 MW**	**198 MW**	**428 MW**	**728 MW**
Considering wind curtailment	3153.0	3189.2	3230.4	30.3	22.6	18.9
Without considering wind curtailment	3153.1	3192.1	3235.5	30.5	23.3	19.6

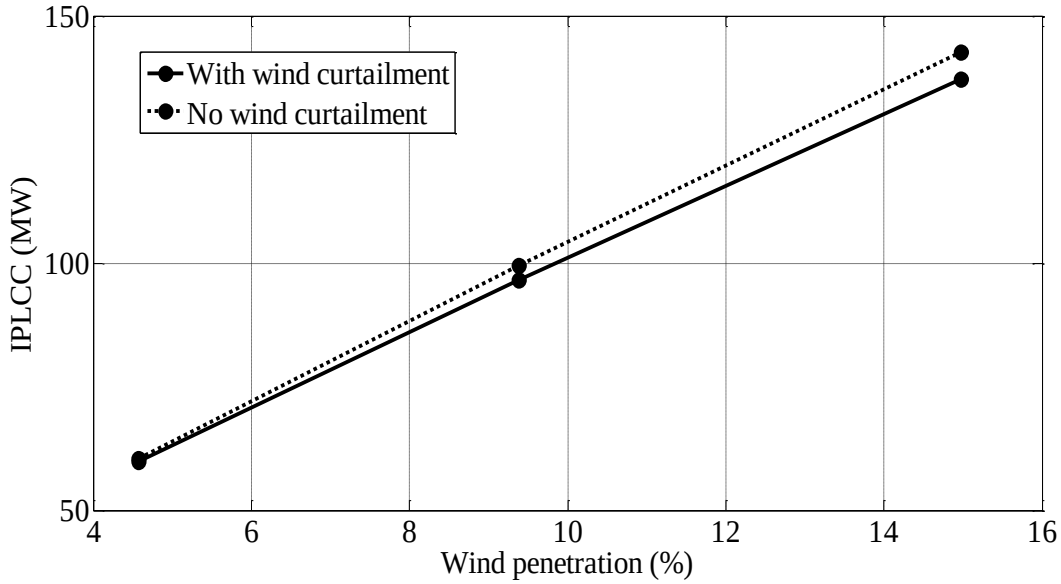

Figure 4.5: Impact of wind growth on the IPLCC

Wind energy indices, wind energy supplied (WES) and wind energy spilled (WESP), were evaluated to assess the impact of wind power growth and wind curtailment on wind energy utilization. The total expected wind energy available at the wind site for the three penetration levels are 500.0, 1080.9 and 1838.5 GWh per year in the increasing order. The WES in GWh increases with wind penetration. However, the WES in percent of the available wind energy decreases with increasing penetration as shown in Figure 4.6 when wind power is curtailed. It can be observed from Figure 4.6 that the wind energy is spilled, and therefore, WES is reduced by 0.02%, 6.30% and 14.20% of the available wind energy due to wind power curtailment when the installed wind capacities are 198 MW, 428 MW and 728 MW respectively. It can be seen that the wind energy spilled increases significantly as the wind penetration increases.

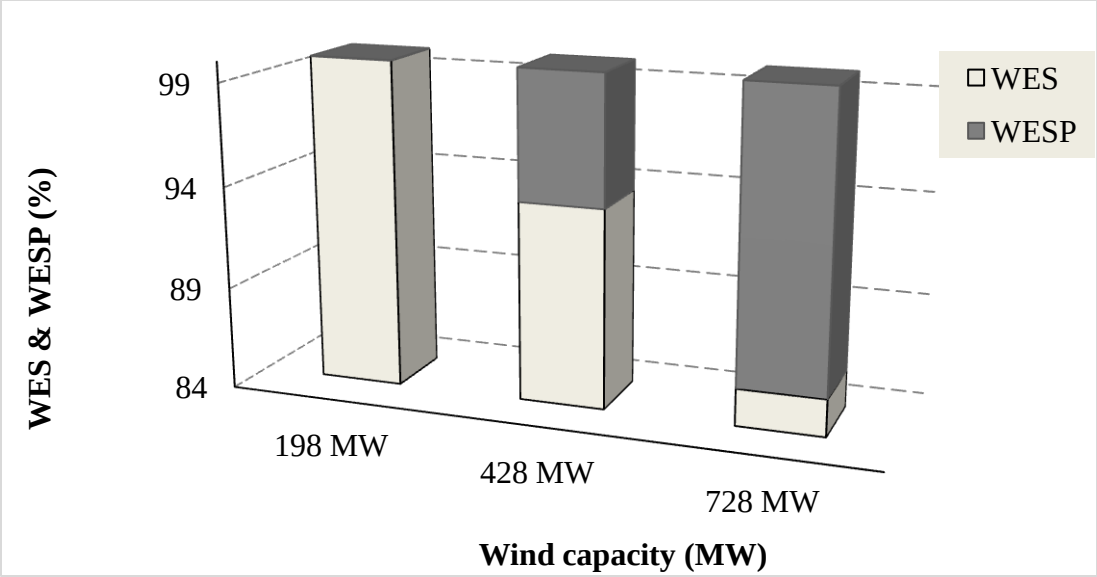

Figure 4.6: Impact of wind power growth on the wind energy utilization

The utilization of wind energy results in conventional fuel savings. The conventional fuel energy offset or saved due to utilization of wind energy can be represented in monetary terms by multiplying the wind energy utilized by the marginal energy cost. Figure 4.7 shows the fuel energy saved in million dollars per year which was calculated using a marginal energy cost of $37.60/MWh. This value was used in the analysis after reviewing technical reports from Canadian utilities, literature and industry experience. It can be seen that the fuel savings increase with wind penetration, but the reduction in fuel savings due to wind power curtailment also increases with the increase in wind power penetration.

The reduction in CO_2, SO_x and NO_x emissions in tonnes per year due to offset in coal and natural gas energy are shown in Table 4.7. The reduction in GHG emissions increases as wind penetration increases. A comparison of the results shows that the environmental benefits from GHG reduction is restricted due to wind power curtailment. As the wind penetration in the system increases, the negative impact of wind power curtailment on the reduction in GHG emissions also increases.

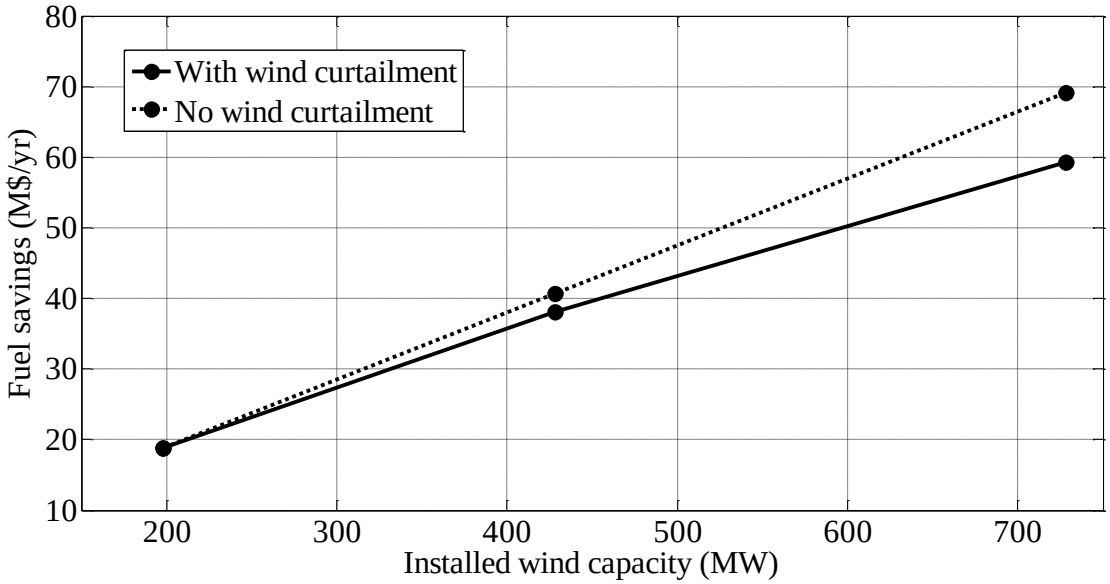

Figure 4.7: Impact of wind growth on the fuel savings

Table 4.7: Reduction in GHG emissions and impact of wind curtailment

	Considering wind curtailment			**No wind curtailment**		
Wind farm capacity	**198 MW**	**428 MW**	**728 MW**	**198 MW**	**428 MW**	**728 MW**
CO_2 reduction (T/yr)	322199	641176	1060036	322252	679952	1176220
SO_x reduction (T/yr)	1379	2744	4537	1379	2910	5034
NO_x reduction (T/yr)	768	1529	2528	769	1622	2806

4.6 Impact of wind diversity on power system reliability and wind energy benefit assessment

The studies presented in this section evaluate the impact of wind diversity on the system reliability and energy indices while considering wind energy curtailments in the evaluation. The

results obtained without considering wind diversity are compared with the case where the installed wind capacity is distributed in two different Saskatchewan sites, Swift Current and Broadview. The correlation in wind speed between the two sites is 0.387.

It is assumed that the installed wind capacity in the example system grows from 198 MW to 428 MW and then to 728 MW. The 198 MW wind capacity consists of two wind farms: a 171.6 MW farm at the Swift Current area and a 26.4 MW farm at the Broadview area. A growth of 230 MW capacity was considered at the Swift Current area to increase the total capacity to 428 MW. An additional 300 MW capacity was considered at the Broadview area to raise the wind capacity to 728 MW in this study. Two years of wind power data were obtained from existing wind farms in these areas, and were used to obtain the wind-integrated load models that incorporate wind diversity.

The seasonal load models considering wind power diversity and curtailment were obtained using the technique described in Section 4.2.2, where only wind power curtailment was considered. The only difference when wind diversity is considered is that *WP(t)* in Eq. (4.1) represents the sum of the hourly power outputs of the Swift Current and Broadview wind farms. The wind power absorbed in hour *t* is calculated using (4.1). The LDCs for different periods of the year can then be created using the modified hourly loads obtained using (4.2). Figure 4.8 compares the winter load models for an installed wind capacity of 728 MW with and without considering wind diversity. All the wind capacity is assumed to be concentrated at the Swift Current area for the case when wind diversity is not considered. The effect of wind energy curtailments are incorporated for both the cases shown in Figure 4.8. The impact of the wind diversity can be seen by the difference in the two load models. Load models incorporating wind power curtailment and diversity were similarly developed for the remaining seasonal periods.

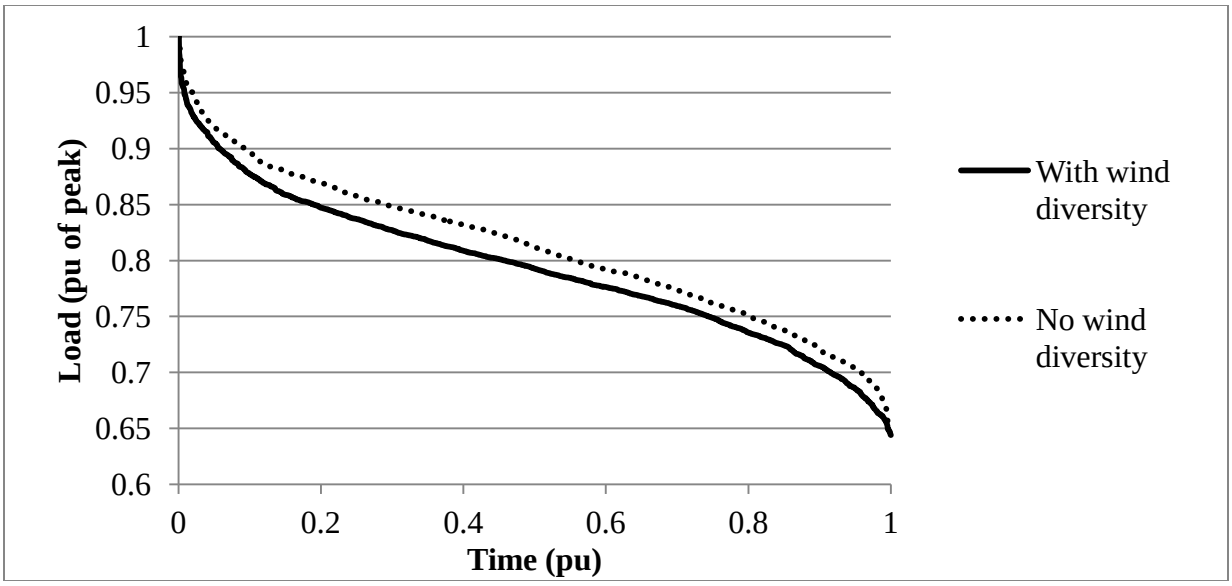

Figure 4.8: Winter load models modified by 728 MW wind capacity with and without considering wind diversity

Table 4.8 shows the reliability indices of the power system for the three wind penetration levels that were obtained using the load models that incorporate wind diversity and wind power curtailments. It can be observed that the LOLE and LOEE values decrease as wind penetration in the system increases from 198 MW to 728 MW. These results are compared with the case when wind diversity is not considered in the evaluation. A comparison of the reliability indices obtained with and without wind diversity show that the system reliability significantly improves when wind diversity is considered. The improvement in the resulting indices increases as the wind power grows in the system. A comparison with the results in Figure 4.4 show that the degradation in system reliability as a result of wind power curtailment at high wind penetration levels can be considerably offset if the total wind capacity is geographically distributed at diverse wind sites.

Table 4.8: Impact of wind diversity on system reliability indices

	LOLE (h/yr)			LOEE (MWh/yr)		
Wind farm capacity	**198 MW**	**428 MW**	**728 MW**	**198 MW**	**428 MW**	**728 MW**
Considering wind diversity	15.95	10.26	6.88	1585.1	982.6	779.1
Without considering wind diversity	17.14	12.51	11.13	1617.1	1114.7	997.7

Table 4.9 shows the PLCC of the system and the wind capacity credit at the three wind penetration levels with and without considering wind diversity. The distribution of the wind resource at diverse geographic locations results in a considerable improvement in the system PLCC. It can be observed from Table 4.9 that the IPLCC due to wind power increases by 1.2 MW, 5.1 MW and 9.1 MW respectively due to the diversity effect of the distributed wind capacity when the total installed wind capacities are 198 MW, 428 MW and 728 MW. It is also observed that there are larger improvements in PLCC benefits due to wind diversity at higher wind penetrations. Table 4.9 shows that wind capacity credit decreases as the wind power grows in the power system. However, the capacity credit of wind increases when wind diversity is considered in the evaluation. The CC of wind is increased by 2.0%, 5.8% and 6.8% respectively due to wind capacity diversification at the three wind penetration levels in the increasing order.

Table 4.10 shows the energy indices to assess the utilization of wind energy in the power system for the three wind penetration levels. A comparison of the WES results with and without the consideration of wind diversity shows that there is increase in the wind energy utilized by the system due to wind capacity diversification, and the benefit increases with wind growth.

Table 4.9: Impact of wind diversity on wind capacity credit

	Considering wind diversity			Without considering wind diversity		
Wind farm capacity	**198 MW**	**428 MW**	**728 MW**	**198 MW**	**428 MW**	**728 MW**
PLCC (MW)	3154.2	3194.8	3239.5	3153.0	3189.7	3230.4
IPLCC (MW)	61.1	101.8	146.4	59.9	96.6	137.3
Capacity credit (%)	30.9	23.9	20.2	30.3	22.6	18.9

Table 4.10: Impact of wind diversity on wind energy indices

	Considering wind diversity			Without considering wind diversity		
Wind farm capacity	**198 MW**	**428 MW**	**728 MW**	**198 MW**	**428 MW**	**728 MW**
WES (%)	99.98	95.50	92.40	99.98	93.70	85.80
WESP (%)	0.02	4.50	7.60	0.02	6.30	14.20
Fuel saving (M$/yr)	20.30	43.48	75.63	18.79	38.09	59.27

Table 4.10 shows that the spillage of wind energy due to wind curtailment is reduced when the wind capacity is diversified, and again the reduction in energy spillage increases with wind penetration. The reductions in wind energy spilled due to wind diversity are 18.0%, 28.6% and 46.5%, respectively at the three wind penetration levels in the increasing order.

Table 4.10 also shows the fuel energy saved in million dollars per year. When wind diversity is considered, there is a further increase in the fuel savings, which increases with the increase in wind power penetration. Table 4.10 shows that the fuel savings are increased by 8.0%, 14.2% and 27.6% respectively due to wind diversity when the wind penetration is 198 MW, 428 MW and 728 MW.

Table 4.11 shows the reduction in CO_2, SO_x and NO_x emissions due to wind power utilization with and without considering wind diversity. There is further reduction in the GHG emissions if the total wind power capacity is diversified. Table 4.11 shows that the wind diversity effect results in additional 8.0%, 16.2% and 23.0% reduction in GHG emissions when the wind penetrations are 198 MW, 428 MW and 728 MW respectively.

Table 4.11: Reduction in GHG emissions and impact of wind diversity

	Considering wind diversity			**Without considering wind diversity**		
Wind farm capacity	**198 MW**	**428 MW**	**728 MW**	**198 MW**	**428 MW**	**728 MW**
CO_2 reduction (T/yr)	347975	745047	1303844	322199	641176	1060036
SO_x reduction (T/yr)	1489	3188	5580	1379	2744	4536
NO_x reduction (T/yr)	829	1776	3109	768	1529	2528

4.7 Conclusions

In this chapter, a methodology to develop a wind power model recognizing the wind power curtailment scenarios was proposed by embedding the wind absorption indices in a load modification approach considering wind power as negative load. The methodology was further modified to incorporate the diversity in wind power profiles at different geographical wind sites. The proposed methodology was then illustrated on a practical power system using wind data from existing wind sites located in Saskatchewan, Canada.

The results from the studies showed that the reliability of the system degrades due to wind

power curtailments. The system could carry a smaller load at the same reliability criterion, or in other words, the capacity credit of wind resources was lowered due to wind power curtailments. This effect was more prominent at high wind penetration levels. There was a reduction in the wind energy utilized by the system due to wind power curtailment. The study results showed that all the wind energy was absorbed by the system and there was no wind energy spillage if there was no wind curtailment. This scenario will only be valid at very low wind penetration levels. At higher penetration levels, wind energy is in fact curtailed due to generation ramping limitations causing wind energy spillage. The spillage in wind energy is increased as more wind capacity is added to the system. Although the savings in conventional fuel are increased with wind penetration, the savings are significantly reduced due to wind energy curtailment.

The environmental benefits from offset in GHG emissions are also considerably reduced due to wind curtailments. The diversity of wind resources generally increases with wind penetration, and therefore, mitigates the adverse impact on system reliability, wind energy utilization and environmental benefits caused by wind curtailments. As the wind penetration continues to grow in a power system, wind energy curtailment and wind diversity will have a significant impact on the power system reliability and wind energy utilization, and should therefore, be considered in system evaluation.

5 INCORPORATION OF WIND CURTAILMENT IN BULK SYSTEM RELIABILITY AND WIND ENERGY BENEFIT ASSESSMENT

5.1 Introduction

Wind power curtailments in a power system can occur due to generating unit limitations in responding to wind power fluctuations as well as transmission constraints. The previous chapters discuss wind curtailments due to generation constraints and the impact on the system reliability, energy and environmental benefits of wind power. Wind power curtailments can also take place due to transmission line constraints depending on factors such as, location of the wind resource in the power system, capacity of the wind resource, and power transfer capacity of the transmission lines connected to the wind farm bus. It is very important to include wind curtailments due to both generation and transmission constraints to conduct a comprehensive reliability modeling of the power system, which can be utilized in the HL II adequacy assessment. This chapter presents a MCS based technique to combine the effects of wind diversity and wind curtailments due to both generation and transmission constraints to assess the reliability, energy and environmental benefits of wind power.

A simple and accurate technique for HL II reliability and wind energy utilization assessment utilizing the MECORE [9] software is presented in this chapter. Wind curtailment is incorporated in the HL II evaluation technique by applying the negative load approach to wind modeling. The effect of additional wind power curtailments due to the transmission constraints is analyzed by utilizing the proposed technique. The technique is further modified in this chapter to incorporate wind speed correlation between diverse wind sites. Further, sensitivity studies are conducted by varying the wind penetration level in the power system.

5.2 Proposed HL II reliability and wind energy benefit assessment technique considering wind curtailment

5.2.1 Conventional generation modeling

Generating unit data such as the location, type, capacity rating, derated capacity and forced outage rate (FOR) [1] are the required inputs to the probabilistic models discussed in Section 2.2 for the conventional generating units. Large coal fired thermal units and combined cycle gas turbine (CCGT) units generally reside in one or more derated states in addition to the fully available and outage states. Such units can be represented by a multi-state model. The hydro units and the simple cycle gas turbine (SCGT) can be represented by two-state generation models.

5.2.2 Transmission line modeling

Transmission lines are represented by two-state Markov models similar to the model shown in Figure 2.3 (a). Transmission line data such as the resistance, reactance, capacity, repair time and failure probability [1] are the required inputs to the probabilistic models for transmission lines.

5.2.3 Load and wind modeling

Annual reliability indices are usually computed using a LDC created using 8760 hourly data. The load data of a typical Saskatchewan year is utilized for the HL II studies. A LDC can be created in the following manner:

1. If wind is present in the system, hourly wind power output of the wind farm is simulated for a year using a time series model.

2. The hourly wind power that can be absorbed by the system is evaluated using (4.1).
3. The hourly wind power absorbed by the power system is subtracted from the hourly chronological system load to obtain a time sequential series of modified system load as described in Section 2.2.3.
4. The maximum value of the modified chronological system load is considered to be the new annual system peak load.
5. The modified hourly loads are arranged in descending order and normalized with respect to the modified peak load value.
6. The total number of hours in the year that each load level is exceeded is evaluated. The values are normalized with respect to the total number of hours in the evaluation period.
7. The modified LDC is created from the load levels arranged in descending order of magnitude.
8. Steps 1 to 7 are repeated for a specified number of yearly samples.
9. The LDCs and peak loads obtained for the yearly samples are averaged to create the modified system LDC that is used in the HL II evaluation of a wind-integrated power system.

Hourly wind speed data is simulated using time series models developed for the particular wind sites, and are used to create the modified load models that incorporate wind power curtailment.

Reference [29] shows that an ARMA model can be used to represent the long term wind characteristics of a specific wind site. The ARMA model time series y_t for the Swift Current wind site in Saskatchewan is shown in (5.1):

$$y_t = 1.1772y_{t-1} + 0.1001y_{t-2} - 0.3572y_{t-3} + 0.0379y_{t-4} + \alpha_t$$
$$- 0.5030\alpha_{t-1} - 0.2924\alpha_{t-2} + 0.1317\alpha_{t-3} \qquad (5.1)$$
$$\alpha_t \in NID(0, 0.524760^2)$$

Where, 1.1772, 0.1001, -0.3572 and 0.0379 are the autoregressive coefficients of the Swift Current wind model. The moving average coefficients of the wind model are -0.5030, -0.2924 and 0.1317. These coefficients are evaluated using historical data of the wind site [29] collected over 15 years. α_t is a Normally and Independently Distributed (NID) white noise process with zero mean and variance of 0.524760^2 at hour *t*. A series of y_t can be generated from (5.1) using the values of α_t randomly generated for each hour and the preceding values of y and α. The simulated hourly wind speeds can then be computed using (5.2).

$$SW_t = \mu_t + \sigma_t \cdot y_t \tag{5.2}$$

Where,

SW_t = simulated wind speed for hour *t*.

μ_t = hourly mean wind speed for hour *t*.

σ_t= hourly standard deviation of wind speed for hour *t*.

The hourly mean and standard deviation of the wind speed at the Swift Current wind site is obtained from Environment Canada [45]. Hourly wind speed data is simulated for 1000 yearly samples using (5.2). Subsequently, the hourly wind power output of the WTG is computed using the power curve relation in (2.6).

The modified annual load models incorporating wind curtailment are built considering wind power as negative load as described above. Equation (4.1) is utilized to evaluate the hourly wind power absorbed, (4.2) is used to find the modified hourly load values and subsequently create the modified LDC.

5.2.4 Load modeling for MECORE application to include wind curtailment in the HL II adequacy evaluation

MECORE utilizes a single load model to represent the load profile at all the load buses in the system to evaluate the annual adequacy indices. In this research work, wind curtailment is included in the adequacy analysis by incorporating wind as negative load. The load profile for the buses connected to wind farms will therefore be very different from that of the other load buses. If these modified load models are to be used to incorporate wind curtailment in the HL II analysis using MECORE, the feature of the software that considers a single load model for all the load buses, is a major limitation. There is an additional feature in MECORE that can be used to obtain annualized reliability indices by considering different load values at the different load buses. In this option, the load at each bus can only be represented by a single peak load value. The annual load models or LDCs with different profiles cannot be used in this option. The diurnal and seasonal variability in load and wind cannot, therefore, be incorporated by using this feature of MECORE.

The proposed method for HL II reliability and wind energy utilization evaluation including wind curtailments by utilizing the MECORE software is presented in this section. The modified LDC at each of the system buses are discretized into *NS* number of states, and a discrete probability distribution is obtained for each load bus. The MECORE software is run *NS* times using different single load values for the different load buses and the annual HL II reliability indices are computed by weighting the annualized indices at every load level by the load level probability. This method can incorporate different load models to represent the loads profiles at different load buses.

The peak load values at individual buses and the system peak load value are known. The annual risk index or wind energy utilization index for a particular load point (LP) collectively denoted as R_{LP} is evaluated using (5.3).

$$R_{LP} = \sum_{i=1}^{NS} R_{i,LP} * p_i \tag{5.3}$$

Where, $R_{i,LP}$ denotes the reliability or energy index obtained using the single value load for load step i, and p_i denotes the probability of load step i. R_{LP} represents a basic risk index (LOLE, LOEE) or a wind energy utilization index obtained by performing the iterative annualized analysis. The wind energy utilization indices for each load step are calculated using the concepts described in Section 4.3. The actual value of the load at each load step is calculated from the per unit value using (5.4) for buses without wind resource, and using (5.5) for buses connected to wind resource.

$$LS_i = LS_{i,p.u.} \times PL_{LP} \tag{5.4}$$

$$LS_i = LS_{i,p.u.} \times MPL_{LP} \tag{5.5}$$

Where,

LS_i = Actual value of the load step.

$LS_{i,p.u.}$ = Per unit value of the load step.

PL_{LP} = Peak load value at the load point.

MPL_{LP} = Modified peak load value at the load point.

The reliability index and the wind energy utilization index for the entire bulk power system can be found by aggregating the individual load point indices using (5.6).

$$R_{system,annual} = \sum_{LP=1}^{NL} R_{LP} \tag{5.6}$$

Where, NL represents the number of load points in the power system.

5.2.5 Load model approximation

It is important to select an appropriate number of load steps or *NS* in (5.3) such that the computation is both fast and reasonably accurate. System reliability studies were conducted using the proposed HL II evaluation technique to determine the appropriate number of load steps. A large number of load steps provides results with high accuracy, but requires significant computation time. Decreasing *NS* will reduce the computation time at the cost of accuracy in the results. Starting with *NS* = 40, the number of load steps was decreased to 30, 20 and 15. The test system, the IEEE-RTS [58], with 32 generating units with capacities ranging from 12 MW to 400 MW was used for the studies. The IEEE-RTS has 24 buses with a total installed generating capacity of 3405 MW and system peak load of 2850 MW.

A range of studies was carried out with and without considering the transmission system, with and without considering wind integration, and at different peak load levels, in order to assess the appropriate number of load steps in the load model at different system configurations. Table 5.1 shows the annual system LOLE and LOEE without considering the transmission system or at the HL I level, considering a system peak load of 2850 MW with no wind integration. Table 5.2 shows the HL I annual system indices for the IEEE-RTS for a peak load value similar to the current Saskatchewan power system peak load of 3500 MW. In Tables 5.3 and 5.4, the LOLE and LOEE are shown for the IEEE-RTS considering the transmission line constraints, or at the HL II level. Table 5.3 shows the results considering a system peak load of 3500 MW without wind integration. Table 5.4 shows the results of the HL II reliability analysis for the same peak load when a 198 MW wind farm located at Swift Current is connected to Bus 6.

Table 5.1: The HL I annual system indices considering a system peak load of 2850 MW

NS	**LOLE (h/yr)**	**LOEE (MWh/yr)**	**Calculation time (seconds)**
15	12.19	1735.9	42.73
20	10.72	1512.2	64.94
30	9.42	1210.7	76.88
40	9.38	1204.9	99.21

Table 5.2: The HL I annual system indices considering a system peak load of 3500 MW

NS	**LOLE (h/yr)**	**LOEE (MWh/yr)**	**Calculation time (seconds)**
15	107.02	15276.1	45.79
20	90.15	12628.8	69.75
30	80.19	10605.7	78.19
40	79.45	10579.1	102.85

Table 5.3: The HL II annual system indices without any wind resource

NS	**LOLE (h/yr)**	**LOEE (MWh/yr)**	**Calculation time (seconds)**
15	151.97	21692.0	197.37
20	121.88	18182.9	257.25
30	112.12	15085.1	299.19
40	111.47	15000.3	345.66

Table 5.4: The HL II annual system indices in presence of 198 MW Swift Current wind farm

NS	**LOLE (h/yr)**	**LOEE (MWh/yr)**	**Calculation time (seconds)**
15	121.57	17353.6	194.32
20	91.88	12125.6	252.10
30	90.05	12005.9	302.84
40	89.17	12000.2	340.91

It is observed that with the increase in the number of load steps from 15 to 40, the values of the reliability indices decrease and more accurate indices are obtained. However, there is an increase in the computation time as *NS* is increased from 15 to 40. Considering the LOLE index using the 40-step load model as the reference in Table 5.1, the error in the LOLE values using the 30-step, 20-step and 15-step load models are 0.4%, 12.3% and 29.9% respectively. From the observation of the results in Table 5.1 to 5.4, it was concluded that a 30-step load model provides reasonable accuracy in the results with reduced computation time.

Figure 5.1 shows the 30-step annual LDC of the IEEE-RTS without wind power. Figure 5.2 shows the load model considering wind curtailment with 198 MW of installed wind capacity at a location with the Swift current wind regime.

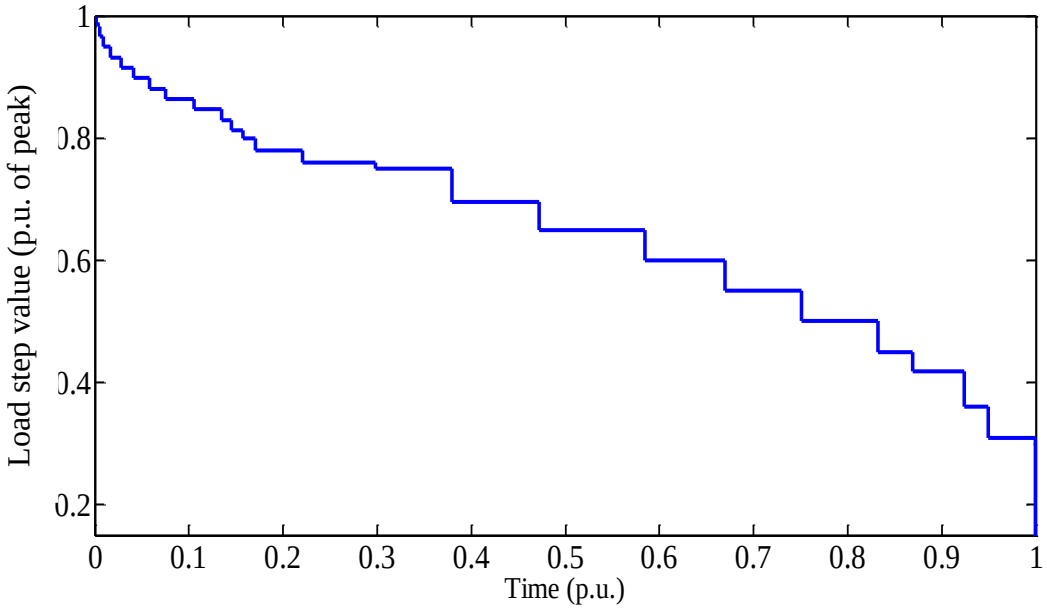

Figure 5.1: Annual 30-step load model of the IEEE-RTS

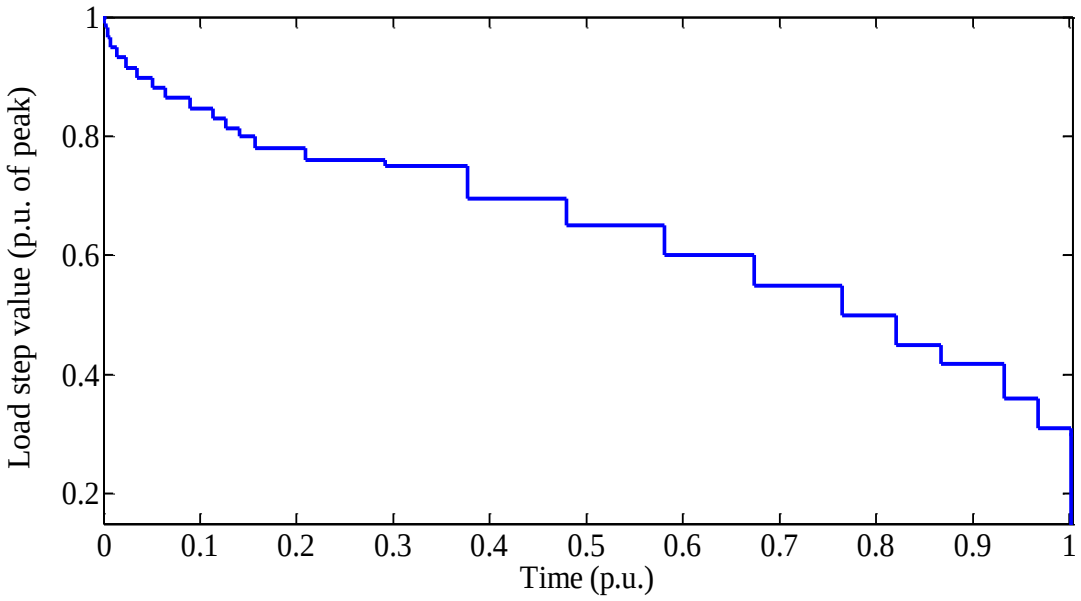

Figure 5.2: Modified annual 30-step load model incorporating wind curtailment from a 198 MW wind farm

5.2.6 Validation of the proposed technique

The accuracy of the technique developed for HL II adequacy analysis including wind curtailments using the 30-step load models is assessed in this section. In order to conduct this assessment, the system reliability indices were first evaluated using the analytical technique described in Chapter 4 for HL I adequacy analysis including wind power curtailments. Subsequently, the same system reliability indices are evaluated using the proposed technique for HL II reliability assessment including wind curtailments.

In order to compare the proposed technique for HL II reliability studies with the previously developed analytical technique for HL I studies, the transmission lines are assumed to be 100% reliable and have no constraints on the power transfer capability. The system considered in the following studies is the IEEE-RTS. A 198 MW wind farm located near Swift Current is

connected to Bus 6 of the power system. The load model in Figure 5.2 was used for Bus 6, whereas the model in Figure 5.1 was used for the remaining load buses in the proposed MCS-based technique using MECORE. The various reliability indices are computed for a peak load of 3500 MW.

The second column in Tables 5.5 shows the values of the reliability and wind energy utilization indices evaluated using the analytical approach described in Chapter 4. The last column shows the same indices using the proposed MCS-based technique using MECORE. It is observed that the numerical values of the indices obtained using the two different evaluation techniques are very close. It can be concluded that the proposed technique for HL II system reliability and wind energy utilization assessment can accurately include wind curtailment scenarios, by applying the negative load approach to wind power modelling.

Table 5.5: Validation of the proposed technique using the HL-I analytical technique

	Analytical technique	**Proposed technique**
LOLE (h/yr)	62.72	63.21
LOEE (MWh/yr)	8465.3	8480.8
PLCC (MW)	2456.7	2456.1
IPLCC (MW)	64.2	64.0
CC (%)	32.4	32.3
WES (GWh/yr)	499.947	499.922
WESP (GWh/yr)	0.082	0.087
Fuel saving (M$/yr)	18.79	18.69
CO_2 (T/yr) reduction	322199	322187
SO_x (T/yr) reduction	1379	1368
NO_x (T/yr) reduction	768	758

5.3 Generation and transmission contribution to wind curtailments and the impact on bulk system reliability

Bulk system reliability evaluation considers the limitation of the transmission line capability in delivering generated power to the bulk load points. A rescheduling of generation is conducted during the evaluation process to alleviate a line congestion event when encountered. The developed methodology is applied to the modified IEEE-RTS to assess the impact on bulk system reliability by considering wind curtailment due to the generation constraints in addition to the transmission limitations.

5.3.1 The modified IEEE-RTS

A single line diagram of the IEEE-RTS [58] is shown in Figure 5.3. The generating system has a total thermal power generating capacity of 1274 MW (37% of total capacity), hydro generating capacity of 300 MW (9%) and combustion turbine-based generating capacity of 80 MW (2%). It should be noted that the current power generation system in Saskatchewan contains 37% of thermal power generating capacity, 21% of hydro generating capacity, and 38% of combustion turbine-based generating capacity. The generating capacity mix of the IEEE-RTS was modified to have the generation type and capacity similar to that of the Saskatchewan power system for comparable studies. Table 5.6 shows the type, location, FOR and MCR data of the generating units added to modify the IEEE-RTS. The buses with relatively poor reliability [18] were selected for connecting the additional generating units in Table 5.6. The modified IEEE-RTS, designated at the MRTS, has a total conventional generating capacity of 3859 MW, and is used for the subsequent HL II studies.

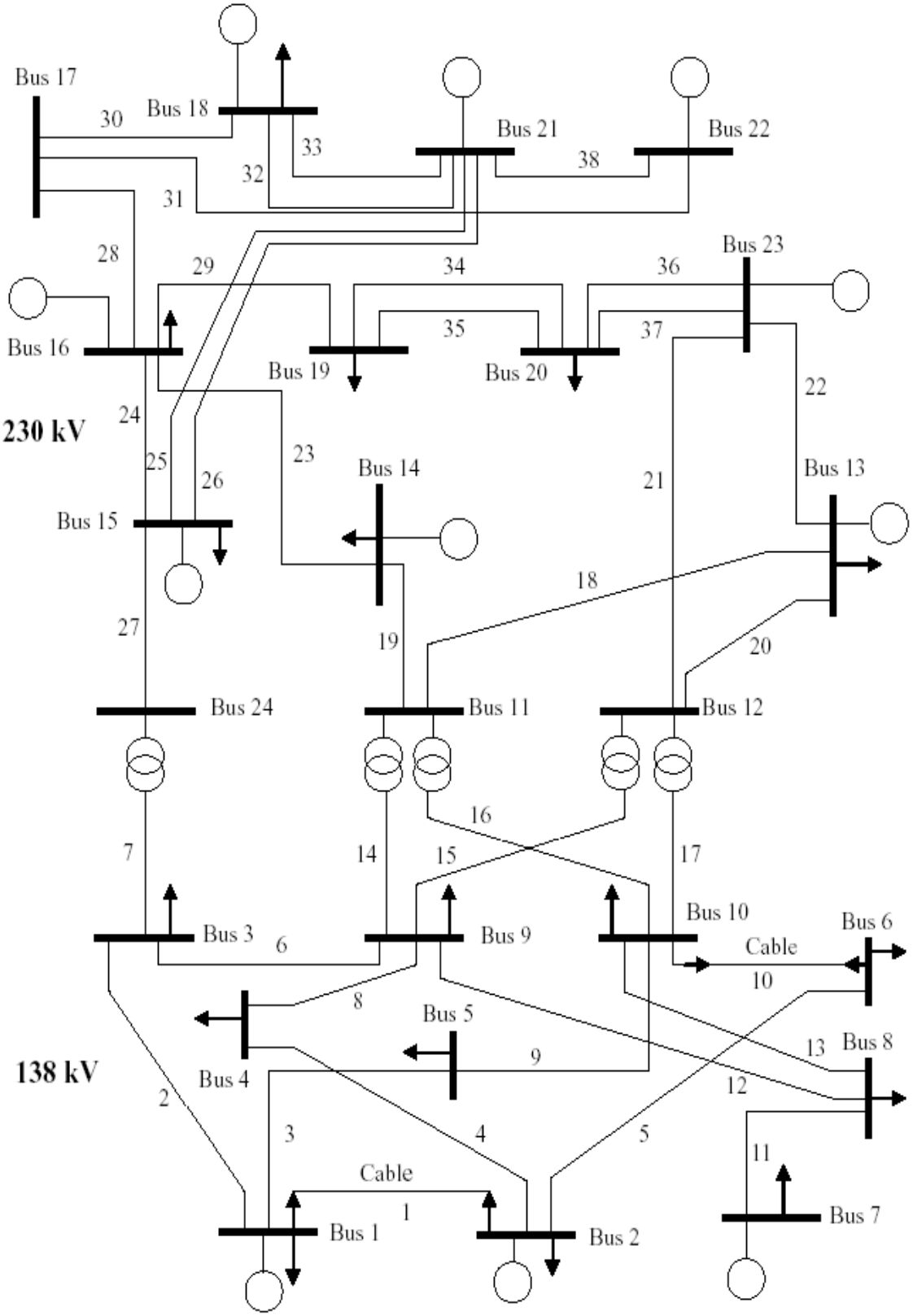

Figure 5.3: Single line diagram of the IEEE-RTS

Table 5.6: Generating units added to the IEEE-RTS

Unit type	Unit name	Bus number	FOR (%)	MCR (MW)
Hydro	H1	6	0.58	62
	H2	6	6.91	62
	H3	6	0.29	62
	H4	2	0.55	34
	H5	2	1.61	34
	H6	2	0.64	34
	H7	2	1.14	34
	H8	2	1.04	34
	H9	2	1.72	34
	H10	10	1.47	42
	H11	10	0.30	42
	H12	3	0.18	14
	H13	3	0.14	14
	H14	3	2.10	14
	H15	3	1.38	14
	H16	3	0.14	15
	H17	3	0.20	15
	H18	3	0.10	15
	H19	13	0.09	85
	H20	13	0.13	85
CCGT	CT1	15	4.50	260
	CT2	14	3.00	228
	CT3	9	6.00	246
	CT4	19	5.18	312
	CT5	20	6.00	246
SCGT	CT6	16	2.40	56
	CT7	16	2.40	56
	CT8	16	2.40	56

5.3.2 Evaluation of the HL II reliability indices

The MRTS consists of a wind farm located near Swift Current connected to Bus 4 of the system. The system LOLE are evaluated for the MRTS considering three wind penetration levels considering installed wind capacities of 198 MW, 428 MW and 728 MW respectively. A 30-step

load model was created for each wind penetration study as described in Section 5.2.3. The system peak load of 3500 MW was considered in the studies.

Table 5.7 shows the results of HL II studies conducted on the wind-integrated MRTS both with and without considering wind curtailment due to generation constraints. The LOLE values in hours per year after conducting the initial HL II study considering wind curtailment due to transmission constraints are shown in Table 5.7. It is observed from Table 5.7 that additional wind curtailment due to generation constraints results in an increase in LOLE for the three wind penetration levels. The difference in percent between the system LOLE values with and without considering wind curtailment due to generation constraints is 4.86%, 11.82% and 19.36% when the wind farm capacity is 198 MW, 428 MW and 728 MW, respectively. It is observed that the percentage difference between the LOLE values increases as the wind penetration increases. Therefore, it is important to consider wind curtailment due to both generation and transmission constraints to obtain a reasonable assessment of system reliability, especially at high wind penetration levels.

Table 5.7: System LOLE considering wind curtailment due to generation and transmission constraints

Wind farm capacity (MW)	**LOLE (h/yr)**	
	Curtailment due to generation & transmission constraints	**Curtailment due to transmission constraints**
198	11.12	10.58
428	8.42	7.41
728	7.59	6.12

5.4 Impact of wind growth on the reliability and wind energy utilization

This section examines the impact of wind power growth on wind energy curtailments, and the resulting reliability and energy indices. It is assumed that the wind penetration in the MRTS

grows from 4.9%, to 9.9%, and then to 16.0% in the following studies. The resulting installed wind capacities are 198 MW, 428 MW and 728 MW respectively. This study considers both the HL I and HL II evaluation to compare the impact of wind curtailment (WC) due to generation and transmission limitations on the system LOLE. Three cases were examined in this study: (1) system reliability evaluation considering no wind curtailment, (2) system reliability evaluation considering wind curtailment due to generation constraints and (3) system reliability evaluation considering wind curtailment due to generation and transmission constraints. The results are shown in Figure 5.4.

It can be seen that the LOLE decreases as wind penetration in the MRTS increases for all three cases. It is observed that highly optimistic reliability evaluation results are obtained when no wind curtailment is considered. The LOLE values are the lowest as shown in the bottom curve in Figure 5.4. There is an increase in the LOLE as seen in the middle curve in Figure 5.4 when wind curtailment due to generation constraints is considered in the reliability evaluation. The LOLE values obtained without considering any wind curtailment increase by 4.35%, 16.22% and 40.19% when wind curtailment due to generation constraints is considered at the three wind penetration levels in increasing order. With the consideration of generation and transmission constraints in the adequacy assessment, the LOLE values increase further by 10.42%, 25.23% and 65.28% at the three wind penetration levels in increasing order, as shown by the top curve in Figure 5.4. The figure shows that the impact of wind curtailments increase substantially as the wind penetration grows in a power system.

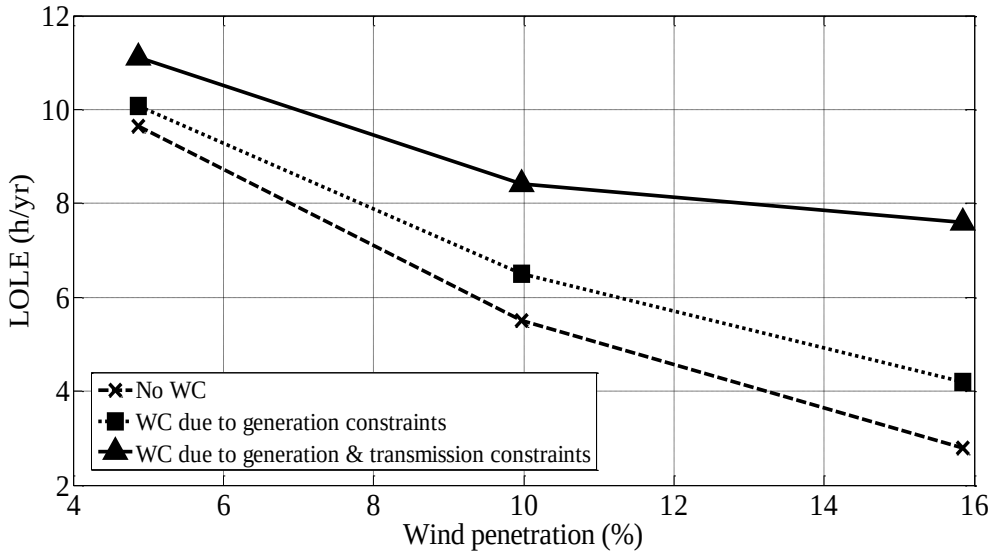

Figure 5.4: Impact of wind growth on system LOLE

The next study evaluates the system load carrying capabilities for the three cases. The system PLCC values were calculated considering a LOLE criterion of 1 hr/yr. The PLCC of the system considering the wind power, and the IPLCC due to wind power contribution are shown in Table 5.8. The capacity credit of wind power is the IPLCC due to its contribution expressed as a percentage of its rated wind farm capacity. Figure 5.5 show the CC of the wind farms for the three cases calculated for the three penetration levels.

Table 5.8: Impact of wind power growth and wind curtailments on load carrying capability

	PLCC (MW)			**IPLCC (MW)**		
Wind farm capacity	**198 MW**	**428 MW**	**728 MW**	**198 MW**	**428 MW**	**728 MW**
Curtailment due to generation & transmission constraints	2653.2	2665.4	2686.4	59.4	94.5	128.2
Curtailment due to generation constraints	2680.5	2702.8	2771.9	64.0	103.2	141.5
No wind curtailment	2681.2	2705.9	2777.9	65.2	107.4	149.7

The PLCC values at the three wind penetration levels without considering wind curtailment are shown in the last row in Table 5.8. When wind curtailment from generation constraints is considered, these values decrease by 0.68 MW, 3.13 MW and 6.12 MW when the installed wind capacities are 198 MW, 428 MW and 728 MW, respectively. The IPLCC values without considering wind curtailment are also shown in the last row in Table 5.8. When wind curtailment from generation constraints is considered, these IPLCC values decrease by 1.2 MW, 4.2 MW and 8 MW, respectively at the three wind penetration levels in the increasing order.

The additional wind power curtailment due to transmission line constraints causes a reduction in the IPLCC due to wind power. The IPLCC values considering wind curtailment from only generation constraints are shown in the fourth row in Table 5.8. It is observed that these IPLCC values are reduced by 4.5 MW, 8.7 MW and 13.3 MW as a result of additional wind power curtailment from transmission constraints when the installed wind capacities are 198 MW, 428 MW and 728 MW respectively. It can be seen that there are larger reductions in PLCC benefits due to wind power curtailment at higher wind penetrations.

It can be seen that wind capacity credit decreases with wind penetration. There is a reduction in the capacity credit of wind when wind power curtailment due to generation constraints is considered in the evaluation, which reduces further when wind curtailment due to transmission constraints is considered. The CC values considering wind curtailment from generation constraints are shown in the middle curve in Figure 5.5. When wind curtailment from both generation and transmission constraints are considered, these values decrease by 4.0%, 8.3% and 9.3%, respectively at the three wind penetration levels in the increasing order.

The wind energy indices, wind energy supplied and wind energy spilled, are evaluated to assess the impact of wind power growth and wind curtailment on the wind energy utilization.

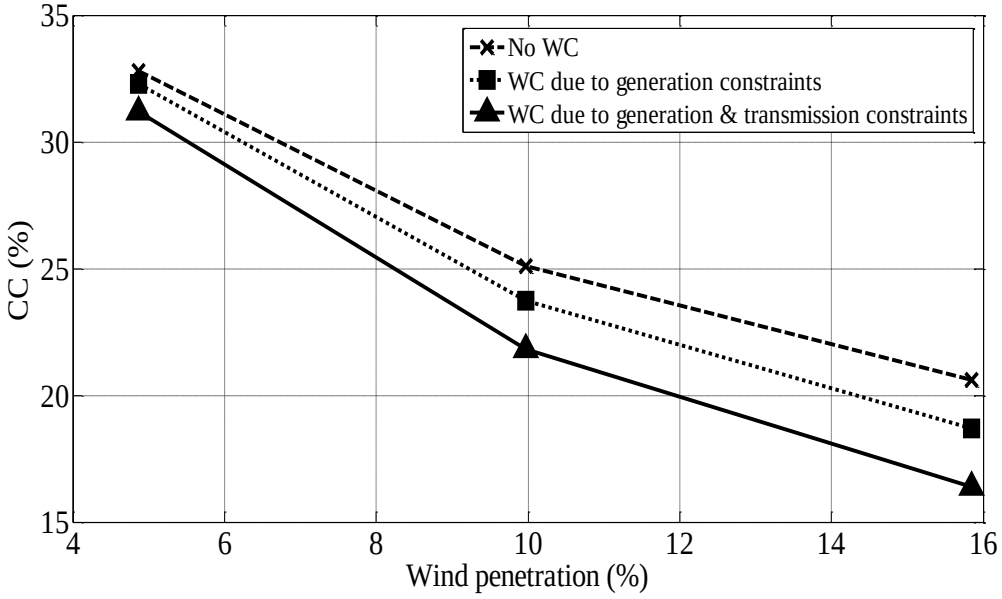

Figure 5.5: Impact of wind growth on the CC

The total expected wind energy available at the wind site for the three penetration levels are 500.0, 1167.6 and 2065.2 GWh per year in the increasing order. The WES in GWh increases with wind penetration. There is no wind energy spillage in the first case study as wind energy curtailments are not considered. The WES and WESP in percent of the available wind energy are shown in Figure 5.6 and Figure 5.7 for the second and third case studies respectively with increasing wind penetration. In these cases, the percent WES decreases as wind energy is spilled with increasing wind penetration as shown. The wind energy spilled increases by 0.04%, 5.00% and 11.12% of the available wind energy due to wind curtailment from generation constraints when the installed wind capacities are 198 MW, 428 MW and 728 MW respectively. The WES is reduced by 1.88%, 16.33% and 20.32% of the available wind energy due to wind energy spillage when wind curtailment due to both generation and transmission limitations are considered. It can be seen that the wind energy spilled increases significantly as the wind

penetration increases, and therefore, it is very important to consider wind energy curtailments in the evaluation.

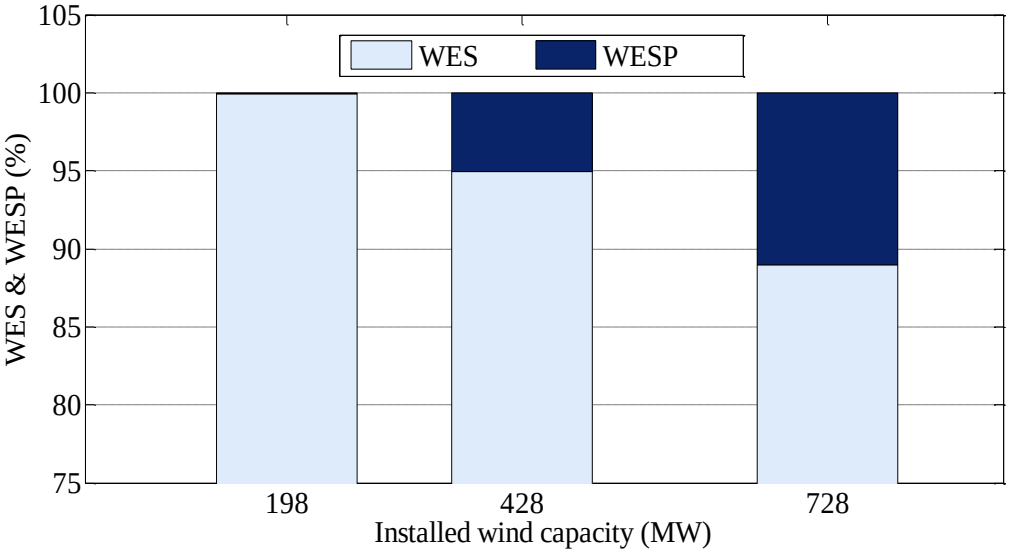

Figure 5.6: Impact of wind growth on the wind energy utilization considering wind curtailment due to generation constraints

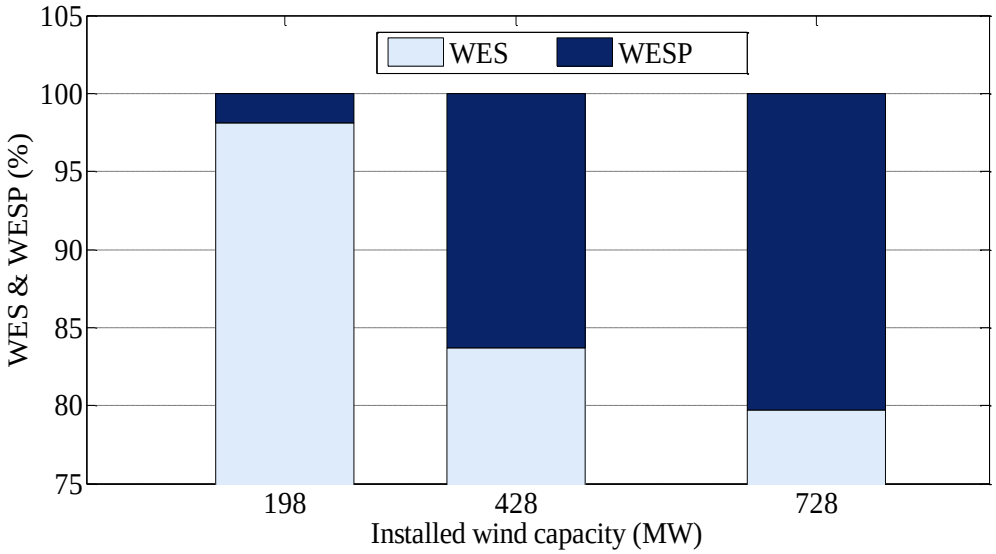

Figure 5.7: Impact of wind growth on the wind energy utilization considering wind curtailment due to generation and transmission constraints

The utilization of wind energy results in conventional fuel savings. The conventional fuel energy offset due to utilization of wind energy can be represented in monetary terms by multiplying the wind energy utilized by the marginal energy cost. Figure 5.8 shows the fuel energy saved in million dollars per year which is calculated using a marginal energy cost of $37.60/MWh. It can be seen that the fuel savings increase with wind penetration, but the reduction in fuel savings due to wind energy curtailment considering both generation and transmission constraints also increases with the increase in wind penetration.

The offset in conventional fuel, mainly coal and natural gas, due to wind energy utilization results in the reduction in greenhouses gas emissions as discussed earlier. The reduction in CO_2, SO_x and NO_x emissions in tonnes per year due to offset in coal and natural gas energy are calculated for the three wind penetration levels, and are shown in Table 5.9. The reduction in GHG emissions increases as the system wind penetration increases from 198 MW to 728 MW.

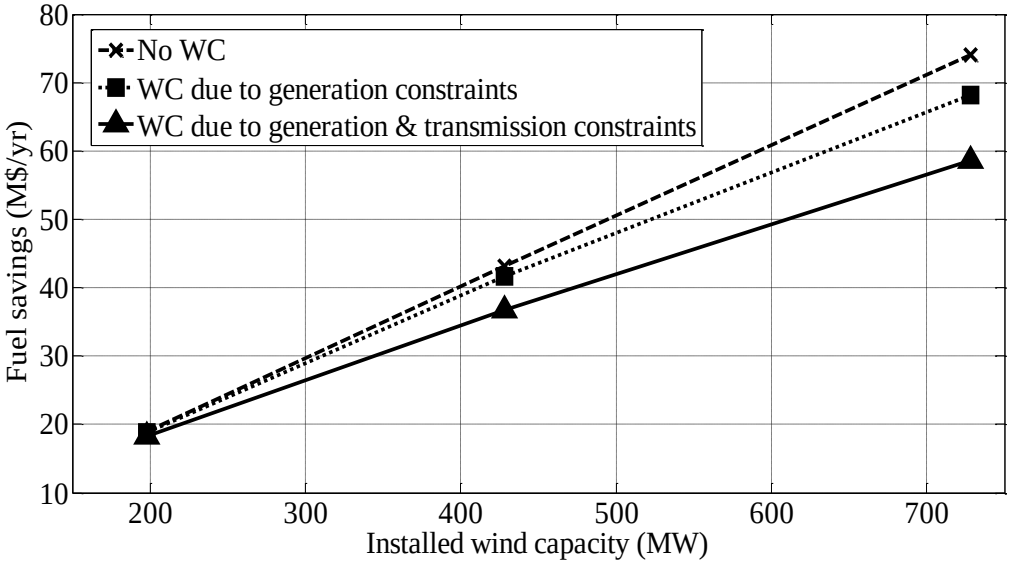

Figure 5.8: Impact of wind growth on the fuel savings

Table 5.9: Impact of wind power curtailment on GHG emissions

	Curtailment due to generation constraints			Curtailment due to generation & transmission constraints		
Wind farm capacity	**198 MW**	**428 MW**	**728 MW**	**198 MW**	**428 MW**	**728 MW**
CO_2 reduction (T/yr)	360336	790885	1345244	346541	771860	1248565
SO_x reduction (T/yr)	1460	3126	5471	1447	2881	4763
NO_x reduction (T/yr)	813	1742	3048	806	1605	2654

A comparison of the results shows that there is a reduction in the environmental benefits from GHG reduction due to wind power curtailment considering generation constraints. This reduction in the environmental benefits from GHG reduction increases further when additional wind power curtailment due to transmission constraints is considered. As the wind penetration in the system increases, the negative impact of wind power curtailment on the reduction in GHG emissions also increases.

5.5 Consideration of wind diversity in bulk power system reliability and wind energy benefit assessment

The location of a wind farm in the power system can have a significant impact on the system reliability indices and wind energy utilization indices. Based on the capacity of the wind farm connected to a particular bus in the power system, the number of transmission lines connected to the bus and also the power transfer capacity of the transmission lines, the system reliability and wind energy utilization benefits can be different.

It has been observed from the HL I studies in Chapter 4 using a practical power system that wind diversity significantly effects the system reliability and wind energy utilization. However,

the transmission line outages and power transfer capability were not considered. The effect of transmission line constraints on the benefits from wind diversity and also on the wind curtailment has been examined in this section.

5.5.1 Development of HL II evaluation technique considering wind speed correlation and wind power curtailment

A power system is considered to be connected to two wind farms, WF1 and WF2, which are located in two different areas having Swift Current and Regina wind characteristics, respectively.

The wind speed characteristic of WF1 is represented by the ARMA model in (5.1), and that of WF2 [29] is represented by the time series, y_t in (5.7).

$$y_t = 0.9336y_{t-1} + 0.4506y_{t-2} - 0.5545y_{t-3} + 0.1110y_{t-4} + \alpha_t$$
$$- 0.2033\alpha_{t-1} - 0.4684\alpha_{t-2} + 0.2301\alpha_{t-3} \tag{5.7}$$
$$\alpha_t \in NID(0, 0.409423^2)$$

The two sets of hourly wind speed data are simulated with correlated random numbers in order to obtain a particular correlation between the two wind sites. The generation of correlated random numbers can be achieved using different techniques. The proposed technique uses the Cholesky Decomposition [59] method. The basic equation for generating a set of correlated random numbers is as follows:

$$X_C = X_1 \cdot \sigma + X_2 \cdot \sqrt{1-\sigma^2} \tag{5.8}$$

Where, X_1 and X_2 are a series of uncorrelated random numbers; σ is the desired correlation coefficient for WF2 which can be varied between 0 and 1. Series X_C obtained using (5.8) has a correlation of σ with series X_1.

The wind speed series for WF1 can be simulated using the random number series X_1 in (5.1) and (5.2). The wind speed series for WF2 can be simulated using the random number series X_C in (5.7) and (5.2). The hourly mean and hourly standard deviation values used for the two wind sites were obtained from Environment Canada [45]. Wind speed data for 1000 yearly samples were simulated for both the wind sites. The hourly wind power outputs for the two sites can then be computed using the power curve relation in (2.6).

The hourly values of the wind power absorbed (WPA) from WF1 are initially found using (4.1). A discrete probability distribution table is then built using these hourly wind power absorbed values. The number of class intervals and the width of each interval in the discrete probability distribution is found using Sturges' rule [57]. The MECORE software allows a maximum of 10 wind power output states. An apportioning method [18] is used to reduce the number of output states in the probability distribution table from 22 to 10, and create a 10-state probability distribution of the wind power absorbed. This wind power model is considered as a generation model, and not as a negative load model as in the previous bulk system studies. A similar approach is followed to create a separate probability distribution of the wind power absorbed from WF2.

The advantage of the technique described in this section is that both the wind power curtailment and diversity effects are included in the HL II analysis and all the load buses use the same load model. The 30-step load model shown in Figure 5.1 represents the load characteristics at all the load buses. The load point reliability and wind energy utilization indices are computed using (5.3). The reliability and the wind energy utilization indices for the entire power system are found using (5.6).

5.5.2 Sensitivity studies considering increase in wind penetration

The subsequent studies on the MRTS consider wind diversity as the wind capacity is assumed to be distributed between the two diversely located wind farms WF1 and WF2 connected at Bus 4 and 19, respectively of the system. The correlation in wind speed, σ between the two sites is 0.38. In the first study, the 198 MW wind capacity is distributed between the two wind farms: a 171.6 MW farm at the Swift Current area and a 26.4 MW farm at the Regina area. A wind capacity growth of 230 MW was considered at the Swift Current area to increase the total capacity to 428 MW. An additional 300 MW capacity was considered at the Regina area to raise the wind capacity to 728 MW in the studies. Wind curtailments due to both generation and transmission constraints are considered. Table 5.10 shows the system reliability and wind energy utilization for the three wind penetration levels.

Table 5.10: Impact of wind diversity on system reliability and wind energy utilization

	LOLE (h/yr)			**WES (%)**		
Wind farm capacity	**198 MW**	**428 MW**	**728 MW**	**198 MW**	**428 MW**	**728 MW**
Considering wind diversity	10.84	6.94	4.55	99.27	91.77	88.18
Without wind diversity	11.32	8.64	7.89	98.12	83.70	79.70

A comparison of the LOLE indices obtained with and without wind diversity show that the system reliability significantly improves when wind diversity is considered. The improvement in the resulting indices increases as the wind power grows in the system. A comparison with the results in Figure 5.4 show that the degradation in system reliability as a result of wind power curtailment at high wind penetration levels can be considerably offset if the total wind capacity is geographically distributed at diverse wind sites. The total expected wind energy available at the

wind sites for the three penetration levels are 500.0, 1167.6 and 2065.2 GWh per year in the increasing order. A comparison of the WES results with and without considering wind diversity shows that there is increase in the wind energy utilized by the system due to wind capacity diversification, and the wind utilization benefit increases with wind growth.

Table 5.11 compares the wind capacity credit for three cases. The results in the second row do not incorporate wind curtailment or diversity in the evaluation, and shows that the wind CC decreases with increase in wind penetration in a power system. The results in the third row show decrease in CC when wind curtailment due to both generation and transmission constraints is considered. The fourth row incorporates both wind curtailment and diversity in the evaluation. A comparison of the results in the third and the last row shows that the wind CC increases due to wind diversity.

Table 5.11: Impact of wind growth on wind capacity credit

Wind farm capacity (MW)	**198**	**428**	**728**
No wind curtailment, no wind diversity	32.8%	25.1%	20.5%
With wind curtailment, no wind diversity	30.0%	22.1%	17.6%
With wind curtailment, and wind diversity	32.0%	24.1%	19.2%

The results in Tables 5.10 and 5.11 were obtained when the wind capacity was diversified between the Swift Current and Regina location, the wind speeds between which has a correlation coefficient, σ of 0.38. Three different correlation coefficients, 0, 0.38 and 0.65 were used in the following studies in order to evaluate the impact of varying the wind diversity between two wind farms connected to a power system. The distribution of the installed wind capacity at the two locations is similar to the previous study. Table 5.12 shows the system LOLE and the wind

energy utilization index, WES obtained considering the three different levels of wind diversity between the two wind farms.

Table 5.12: Impact of wind diversity on system reliability and wind energy utilization

	LOLE (h/yr) for wind capacity of			**WES (%) for wind capacity of**		
Correlation coefficient, σ	**198 MW**	**428 MW**	**728 MW**	**198 MW**	**428 MW**	**728 MW**
0.65	11.09	7.57	5.39	99.16	88.55	85.89
0.38	10.84	6.94	4.55	99.27	91.77	88.18
0.00	10.53	6.20	3.61	99.42	94.67	91.06

The level of system reliability and WES indices of the MRTS are the highest when there is no correlation between the wind speeds at Swift Current and Regina. When σ is increased to 0.38, the system LOLE values increased by 2.94%, 10.90% and 26.03%, at the three wind penetration levels in the increasing order. The system LOLE values increased further by 2.31%, 9.50% and 26.03%, when σ is subsequently increased to 0.65. It is observed that the percentage difference between the LOLE and WES values obtained when the wind farms are independent and when the wind farms are correlated increases with the increase in wind penetration. It is clearly seen that the level of wind speed correlation plays an important role in the reliability and wind energy utilization benefits obtained from wind diversity.

Table 5.13 shows the wind capacity credit, CC obtained considering the three different levels of wind diversity between the two wind farms. The CC values are the highest when no correlation existed between the wind speeds at Swift Current and Regina. When σ is increased to 0.38, the CC values decreased by 2.14%, 5.37% and 8.89%, at the three wind penetration levels in the increasing order. The CC decreased further by 1.88%, 4.85% and 7.79%, when σ is subsequently increased to 0.65. It is also observed that the percentage difference between the CC

values obtained when the wind farms are independent and when the wind farms are correlated increases with the increase in wind penetration.

Table 5.13: Impact of wind growth on wind capacity credit

	CC (%) for wind capacity of		
Correlation coefficient, σ	**198 MW**	**428 MW**	**728 MW**
0.65	31.4	23.1	17.8
0.38	32.0	24.1	19.2
0.00	32.7	25.2	20.6

5.6 Conclusions

This chapter presents new techniques for HL II reliability and wind energy utilization assessment considering wind power both as negative load model and as generation model. Wind curtailment was initially incorporated in the HL II evaluation technique by applying the negative load approach to wind modeling. The impact of wind power curtailments due to both transmission and generation constraints was analyzed by utilizing the proposed HL II evaluation technique. It is seen that the additional wind energy curtailment due to transmission line constraints results in a decrease in system reliability and wind energy utilization in a wind-integrated bulk power system. The reduction in system reliability and wind energy benefits increases as the wind penetration increases to higher levels.

A HL II evaluation technique was also developed considering wind power as generation model to incorporate wind speed correlation between two diverse wind sites. The proposed technique was simple and demonstrated high accuracy. Further sensitivity studies were also conducted by varying the wind penetration level in the power system. It is seen that at the HL II level, wind diversity significantly offsets the degradation in wind energy utilization and system reliability due to wind energy curtailments. It is also seen that the level of wind speed correlation

significantly affects the degree of reliability and wind utilization benefits obtained due to the diversification of wind resource. The percentage difference between the system reliability and wind energy utilization indices obtained when the wind farms are independent and when the wind farms are correlated increases with the increase in wind penetration.

6 SUMMARY AND CONCLUSIONS

Electric utilities in many countries are supported by their governments to increase the utilization of renewable energy resources such as wind energy to reduce the impact of GHG emissions on the environment. It has been seen over the past decade that the application of wind energy resources in power systems has increased rapidly. With the increase in wind penetration, the curtailment of wind energy increases due to transmission line constraints and generating unit limitations arising from the intermittent and uncertain nature of wind power. The combined effect of factors such as wind curtailment and wind diversity has not been considered in existing techniques for adequacy assessment of wind integrated power systems. The primary goal of this research was to evaluate the reliability and energy contribution of large scale wind energy systems considering the forced curtailment of wind power with the increase in wind growth in power systems. Various reliability and wind energy utilization indices are used in this thesis for conducting studies on test power systems.

Chapter 1 describes the existing research on reliability evaluation of wind integrated power systems and also some of the problems which have not been addressed by researchers. The chapter also presents the problem statement and the outline of the thesis. Chapter 2 describes the fundamental concepts for reliability evaluation of a wind integrated power system. The chapter describes the detailed procedure of modelling the system load and the power system generation. A small power system with four conventional generating units and one wind farm was considered to further explain the different concepts and the procedure of reliability and wind energy utilization assessment. By using a simple wind integrated power system model, the basic concepts and reliability evaluation techniques were illustrated. The key concepts required to

conduct a Monte Carlo simulation, and obtain the reliability indices of a bulk power system were also discussed in Chapter 2.

Chapter 3 introduces a technique to accurately evaluate the wind power absorption capability of large scale power systems. The chapter considered a realistic power system in the analysis, consisting of different types of generating units. The analysis considered the response rates of the various generating units such as hydro, coal, gas and steam units to change in loading. An analysis of the wind power absorption capability of the system was carried out for all possible operating conditions of the system. The generating units were added, one at a time according to the priority loading order, to the base case generation schedule. The loading conditions were grouped into the low load and high load periods, and expected WPAC values were evaluated for each period. It was seen that the dispatch order of generating units and response rate of the conventional generating units to load change affected the WPAC of the power system, and significantly affected the adequacy of a wind integrated power system. These factors were considered in the system evaluation techniques described in Chapters 4 and 5.

Chapter 4 describes a new procedure for wind power modelling including the effect of wind curtailment. The indices related to the wind absorption capability were included in the analysis by following a negative wind power load modification approach. The proposed methodology was also capable of incorporating the diversity in wind power profiles at different geographical wind sites in the system studies. A realistic power system and wind data from wind farms in Saskatchewan, Canada were used to test the performance of the proposed technique.

The studies conducted in Chapter 4 clearly showed the degradation in system reliability as a result of wind curtailments. The wind power curtailments also resulted in a reduction in the system peak load carrying capability and the capacity credit of the connected wind farms. At

high levels of wind penetration, these effects were even more notable. There was also a reduction in the utilized wind energy by the system due to wind energy curtailment. If wind power curtailment is not considered in adequacy evaluation, the system utilizes all the available wind energy, resulting in no wind energy spillage. However, the limitations in generation ramping capabilities resulted in wind energy curtailment causing wind energy spillage. The increase in the installed wind capacity in the power system resulted in further spillage of wind energy.

The increase in the wind penetration resulted in conventional fuel savings; however the increase in these savings was constrained due to wind energy curtailment. Wind energy curtailments also reduced the environmental benefits from the reduction in GHG emissions. As the wind penetration increased, the wind resources were diversified between multiple wind farm locations. The wind capacity diversification alleviated the deterioration of system reliability, wind energy utilization and environmental benefits caused by wind curtailments. The combined impact of wind energy curtailment and diversity would increase further with the growth of the installed wind capacity in power systems, which makes it very important to be considered in system reliability and wind energy utilization assessment.

Chapter 5 presents novel techniques for HL II system reliability and wind energy utilization assessment. The techniques were capable of including wind curtailment scenarios in the system studies by utilizing the negative load approach to wind modelling. An analysis was also conducted to determine the optimal number of steps to be used for load modelling, which would result in an accurate and relatively fast evaluation of the reliability and wind energy utilization indices. The proposed bulk power system evaluation technique was capable of including the effect of wind power curtailments due to both transmission and generation constraints in the system studies. The additional wind curtailments due to transmission line constraints

significantly affected the reliability and wind energy utilization assessment of the wind-integrated bulk power system, particularly at a high wind penetration.

The HL II evaluation technique was further modified to incorporate wind speed correlation between two geographically diverse wind farms. The total wind capacity was diversified between two wind farm locations: Swift Current and Regina in Saskatchewan. However, the proposed technique can be easily applied to a power system with more than two geographically diverse wind farms connected to the system. Sensitivity studies were also conducted by varying the wind penetration level in the power system. The wind diversity substantially mitigated the degradation in wind energy utilization and system reliability due to wind curtailments. The wind speed correlation level between the geographically diverse wind farms also contributed to the degree of reliability and wind utilization benefits obtained due to wind capacity diversification. The level of system reliability and wind energy utilization in the power system were the highest when there was no correlation between the wind speeds at Swift Current and Regina. When the wind speed correlation level was increased to higher values, there was a reduction in the system reliability and wind energy utilization. The reduction in system reliability and wind energy utilization benefits increases with the increase in wind penetration.

Simple and accurate techniques that can be utilized to incorporate wind power in the reliability and the wind energy utilization assessment of a power generation system and bulk power system were developed in this thesis. The sensitivity of reliability and wind energy utilization indices to important factors such as wind curtailment and diversity are emphasized through the studies conducted in this thesis. As the wind penetration continues to grow in power systems, the techniques developed and the results obtained in this thesis would prove very useful to system planners for making decisions related to wind power integration.

LIST OF REFERENCES

[1] R. Billinton and R. N. Allan, “Reliability Evaluation of Power Systems,” 2nd ed. New York: Plenum, 1996.

[2] R. Billinton, “Criteria used by Canadian utilities in the planning and operation of generating capacity,” IEEE Trans. Power Syst., vol. 3, no. 4, pp. 1488–1493, 1988.

[3] P. Giorsetto and K. F. Utsurogi, “Development of a new procedure for reliability modeling of wind turbine generators,” IEEE Trans. Power Appar. Syst., vol. PAS-102, no. 1, pp. 134–143, 1983.

[4] S. H. Karaki, B. A. Salim, and R. B. Chedid, “Probabilistic model of a two-site wind energy conversion system,” IEEE Trans. Energy Convers., vol. 17, no. 4, pp. 530–536, 2002.

[5] F. C. Sayas and R. N. Allan, “Generation availability assessment of wind farms,” in IEE Proc. Gener. Transm. Distribution, vol. 143, no. 5, pp. 507–518, 1996.

[6] A. Sankarakrishnan and R. Billinton, “Sequential Monte Carlo Simulation for Composite Power System Reliability Analysis with Time Varying Loads,” IEEE Trans. Power Syst., vol. 10, no. 3, pp. 1540–1545, 1995.

[7] N. M. Pindoriya, P. Jirutitijaroen, D. Srinivasan, and C. Singh, “Composite Reliability Evaluation using Monte Carlo Simulation and Least Squares Support Vector Classifier,” IEEE Trans. Power Syst., vol. 26, no. 4, pp. 2483–2490, 2011.

[8] R. Karki, P. Hu, and R. Billinton, “Reliability Evaluation Considering Wind and Hydro Power Coordination,” IEEE Trans. Power Syst., vol. 25, no. 2, pp. 685–693, 2010.

[9] W. Li, “Installation Guide and User's Manual for the MECORE Program,” July 1998.

[10] C. W. E. Association, “Economic Benefits of Wind Energy,” 2013. [Online]. Available:http://www.canwea.ca/images/uploads/File/NRCan_-_Fact_Sheets/canwea-factsheet economic-web.pdf. [Accessed: 20-Apr-2015].

[11] SaskPower, “SaskPower Annual Report 2013,” 2013. [Online]. Available: http://www.saskpower.com/wp-content/uploads/2013_saskpower_annual_report.pdf. [Accessed: 30-Apr-2015].

[12] R. Billinton and G. Bai, “Generating Capacity Adequacy Associated With Wind Energy,” IEEE Trans. Energy Convers., vol. 19, no. 3, pp. 641–646, 2004.

[13] R. Karki and P. Hu, “Wind power simulation model for reliability evaluation,” in Proc. 2005 Canadian Conference on Electrical and Computer Engineering (CCECE), vol. 1, pp. 541–544, 2005.

[14] R. Karki, P. Hu, and R. Billinton, “A Simplified Wind Power Generation Model for Reliability Evaluation,” IEEE Trans. Energy Convers., vol. 21, no. 2, pp. 533–540, 2006.

[15] W. Wangdee and R. Billinton, “Considering load-carrying capability and wind speed correlation of WECS in generation adequacy assessment,” IEEE Trans. Energy Convers., vol. 21, no. 3, pp. 734–741, 2006.

[16] R. Billinton and B. Bagen, “A sequential simulation method for the generating capacity adequacy evaluation of small stand-alone wind energy conversion systems,” in Proc. 2002 Canadian Conference on Electrical and Computer Engineering (CCECE), vol. 1, pp. 72–77, 2002.

[17] Y. Gao and R. Billinton, “Adequacy assessment of generating systems containing wind power considering wind speed correlation,” IET Renew. Power Gener., vol. 3, no. 2, pp. 217–226, 2009.

[18] Y. Gao, “Adequacy assessment of electric power systems incorporating wind and solar energy,” University of Saskatchewan, 2006.

[19] M.-R. Haghifam and M. Omidvar, “Wind Farm Modeling in Reliability Assessment of Power System,” in Proc. 9th International Conference on Probabilistic Methods Applied to Power Systems, pp. 1–5, 2006.

[20] Y. Gao, R. Billinton, and R. Karki, “Composite generation and transmission system adequacy assessment considering wind energy seasonal characteristics,” in Proc. 2009 IEEE Power & Energy Society General Meeting, pp. 1–7, 2009.

[21] R. Billinton, R. Karki, Y. Gao, D. Huang, P. Hu, and W. Wangdee, “Adequacy Assessment Considerations in Wind Integrated Power Systems,” IEEE Trans. Power. Syst., vol. 27, no. 4, pp. 2297–2305, 2012.

[22] R. Billinton and W. Wangdee, “Reliability-Based Transmission Reinforcement Planning Associated With Large-Scale Wind Farms,” IEEE Trans. Power. Syst., vol. 22, no. 1, pp. 34–41, 2007.

[23] F. Chen, F. Li, Z. Wei, G. Sun, and J. Li, “Reliability models of wind farms considering wind speed correlation and WTG outage”, Electr. Pow. Syst. Res. (Elsevier), vol. 119, pp. 385–392, 2015.

[24] R. Karki, D. Dhungana, and R. Billinton, “An appropriate wind model for wind integrated power systems reliability evaluation considering wind speed correlations,” Appl. Sci., vol. 3, pp. 107–121, 2013.

[25] D. Dhungana and R. Karki, “Quantifying System Adequacy Benefit of Wind Power Diversity,” in Proc. 2014 IEEE Electrical Power and Energy Conference (EPEC), pp. 82–86, 2014.

[26] Y. Degeilh and C. Singh, “A quantitative approach to wind farm diversification and reliability,” Int. J. Electr. Power Energ. Syst. (Elsevier), vol. 33, no. 2, pp. 303–314, 2011.

[27] R. Billinton, Y. Gao, and R. Karki, “Composite System Adequacy Assessment Incorporating Large-Scale Wind Energy Conversion Systems Considering Wind Speed Correlation,” IEEE Trans. Power Syst., vol. 24, no. 3, pp. 1375–1382, 2009.

[28] R. Billinton and D. Huang, “Incorporating Wind Power in Generating Capacity Reliability Evaluation Using Different Models,” IEEE Trans. Power Syst., vol. 26, no. 4, pp. 2509–2517, 2011.

[29] R. Billinton, H. Chen, and R. Ghajar, “Time-series models for reliability evaluation of power systems including wind energy,” Microelectron. Reliab., vol. 36, no. 9, pp. 1253–1261, 1996.

[30] P. M. T. Broersen, “Automatic Autocorrelation and Spectral Analysis,” ser. Springer eBooks. London, U.K.: Springer-Verlag London Limited, 2006.

[31] R. Billinton and Y. Li, “Incorporating multi-state unit models in composite system adequacy assessment,” Eur. Trans. Elect. Power, vol. 17, no. 4, pp. 375–386, Jul./Aug. 2007.

[32] R. Billinton, B. Karki, R. Karki, and G. Ramakrishna, “Unit Commitment Risk Analysis of Wind Integrated Power Systems,” IEEE Trans. Power Syst., vol. 24, no. 2, pp. 930–939, 2009.

[33] D. J. Burke and M. J. O’Malley, “Factors Influencing Wind Energy Curtailment,” IEEE Trans. Sustain. Energ., vol. 2, no. 2, pp. 185–193, 2011.

[34] E. McKenna, P. Grünewald, and M. Thomson, “Going with the wind: temporal characteristics of potential wind curtailment in Ireland in 2020 and opportunities for demand response,” IET Renew. Power Gen., vol. 9, no. 1, pp. 66–77, 2015.

[35] Y. Gu, L. Xie, B. Rollow, and B. Hesselbaek, “Congestion-induced wind curtailment: Sensitivity analysis and case studies,” in Proc. 2011 North American Power Symposium (NAPS), pp. 1–7, 2011.

[36] Y. Gu and L. Xie, “Fast Sensitivity Analysis Approach to Assessing Congestion Induced Wind Curtailment,” IEEE Trans. Power Syst., vol. 29, no. 1, pp. 101–110, 2014.

[37] I. Pierre et al, “Flexible Generation: Backing Up Renewables,” Eurelectric Renewables Action Plan, Eurelectric, Brussels, D/2011/12.105/47, 2011.

[38] B. Kirby and E. Hirst, “Generator Response to Intrahour Load Fluctuations,” IEEE Trans. Power Syst., vol. 13, no. 4, pp. 1373–1378, 1998.

[39] R. Karki, D. Dhungana, S. Shimu, and R. Billinton, “Reliability evaluation incorporating the load following capability of wind generation,” in Proc. 2013 26th Annual IEEE Canadian Conference on Electrical and Computer Engineering (CCECE), pp. 1–4, 2013.

[40] S. Martín-Martínez, E. Gómez-Lázaro, A. Molina-Garcia, and A. Honrubia-Escribano, “Impact of Wind Power Curtailments on the Spanish Power System Operation,” in Proc. 2014 IEEE PES General Meeting Conference & Exposition, pp. 1–5, 2014.

[41] C. Singh and A. Lago-Gonzalez, “Reliability modeling of generations systems including unconventional energy sources,” IEEE Trans. on Power Apparatus and Systems, vol. PAS-104, no. 5, pp. 1049–1055, 1985.

[42] B. Cleary et al., “Assessing the Economic Benefits of Compressed Air Energy Storage for Mitigating Wind Curtailment,” IEEE Trans. Sustain. Energ., vol. PP, no. 99, pp. 1–8, 2015.

[43] M. Moradzadeh, B. Zwaenepoel, J. Van de Vyver, and L. Vandevelde, “Congestion-induced wind curtailment mitigation using energy storage,” in Proc. 2014 IEEE International Energy Conference (ENERGYCON), pp. 572–576, 2014.

[44] R. Karki and D. Dhungana, “Reliability evaluation of the SaskPower system considering regional wind power integration,” Power Systems Research Group, University of Saskatchewan, 2013.

[45] Environment Canada, “Canadian Weather Energy and Engineering Datasets (CWEEDS).” [Online]. Available:ftp://ftp.tor.ec.gc.ca/Pub/Engineering_Climate_Dataset/Canadian_Weather_Energy_Engineering_Dataset_CWEEDS_2005/ZIPPED FILES/ENGLISH/. [Accessed: 22-Feb-2014].

[46] T. R. Oke, “Initial Guidance to Obtain Representative Meteorological Observations at Urban Sites,” Geneva, 2006.

[47] J. H. Seinfeld and S. N. Pandis, “Atmospheric Chemistry and Physics: From Air Pollution to Climate Change,” 2nd ed. Hoboken, New Jersey: WILEY, 2006.

[48] W. Katzenstein, “Wind power variability, its cost, and effect on power plant emissions,” Carnegie Mellon University, 2010.

[49] R. Billinton and Y. Gao, “Multistate wind energy conversion system models for adequacy assessment of generating systems incorporating wind energy,” IEEE Trans. Energy Convers., vol. 23, no. 1, pp. 163–170, 2008.

[50] Resource and Transmission Adequacy Task Force of the NERC Planning Committee, "Resource and Transmission Adequacy Recommendations," NERC Board of Trustees, June 15, 2004.

[51] R. Billinton and W. Li, "Hybrid approach for reliability evaluation of composite generation and transmission systems using Monte-Carlo simulation and enumeration technique," IEE Proceedings-C, vol. 138, no. 3, pp. 233–241, 1991.

[52] R. Billinton and W. Wangdee, "Impact of Utilizing Sequential and Non-Sequential Simulation Techniques in Bulk Electric System Reliability Assessment," IEE Gener. Transm. Distribution, vol.152, no. 5, pp. 623–628, 2005.

[53] R. Billinton and W. Li, "Reliability Assessment of Electrical Power System Using Monte Carlo Methods," Plenum Press, New York, 1994.

[54] F. Aminifar, M. Fotuhi-Firuzabad, and M. Shahidehpour, "Unit Commitment With Probabilistic Spinning Reserve and Interruptible Load Considerations," IEEE Trans. Power Syst., vol. 24, no. 1, pp. 388–397, 2009.

[55] E. Arriagada et al, "A probabilistic economic dispatch model and methodology considering renewable energy, demand and generator uncertainties," Electr. Pow. Syst. Res., vol. 121, pp. 325–332, 2015.

[56] P. Jaramillo, W. M. Griffin, and H. S. Matthews, "Comparative Life-Cycle Air Emissions of Coal, Domestic Natural Gas, LNG, and SNG for Electricity Generation," Environ. Sci. Technol., vol. 41, pp. 6290–6296, 2007.

[57] H. A. Sturges, "The choice of a class interval," J. Am. Stat. Assoc., vol. 21, no. 153, pp. 65–66, 1926.

[58] A. P. M. Subcommittee, “IEEE Reliability Test System,” IEEE Trans. Power Appar. Syst., vol. PAS-98, no. 6, pp. 2047–2054, 1979.

[59] G. H. Golub and C. F. Van Loan, “Matrix computations,” vol. 3, Johns Hopkins Univ Pr., 1996.